

FEHRL Report 2006/01

**Harmonization of European
Routine and research
Measuring Equipment
for Skid Resistance**

FEHRL Report 2006/01

Title: Harmonization of European Routine and research Measuring Equipment for Skid Resistance

Authors: G. Descornet – BRRC, Belgium
B. Schmidt – DRI, Denmark
M. Boulet – LCPC, France
M. Gothié – LCPC, France
M-T. Do – LCPC, France
J. Fafié – DWW, Netherlands
M. Alonso – CEDEX, Spain
P. Roe – TRL, United Kingdom
R. Forest – TRL, United Kingdom
H. Viner – TRL, United Kingdom

Keywords: Roads, Skid Resistance, Measurements, Harmonization.

Although the FEHRL has done its best to ensure that any information given is accurate, no liability or responsibility of any kind (including liability of negligence) is accepted in this respect by FEHRL, its members or its agents.

© FEHRL 2006

ISSN 1362-6019

All rights reserved. No part of this publication may be reproduced, stored in a retrieval system, or transmitted in any form or by any means, electronic, mechanical, photocopying, recording or otherwise, without the prior written permission of FEHRL.

FEHRL Secretariat: S. Phillips
Boulevard de la Woluwe, 42
Bte 3, B-1200 Brussels
Belgium

Tel: +32 2 775 82 38

Fax: +32 2 775 82 29

E-mail: info@fehl.org

Web site: www.fehl.org

Table of Contents

FOREWORD	V
THE HERMES PROJECT	V
SPECIFIC OBJECTIVES.....	V
WORK PROGRAMME SUMMARY	VI
FINANCING.....	VI
RESEARCH CONSORTIUM.....	VII
STEERING COMMITTEE.....	VII
PARTICIPANTS IN THE FIELD TRIALS	VIII
1 INTRODUCTION.....	1
2 THE HERMES CALIBRATION EXERCISES	4
2.1 GENERAL DESCRIPTION OF TRIALS.....	4
2.1.1 Overview	4
2.1.2 Participating devices.....	5
2.1.3 Trial Planning.....	8
2.1.4 The trials – general principles.....	11
2.1.5 The trials – Round 1.....	15
2.1.6 The trials – Round 2.....	18
2.1.7 The trials – Round 3.....	20
2.1.8 The test surfacings.....	20
2.1.9 Discussion of practical technical issues.....	22
2.2 NON-TECHNICAL ISSUES	27
2.2.1 Use of questionnaires.....	27
2.2.2 Logistics.....	29
2.2.3 Safety issues.....	31
2.2.4 Financial aspects.....	32
2.3 SUMMARY OF THE HARMONISATION PROCESS	33
2.3.1 Calculation of the IFI using the PIARC-model.....	33
2.3.2 From IFI to EFI.....	34
2.3.3 Determination of the EFI.....	34
2.3.4 The calibration procedure.....	35
2.4 EXPERIMENTAL RESULTS.....	37
2.4.1 Introduction.....	37
2.4.2 Characteristics of the test surfaces.....	37
2.4.3 Texture measurements	38
2.4.4 Friction device-specific parameters.....	41
2.4.5 The database collected.....	42
2.4.6 Repeatability of F	42
2.4.7 Reproducibility of F	44
2.4.8 Curve fitting on $F(S)$	47
2.4.9 Deriving S_0 from MPD	48
2.4.10 Applying statistical tests to the EFI measurements	48
2.4.11 Calibration results.....	49
2.4.12 Discussion	52
3 REVISION OF THE FRICTION MODEL	55
3.1 INTRODUCTION.....	55
3.2 FURTHER IMPROVEMENTS TO THE MODEL.....	55
3.2.1 Calculation of S_0 vs. MPD_{ISO} per device	55
3.2.2 Quadratic regression analysis	58
3.2.3 The LCPC-model.....	63
3.2.4 Investigation of alternative characteristics of surface texture depth.....	80
3.3 DISCUSSION.....	85
4 ALTERNATIVE PROCESSING OF EXPERIMENTAL DATA	88

4.1	INTRODUCTION	88
4.2	IMPROVED MODEL FOR S_0 VS. MPD	88
4.3	STATISTICAL TESTS	90
4.4	SCENARIO #2: APPLYING NEW STATISTICAL TESTS	91
4.5	SCENARIO #3: APPLYING SIMPLER STATISTICAL TESTS	92
4.6	SCENARIO #4: REVERSING THE REGRESSION CALCULATION	97
4.7	SCENARIOS #5 TO #7: FORCING "A" TO ZERO	100
4.8	SCENARIO #8: TREATING <i>BFC</i> - AND <i>SFC</i> -DEVICES SEPARATELY	105
4.9	SCENARIOS #9 TO #11: IMPROVED MODEL FOR $F(S)$	106
4.10	ANALYSIS OF DEVIATIONS	110
4.11	SCENARIO #12: USING ACTUAL VALUES OF S_0 INSTEAD OF PREDICTIONS	111
4.12	REPEATABILITY OF <i>EFI</i>	112
4.13	SCENARIO #13. AVERAGING OUT THE REPEATABILITY DEVIATIONS OF <i>EFI</i>	114
4.14	RECAPITULATION	119
4.15	DISCUSSION	120
5	ALTERNATIVE APPROACHES TO REFERENCE LEVELS	122
5.1	INTRODUCTION	122
5.2	A SINGLE REFERENCE DEVICE	122
5.2.1	<i>Purpose</i>	122
5.2.2	<i>Approach</i>	122
5.2.3	<i>Historic and technical background</i>	123
5.2.4	<i>European needs</i>	124
5.2.5	<i>Proposed specification requirements</i>	128
5.3	REFERENCE SURFACES	131
5.3.1	<i>The purpose of reference surfaces</i>	131
5.3.2	<i>Requirements for reference surfaces</i>	131
5.3.3	<i>Past experience and existing practice</i>	132
5.3.4	<i>Possible solutions</i>	136
5.3.5	<i>Outline specification for calibration reference surfaces</i>	141
5.3.6	<i>Further research</i>	144
6	CONCLUSIONS	146
7	RECOMMENDATIONS	150
7.1	REVIEW OF THE CURRENT SITUATION	150
7.2	SPECIFIC RECOMMENDATIONS	151
	REFERENCES	152
	ANNEX A: GLOSSARY OF TERMS	ERROR! BOOKMARK NOT DEFINED.
	ANNEX B: EXPERIMENTAL RESULTS-GRAPHS OF $F(S)$...	ERROR! BOOKMARK NOT DEFINED.
	ANNEX C: EXPERIMENTAL RESULTS-GRAPHS OF S_0 V <i>MPD</i>	ERROR! BOOKMARK NOT DEFINED.
	: EXPERIMENTAL RESULTS-CALIBRATION GRAPHS <<EFI>> V <i>EFI</i>	ERROR! BOOKMARK NOT DEFINED.
	ANNEX E: <i>LCPC</i>-MODEL CONSTANTS	ERROR! BOOKMARK NOT DEFINED.
	ANNEX F: ALTERNATIVE PROCESSING-GRAPHS OF S_0 V <i>MPD</i>	ERROR! BOOKMARK NOT DEFINED.
	ANNEX G: ALTERNATIVE PROCESSING-CALIBRATION GRAPHS <<EFI>> V <i>EFI</i>	ERROR! BOOKMARK NOT DEFINED.
	ANNEX H: ALTERNATIVE PROCESSING-GRAPHS OF F V S	ERROR! BOOKMARK NOT DEFINED.
	ANNEX I: ALTERNATIVE PROCESSING-CALIBRATION GRAPHS <<EFI>> V <EFI> ...	ERROR! BOOKMARK NOT DEFINED.

ANNEX J: REVISED DRAFT FOR ANNEX B OF PREN 13036-2ERROR! BOOKMARK NOT DEFINED.

ANNEX K: REFERENCE DEVICE QUESTIONNAIREERROR! BOOKMARK NOT DEFINED.

ANNEX L: PROPOSED SPECIFICATION FOR A REFERENCE DEVICE..... ERROR! BOOKMARK NOT DEFINED.

ANNEX M: SYMBOLS AND ABBREVIATIONSERROR! BOOKMARK NOT DEFINED.

Foreword

The *HERMES* Project

HERMES – “Harmonization of European Routine and research Measuring Equipment for Skid Resistance” was a *FEHRL*-funded pre-normative project that aimed to lay the foundations for consistent European standardisation of skid resistance measurement on roads and runways. Underlying the work was the idea that the project should give the initial impetus to the implementation of a common scale of friction, the so-called *EFI* (European Friction Index), together with an associated harmonised calibration procedure, in all European countries.

Specific objectives

The project had five specific objectives relating to theoretical, practical and longer-term aspects of harmonising skid resistance measurements in Europe, namely:

1. To improve the model on which *EFI* is based, which relates the friction coefficient to the measurement speed, slip ratio and road surface texture, by taking account of recent developments in this field.
2. To demonstrate the reliability and feasibility of the procedure proposed by CEN/TC227/WG5 for inter-laboratory calibrations of the various devices used in Europe.
3. To produce a revised draft standard incorporating the findings from items 1 & 2.
4. To provide *FEHRL* with a practical scheme for setting up an organisation for the calibration of skid resistance devices in Europe.
5. To submit draft specifications for a reference device and/or reference surfaces to the member laboratories of *FEHRL* with a view to developing the next generation of standards.

Work programme summary

To meet those five objectives, the following tasks were identified:

- 0 Scientific management.
- 1 Improvement of models.
- 2 Evaluation of proposed calibration procedures and their organisation.
 - 2.1 Organisation of calibration exercises.
 - 2.2 Analysis of the results.
 - 2.3 Evaluation of non-technical aspects.
- 3 Definition of references for the future.
 - 3.1 Specifications for a reference device.
 - 3.2 Specification for reference surfaces.

Financing

The members of the *HERMES* Working Group thank the following institutions for their contributions to the financing of this research:

Belgium:	Ministère fédéral des Affaires Economiques - Division Compétitivité NG III Belgian Road Research Centre (<i>BRRC</i>)
Denmark:	Danish Road Institute Danish Road Directorate
France:	Ministère de l'Équipement, du Logement et des Transports Ministère de l'Éducation Nationale, de la Recherche et de la Technologie
Netherlands:	Directorate-general of Public Works and Water Management (<i>RWS</i>)
Spain:	Centro de Estudios y Experimentación de Obras Públicas (<i>CEDEX</i>)
United Kingdom:	Highways Agency

Research consortium

The following consortium of FEHRL laboratories was responsible for carrying out the research. Individual laboratories took responsibility for leading specific tasks within the programme and all contributed to other tasks.

Laboratory	Role
<i>BRRC</i> (BE) Belgian Road Research Centre	Project co-ordinator, task 0 Contributor task 2.1 Leader task 2.2
<i>CEDEX</i> (ES) Centro de Estudios y Experimentación de Obras Públicas	Contributor task 2.1 Contributor task 3.1 Contributor task 3.2
<i>DRI</i> (DK) Danish Road Institute	Leader task 2.3 Contributor task 3.1 Contributor task 3.2
<i>DWW</i> (NL) Dienst Weg- en Waterbouwkunde	Contributor task 2.1 Leader task 1
<i>LCPC</i> (FR) Laboratoire Central des Ponts et Chaussées	Contributor task 1 Contributor task 2.1 Leader task 3.1 Contributor task 3.2
<i>TRL</i> (GB) Transport Research Laboratory	Contributor task 1 Leader task 2.1 Leader task 3.2

Steering committee

The project was carried out by a *FEHRL* Working Group, the membership of which is as follows:

Guy DESCORNET (Convenor)	BRRC	Belgium
Bjarne SCHMIDT	DRI	Denmark
Michel BOULET	LCPC	France
Michel GOTHIE	LCPC	France
Minh-Tan DO	LCPC	France
Jeannot FAFIÉ	DWW	Netherlands
Marta ALONSO ANCHUELO	CEDEX	Spain
Peter ROE	TRL	United Kingdom
Rozenn FOREST	TRL	United Kingdom
Helen VINER	TRL	United Kingdom

Participants in the field trials

In addition to the work of the main research consortium, the following organizations sent their equipment and teams to participate in calibration exercises several times, and in different countries, during the course of the project. The Steering Group offer their wholehearted thanks for these contributions, without which the project could not have been carried out¹.

Organization	Country	Particular thanks to:
<i>BRRC</i> - Belgian Road Research Centre	Belgium	Michel GORSKI
<i>MET</i> - Ministère wallon de l'Équipement et des Transports – Division de Structures routières	Belgium	Guy LEFÈBVRE
<i>DRI</i> – Danish Road Institute	Denmark	B. Roland JENSEN
<i>CETE</i> - Centre d'Études Techniques de l'Équipement de Lyon	France	Michel GOTHIE
<i>STBA</i> – Service Technique des Bases Aériennes	France	Jean-Claude DEFFIEUX
<i>TRL</i> - Transport Research Laboratory	United Kingdom	Paul FÈVRE
<i>DWW</i> - Rijkswaterstaat - Dienst Weg- en Waterbouwkunde	Netherlands	Jeannot FAFIÉ
Staten Vegvesen	Norway	Bjorne Ove OFSTAD
<i>NPRA</i> – <i>NRRL</i> – Norwegian Road Research Laboratory	Norway	Per Harald HANSEN
<i>IBDIM</i> – Road and Bridge Research Institute	Poland	Bogumil SZWABIK ²
<i>CEDEX</i> – Centro de Estudios y Experimentación de Obras Públicas	Spain	Marta ALONSO ANCHUELO

¹ The experimental data collected in this project will remain the property of FEHRL. They can be made available on request to FEHRL-member laboratories as well as other non-FEHRL participants in field trials.

² The authors note with sadness that Mr Szwabik died before the project was completed. The HERMES team would like to acknowledge his enthusiastic personal contribution to the field trials and offer their condolences to his colleagues, family and friends.

1 Introduction

The skid resistance of a road surface is affected by a great many factors, some to do with the road and others to do with the measurement technique and conditions.

In Europe more than twelve different types of device are used to measure skid resistance. Some make use of different principles and those that use similar principles may have detail differences that affect their relative measurements. Devices may be operated at different speeds and this, too affects the results. The effect that speed has on the measurements depends upon a property of the road surface known as “macro texture” or texture depth. This is a major factor that contributes to the differences between measurements made by different devices.

Historically, each country has used one or two types of device and the requirements of their standard tender specifications and maintenance policies have been set to match them. The opening up of the single market, however, has created a need for harmonisation, to encourage the development of homogeneous conditions of safety from one country to the next. This harmonisation has been undertaken in CEN group TC227/WG5. One of the objectives of that group is to develop a draft standard defining a uniform procedure to determine skid resistance from a dynamic measurement.

It is unrealistic to expect such a procedure to rely on a single device if it is to be acceptable to a majority of countries. That is why a philosophy has been adopted that there should be a means of converting results delivered by different devices to values on a common, harmonised, scale so that individual countries can continue to use their own method – at least during a period of transition – but at the same time offering them the possibility of relating their measurements to those used elsewhere.

However, because skid resistance is not constant and is affected by so many factors, there is no absolute measure of friction that can be used to compare different skid-resistance measurement devices. Therefore, a scale is needed that, in effect, can use the “average” of all devices as a surrogate for the “correct” answer. If individual devices could be linked to this scale in a way that takes account of their particular characteristics, then the required harmonisation could be achieved.

Anticipating this need, in 1992, *PIARC* conducted an international experiment to compare different devices and methods in use to measure friction and surface texture on road and airfield pavements [1]. All the devices and methods used in Europe at that time were represented. The experiment showed that virtually all of the participating devices could be harmonised using a single equation to relate their outputs to a common scale, provided that an allowance was made for a measurement of macro texture. The proposed scale was called the International Friction Index (*IFI*). There were concerns, however, that this scale was not sufficiently precise to be of effective practical value in Europe where so many different devices were used.

A further analysis of the database from this experiment and additional tests were performed in 1997-1998 under a contract with the Belgian Federal Government [2]. The objective was to adapt the definition of *IFI* to relate more specifically to the sub-set of devices used in Europe and to update it by taking into account new road surfacing materials (for example porous asphalt, stone mastic asphalt and slurry seals) not covered by the *PIARC* experiment.

This resulted in a proposal for a European Friction Index (*EFI*) that would, potentially, provide the harmonisation sought between the various types of device used in Europe. The proposed *EFI*, building on the experience gained from the PIARC experiment and Belgian research, uses the overall average of all devices used in Europe to define the common scale and uses mathematical models that represent the effect of texture and speed to adjust the measured values made at a particular test speed by a particular device to their equivalent on this common scale at a reference speed. How this is done is explained in more detail in Chapter 2.3 of this report.

It was also recognised that, for the system to operate effectively, a means of regularly calibrating individual devices to the scale and for verifying that the scale itself remained stable was also needed. This would also need to make provision for new devices to be added to the system when necessary.

Based on this work, in 1998 a proposal was submitted to *CEN/TC227/WG5* that defined both the *EFI*³ and a procedure for calibrating measuring devices based on that index. The proposal was included in a draft standard in preparation, as an informative Annex [3].

However, after several examinations and subsequent revisions of the draft, the group considered it necessary to test the proposed calibration procedure before formalising it in a standard. The questions that remained unanswered related mainly to the reproducibility of the *EFI*-values delivered by the various devices, the real magnitudes of the drifts of the devices and, consequently, the required frequency of calibration needed to maintain the desired accuracy. Non-technical aspects such as costs and any difficulties in practice also required examination. Further, in the intervening period, new research results had become available that might permit some improvements in the precision of *EFI* by allowing for an additional parameter, namely, the *slip ratio* between the test tyre and the tested surface.

Meanwhile, the *FEHRL* working group on “European Harmonisation of Friction, Texture and Evenness Measurements” had been mandated as early as in 1997 by the *FEHRL* Board of Directors to work on the development of basic specifications for a European reference device for use with the next generation of skid resistance standards. As there were doubts about the real possibility of relying on *EFI*, that alternative option was to be seriously considered despite its own inherent difficulties. One such difficulty is that such a device has itself to be calibrated somehow, which requires some friction standard(s) to be available. Therefore, the possibility of using reference surfaces for that purpose had to be investigated as well.

The *HERMES* project was therefore conceived by the *FEHRL* working group to address these issues, with specific objectives as set out in the Foreword to this report. The work would be carried out by a core team of experts from laboratories represented in this group, assisted by contributions from other *FEHRL* laboratories and organisations in member countries.

³ The Draft prEN-13036-2 [3], proposes the term Skid Resistance Index (SRI) to describe the harmonised scale, instead of European Friction Index (EFI). However, because EFI has been used in several previous publications, and in order to avoid confusion in readers' minds, EFI is also used in this report. A change to using the term SRI may be eventually necessary if the prEN retains that terminology and when it is used as a standard.

This report presents the results of the project in five main Chapters.

Chapter 2 describes the experimental part of the project that aimed to test the feasibility of the proposed calibration procedures under realistic conditions. Not only technical activities (Section 2.1) but also practical aspects (Section 2.2) are evaluated. Section 2.3 explains briefly the way in which the harmonisation process in the draft standard operates, and how the associated calculations are made. Finally, Section 2.4 summarises the measurements made and gives an initial analysis of the results obtained when the procedures set out in the draft standard were followed.

Chapter 3 presents the results of various attempts to improve the mathematical models on which the definition of *EFI* is based, with a view to possible improvements to the precision and reliability of the index itself.

Chapter 4 presents a number of alternative ways of processing the results from the calibration exercises (described in Section 2.3) that were considered with a view to optimising the reproducibility of *EFI* as delivered by the different participating devices.

Chapter 5 looks to the future. Section 5.1 proposes specifications for a future single standard skid resistance measurement device, based upon a consultation of users of current equipment and detailed discussions within the project steering group. Section 5.2 discusses the background to past work in the field and the future possibilities for designing, building and maintaining stable and reproducible reference surfaces for calibrating friction measurement devices.

2 The HERMES calibration exercises

2.1 General description of trials

2.1.1 Overview

As explained in Chapter 1 of this report, the *EFI*, in the absence of an absolute reference value, is based upon the idea of relating different measurement devices to a common scale that itself represents an overall “average” of all devices. However, because devices could change over time, it is essential to ensure that the index itself does not change significantly or gradually drift and that individual types of device are regularly calibrated to the index.

To achieve this, the *prEN* [3] requires calibration exercises, in which different combinations of a few devices would meet to re-establish the links with the main index and keep the index itself consistent with the current status of the devices. This process would lead to devices being established as “reference devices”⁴ that had been calibrated to the index through one of these meetings, allowing other similar devices in national fleets to be calibrated to the reference device and hence to the index. In due course, new devices could join in a calibration trial and then themselves join the set of “reference devices” for subsequent occasions.

The *prEN* [3] anticipated that such meetings would occur annually for reference devices.

The purposes of the *HERMES* calibration exercises (referred to subsequently in this chapter and elsewhere by the shorthand “trials”) were therefore twofold:

To assess the practicality of following the procedure set out in the *prEN*.

To provide data that would allow the stability and precision of the *EFI* to be assessed across a realistic range of European devices.

To consider the precision of the *EFI*, the programme therefore needed to include a range of devices that would have to meet in different combinations at different times. The first round of tests would allow the device-dependent coefficients to be recalculated (Section 2.3.12). Subsequent rounds of trials would provide for further refinement of the coefficients and the index.

To assess the stability of the index over time, a number of trial cycles would be necessary. To assess this within a practical overall project time, it was decided to accelerate the programme of trials to mimic a three-year cycle, but within a one-year timetable. A series of trials was therefore planned, with three “rounds”, each containing three individual meetings.

In principle, each participating device would attend one trial in each round and, generally, visit a different location and meet with a different group of devices on each occasion. This

⁴ The term “reference device” here is used specifically to mean devices that have been through this process of calibration against the skid resistance index and on which the index is based. It does not have the same meaning as an absolute reference against which other devices can be compared, except as a means of relating other devices of the same type to the index in what is known as a “Type-3 calibration”.

would enable the variation in the device coefficients to be checked and gradually refined and also assess any inherent variation in the *EFI*. More details of the way in which this was achieved are given in Section 2.1.3









2.1.2 Participating devices

Altogether, fifteen skid resistance-measuring devices and eight texture-measuring devices took part in the *HERMES* project. Some devices were initially considered to be “reference devices” because they had taken part in the 1992 *PIARC* International Experiment. This meant that initial values for the regression coefficients were available and their results provided the overall average on which the *EFI* would be based.

Other devices were newcomers to the set, but once they had participated at one exercise they joined the set of reference devices for the later meetings. The set of friction devices originally invited to participate covered practically the full range of systems currently in use on roads in Europe, including both longitudinal (*BFC*) and transverse (*SFC*) measurements with *slip ratios* from 14% to 100% (locked wheel). Table 2.1 provides a brief description of each skid resistance device participating. One device used on airfields in France was added later in the programme.

In order to apply the mathematical models to harmonise the devices, it was necessary to have measurements of texture depth (as Mean Profile Depth, *MPD*) for the test surfaces. Measurements were made both by the organisers of each trial and by participating devices where they were capable of measuring *MPD*. The various texture devices used are listed in Table 2.2. Some were fitted to the friction device, others were separate, but all of the texture devices complied with *ISO 13473-1*, 1996.

Table 2.1 Skid resistance devices taking part in the HERMES trials

Code	Device Name	Operator Organisation (Country)	Key Operating Principles*	Thumb-nail Photograph
F01	DWW Trailer	DWW Rijkswaterstaat (NL)	86% Fixed Slip. PIARC Radial smooth tyre at 200 kPa. 0,5 mm water film thickness.	
F02	ADHERA	CETE de Lyon (FR)	Locked Wheel. smooth PIARC tyre at 180kPa. 1,0 mm water film thickness.	
F03	SCRIM	CEDEX (ES)	Side Force 20° wheel angle. Avon SCRIM smooth tyre at 350 kPa. 0,5 mm water film thickness.	
F04	SCRIM	MET (BE)	Side Force 20° wheel angle. Avon SCRIM smooth tyre at 350 kPa. 0,5 mm water film thickness.	
F05	GripTester	MET (BE)	15% fixed slip. 254 mm (10") dia. smooth tyre at 138 kPa. 0,5 mm water film thickness.	
F06	ROAR	DRI (DK)	Variable slip device run at 20% fixed slip. ASTM 1551 smooth tyre. 0,5 mm water film thickness.	
F07	ROAR	DWW Rijkswaterstaat (NL)	Variable slip device run at 86% fixed slip. ASTM 1551 smooth tyre. 0,5 mm water film thickness.	
F08	Odoliograph	BRRC (BE)	Side Force 20° wheel angle. PIARC ASTM E525 88 smooth tyre. 0,5 mm water film thickness spread by preceding tanker.	

Code	Device Name	Operator Organisation (Country)	Key Operating Principles*	Thumb-nail Photograph
F09	PFT	TRL (GB)	Locked wheel. ASTM E524 smooth tyre at 200 kPa. 1,0 mm water film thickness.	
F10	OSCAR	(NPRA/NRRL) (NO)	Variable slip device run at 18% fixed slip. ASTM E524 smooth tyre at 207 kPa. 0,5 mm water film thickness.	
F11	ROAR II	Statens Vegvesen (NO)	Variable slip device run at 18% fixed slip. ASTME1551 smooth tyre. 0,5 mm water film thickness.	
F12	SRT-3	IBDIM (PL)	Locked wheel. Commercial patterned tyre at 200 kPa. 0,5 mm water film thickness.	
F13	SCRIM	TRL (UK)	Side Force 20° wheel angle. Avon SCRIM smooth tyre at 350kPa. Water flow 0.95l/s giving 0,5mm water film thickness at 50km/h and 0,25mm at 90km/h.	
F14	Odoliograph	MET (BE)	Side Force 20° wheel angle. PIARC ASTM E525 88 smooth tyre. 0,5 mm water film thickness spread by preceding tanker.	
F15	IMAG	STBA (FR)	15% Fixed slip. Smooth PIARC tyre. 1,0 mm water film thickness.	

Code	Device Name	Operator Organisation (Country)	Key Operating Principles*	Thumb-nail Photograph
<p>Tyre pressures are given in SI units to the nearest kPa based upon information provided by the Operating Organisation (<i>some operators use Imperial (UK) or Metric units</i>). The water film thickness given here is the theoretical water film thickness at which the device normally operates when wetting the road for a test, as advised by the Operating Organisation. (<i>For some devices this is controlled automatically by varying the flow rate according to the test speed, for others a fixed flow rate may be used that results in a slight variation in water film thickness at different operating speeds. In most cases in the HERMES trials, apart for the first machine on the first test run, the road surface had already been wetted by preceding devices</i>).</p>				

Table 2.2 Texture devices used in HERMES trials

Device Code	Name of Equipment	Nationality	Operator Organisation
T1	GREENWOOD	DK	Danish Road Institute
T2	ARAN	NL	DWW Rijkswaterstaat
T3	Rugolaser	FR	CETE de Lyon
T4	GEOCISA	ES	CEDEX
T5	HARRIS	GB	TRL
T6	ROAR	NO	Statens Vegvesen
T7	SCRIMTEX	GB	TRL
T8	Stat TX meter	BE	BRRC

2.1.3 Trial Planning

So that the project would include a representative sample of European highway surfaces and encompass the wide range of environmental conditions across Europe, the trials were planned to take place in more than one country. Sites on test tracks and sites on public roads would be included in order to assess the advantages and disadvantages of each type of location. Holding the trials in more than one country would also allow a wider range of important non-technical issues to be assessed than would be possible if the trials were held in just one country.

It was arranged that five of the Steering Group members would host or arrange trial exercises in their countries. These would be *TRL* (United Kingdom), *CEDEX* (Spain), *DWW* (Netherlands), *LCPC* (France) and *BRRC* (Belgium), with overall co-ordination by *TRL*, the Task Leader. As Task Leader, the *TRL* representative on the Steering Group attended all of the trials apart from the last two, either as an independent observer or as a device operator. This provided for continuity of observation at all of the different locations (every member of the Steering Group attended at least one of the trials).

The trial schedule was constrained by the overall duration of the project and the need to simulate the calibration periods specified in the *prEN* [3]. It was also necessary to provide a realistic interval between the first and last set of trials so that any drift in the results of

any one device could be identified and realistically incorporated in the data set, thus ensuring that the derived procedures would be robust.

Overall, nine trial exercises would be held in three trial rounds, with three meetings in each round. Each host organisation would arrange two trials, except *CEDEX* who would only host one trial. The trial rounds were planned for autumn 2001, spring 2002 and autumn 2002. The number of trials required was based on the number of participating devices, allowing most devices to participate at least once in each trial round. Some devices participated more than once in a trial round, usually when they were attached to the host organisation for one of the trials.

The order of the trials was chosen to reduce the possibility of disruption due to bad weather. For example, in the first round, which took place during autumn 2001, the United Kingdom trial was held first, followed by the Netherlands and then Spain. Even so, heavy rain affected several of the trials and snow on the roads in the preceding week almost forced the postponement of the Spanish trial. In Belgium, *BRRC* worked through *MET* (the Ministère Wallon de l'Équipement et des Transports) that carried out the detailed organisation and ran the two trials there. Table 2.3 summarises the trial round programme.

Table 2.3 Summary of trial rounds

Round, Trial	Host, Country	Dates	No. of devices		Location and type of site	No. of test sections
			Friction	Texture		
1,1	<i>TRL</i> , GB	23-25/10/01	5	1	Crowthorne, <i>TRL</i> test track	8
1,2	<i>DWW</i> , NL	29-31/10/01	4	2	Joure and Lelystad, Motorway + test track	6
1,3	<i>CEDEX</i> , ES	20-22/11/01	4	2	Valencia area, Motorway, main road	6
2,1	<i>MET</i> , BE	19-21/03/02	7	3	Nivelles and Borders areas, Motorway, main road, local roads	7
2,2	<i>LCPC</i> , FR	26-28/03/02	5	1	Nantes, <i>LCPC</i> test track	6
2,3	<i>DWW</i> , NL	23-25/04/02	6	3	Cuijk area, Motorway, main roads	7
3,1	<i>TRL</i> , GB	01-03/10/02	3	3	Crowthorne, <i>TRL</i> test track	8
3,2	<i>MET</i> , BE	08-10/10/02	6	1	Nivelles and Borders areas, Motorway, main road, local roads	7
3,3	<i>LCPC</i> , FR	15-17/10/02	7	2	Nantes, <i>LCPC</i> Test track	6

At the outset of the work it was recognised that there could be more devices available than was necessary for the purposes of the project and that some might have constraints on their availability that would rule them out. Therefore, an initial letter was sent to all of the *FEHRL* Laboratories introducing the project and inviting them to consider taking part. The letter included a general proposal regarding the trial schedule and the level of commitment being requested. Each potential participant was asked to identify dates that were most suitable for them. They were also asked to indicate whether they would be able to attend any particular country. The final decision as to which devices would be invited to join in the project and which trials they would attend rested with the project Steering Group.

Based on the response from this initial approach, a participation matrix was planned. In principle, each device would attend three trials, in three different countries. In order to reduce costs, one of these would be the trial of its host country where possible. In addition, "host" devices would also attend subsequent trials in their own countries in addition to the visiting devices.

The matrix was initially designed to ensure that the sets of devices that met at any one trial were mixed in relation to measurement type and in such a way as to avoid repetitions of meeting sets on subsequent occasions. In the event, equipment failures and other operational commitments meant that some re-arrangement and substitution was necessary and some devices experienced difficulties that prevented them from taking part fully in all the trials that they attended.

Table 2.4 lists the devices attending each trial. Table 2.5 shows the full participation matrix, indicating the trials where each device met the other devices.

Table 2.4 Devices attending each trial

Trial Reference	Country	Friction Devices attending	Texture devices attending
1,1	UK	F09, F10, F11, F12, F13	T5
1,2	Netherlands	F01, F04, F07, F05, F06	T1, T2
1,3	Spain	F01, F03, F02, F08	T3, T4
2,1	Belgium	F01, F06, F09, F10, F05, F14	T6
2,2	France	F02, F05, F08, F12, F15	T3
2,3	Netherlands	F01, F03, F04, F11, F13, F15	T4, T6, T7
3,1	UK	F01, F06, F13	T1, T5, T7
3,2	Belgium	F04, F05, F13, F15	T6, T8
3,3	France	F02, F03, F04, F05, F10, F11, F12	T3, T4

Table 2.5 Participation matrix – trials attended by each device

Device	F01	F02	F03	F04	F05	F06	F07	F08	F09	F10	F11	F12	F13	F14	F15
F01		1,3	1,3 2,3	1,2 2,1 2,3	1,2 2,1	1,2 2,1 3,1	1,2	1,3	2,1	2,1	2,3		2,3 3,1	2,1	2,3
F02	1,3		1,3 3,3	3,3	2,2 3,3			1,3 2,2		3,3	3,3	2,2 3,3			2,2
F03	1,3 2,3	1,3 3,3		2,3 3,3	3,3			1,3		3,3	2,3 3,3	3,3	2,3		2,3
F04	1,2 2,1 2,3	3,3	2,3 3,3		1,2 2,1 3,2 3,3	1,2 2,1	1,2	3,2	2,1	2,1 3,3	2,3 3,3	3,3	2,3 3,2	2,1 3,2	2,3 3,2
F05	1,2 2,1	2,2 3,3	3,3	1,2 2,1 3,2 3,3		1,2 2,1	1,2	2,2 3,2	2,1	2,1 3,3	3,3	2,2 3,3	3,2	2,1 3,2	2,2 3,2
F06	1,2 2,1 3,1			1,2 2,1	1,2 2,1		1,2		2,1	2,1			3,1	2,1	
F07	1,2			1,2	1,2	1,2									
F08	1,3	1,3 2,2	1,3	3,2	2,2 3,2							2,2	3,2	3,2	2,2 3,2
F09	2,1			2,1	2,1	2,1				1,1 2,1	1,1	1,1	1,1	2,1	
F10	2,1	3,3	3,3	2,1 3,3	2,1 3,3	2,1			1,1 2,1		1,1 3,3	1,1 3,3	1,1	2,1	
F11	2,3	3,3	2,3 3,3	2,3 3,3	3,3				1,1	1,1 3,3		1,1 3,3	1,1 2,3		2,3
F12		2,2 3,3	3,3	3,3	2,2 3,3			2,2	1,1	1,1 3,3	1,1 3,3		1,1		2,2
F13	2,3 3,1		2,3	2,3 3,2	3,2	3,1		3,2	1,1	1,1	1,1 2,3	1,1		3,2	2,3 3,2
F14	2,1			2,1 3,2	2,1 3,2	2,1		3,2	2,1	2,1			3,2		3,2
F15	2,3	2,2	2,3	2,3 3,2	2,2 3,2			2,2 3,2			2,3	2,2	2,3 3,2	3,2	

2.1.4 The trials – general principles

The general trial procedure was standardised, although some local variation was necessary in the light of experience or to take account of local circumstances or events as they developed. Generally, each trial was planned to take place over a working week. In principle, the Monday and Tuesday mornings were available for the participants to travel to the location ready to attend a briefing and familiarisation session on the Tuesday afternoon. The main test runs were carried out on the Wednesday and Thursday, followed by a de-briefing session. Teams would then travel home on the Friday. The Friday was also reserved for further testing in case bad weather or other unforeseen problems interrupted the main programme. In principle, the preceding and succeeding weekends would be available for travelling for devices with longer journeys.

At each trial, a range of surfaces was to be tested by each device at three different speeds: 30km/h, 90km/h and an intermediate speed that corresponded to the normal survey speed for the specific device. A target of five replicate measurements on each surface at each speed was set, with the intention of achieving at least three passes by each device in the event of delays or disruptions. The order in which devices would test the surfaces would generally be randomised between replicates. Figure 2.1 is an example of a timetable chart from one of the trials, illustrating the randomisation process.

Each host organisation was responsible for measuring and reporting the texture depth of the test sections but, in addition, an opportunity was provided to enable the visiting devices that could measure texture to survey the test sections on the dry surface before the commencement of the main wet-testing programme.

Each trial surface selected was to be of homogeneous friction and texture and not less than 100 m long. The trial organisers were encouraged to select as wide a range of surfaces as was practical, including asphalt and cement concrete, dense and porous. It was intended that across all the trials the surfaces selected should vary in type, age and condition and should include modern thin surfacings. The surfacings are discussed in more detail in Section 2.1.8.

Device operators would process the data from their own machine and complete a standardised data sheet with the results (i.e. the average skid resistance and actual test speed recorded on each section for each run), either before leaving the trial location for home or as soon as possible afterwards. Figure 2.2 shows an example of a completed results sheet. This was part of a Microsoft Excel spreadsheet that contained a number of similar worksheets to record the results from each device participating in the particular trial, together with other information relating to the trial. Once completed for all the devices in the trial, the data were sent to *BRRC* for further analysis.

In addition to recording their data, each device team was asked to complete a questionnaire seeking feedback on various non-technical aspects of the trial. These were subsequently used to review the major non-technical issues that are discussed in detail in Section 2.2 below.

APPENDIX 1

TRIAL MATRIX

WEDNESDAY 2ND OCTOBER

Route 1

Practice Run

NO WATER

TimeNoSpeed

09:0013Any

9Any

1Any

6Any

Route 1

Texture Run

NO WATER

TimeNoSpeed

09:151350

150

660

Route 1

Replicate 1

Replicate 2

Replicate 3

Replicate 4

Replicate 5

TimeNoSpeed

9:30130

630

930

1330

9:40150

660

960

1350

9:50190

690

990

1390

TimeNoSpeed

10:10630

1330

130

930

10:20660

1350

150

960

10:30690

1390

190

990

TimeNoSpeed

10:501330

130

930

630

11:001350

150

960

660

11:101390

190

990

690

TimeNoSpeed

11:301330

930

630

130

11:401350

960

660

150

11:501390

990

690

190

TimeNoSpeed

12:10930

630

1330

130

12:20960

660

1350

150

12:30990

690

1390

190

LUNCH 12:45 to 13:30

TRANSPORT WILL BE PROVIDED TO ROOM B0151

Route 2

Practice Run

NO WATER

TimeNoSpeed

13:4513Any

9Any

1Any

6Any

Route 2

Texture Run

NO WATER

TimeNoSpeed

14:001350

150

660

Route 2

Replicate 1

Replicate 2

Replicate 3

Replicate 4

Replicate 5

TimeNoSpeed

14:20130

630

930

1330

14:30150

660

960

1350

TimeNoSpeed

15:00630

1330

130

930

15:10660

1350

150

960

TimeNoSpeed

15:401330

130

930

630

15:501350

150

960

660

TimeNoSpeed

16:201330

930

630

130

16:301350

960

660

150

TimeNoSpeed

17:00930

630

1330

130

17:10960

660

1350

150

17:20990

690

1390

190

Figure 2.1 Example of trial running timetable


<div>  <div> Harmonisation of European Routine and Research Measuring Equipment for Skid Resistance of Roads and Runways </div> </div>										
CALIBRATION TRIAL MEETING - RESULTS SPREADSHEET - FRICTION TEST RESULTS										
This sheet summarises the results from Device 1 (SCRIM from UK), at calibration meeting 1.1 held in United Kingdom on 23-25 October 2001										
Section Identifier (eg UK1, NL5)	Section name	Target speed 30km/h			Intermediate speed			Target speed 90km/h		
		Run	actual speed	friction value	Run	actual speed	friction value	Run	actual speed	friction value
UK1	Grooved concrete	1	29.8	0.550	1	50.4	0.523	1	89.3	0.453
		2	30.2	0.555	2	50.1	0.529	2	88.8	0.450
		3	30.7	0.550	3	50.0	0.530	3	89.1	0.455
		4	31.2	0.550	4	50.0	0.531	4	89.1	0.448
		5	31.0	0.556	5	49.6	0.531	5	89.5	0.452
UK2	Brushed concrete	1	29.2	0.546	1	50.1	0.479	1	90.3	0.349
		2	30.1	0.560	2	49.8	0.493	2	90.6	0.342
		3	30.4	0.548	3	50.0	0.502	3	89.3	0.358
		4	30.5	0.556	4	49.8	0.495	4	90.5	0.339
		5	30.1	0.555	5	50.1	0.496	5	89.9	0.340
UK6	"MARS" 14mm	1	31.0	0.687	1	49.8	0.652	1	89.3	0.611
		2	31.0	0.718	2	50.0	0.691	2	90.1	0.610
		3	31.0	0.718	3	50.2	0.708	3	91.0	0.605
		4	30.0	0.737	4	49.7	0.688	4	88.1	0.602
		5	30.3	0.739	5	50.1	0.700	5	92.9	0.584
UK5	"ENCAP"	1	30.0	0.704	1	50.0	0.699	1	89.1	0.603
		2	31.5	0.686	2	49.6	0.709	2	90.4	0.570
		3	30.0	0.753	3	50.0	0.691	3	91.0	0.573
		4	30.2	0.715	4	50.0	0.681	4	90.8	0.550
		5	31.0	0.718	5	50.0	0.689	5	90.8	0.552
UK8	Hot Rolled Asphalt	1	30.4	0.653	1	50.2	0.647	1	87.5	0.595
		2	30.5	0.642	2	49.8	0.684	2	89.5	0.606
		3	30.3	0.661	3	50.0	0.683	3	90.6	0.606
		4	31.0	0.662	4	49.9	0.700	4	90.4	0.601
		5	30.9	0.666	5	50.0	0.682	5	90.6	0.599
UK7	Epoxy	1	31.0	0.134	1	51.0	0.071	1	91.7	0.028
		2	30.8	0.157	2	50.3	0.079	2	91.6	0.029
		3	30.4	0.141	3	50.7	0.078	3	89.6	0.030
		4	30.0	0.144	4	49.9	0.075	4	91.4	0.035
		5	31.0	0.142	5	49.7	0.095	5	89.9	0.026
UK3	fine cold asphalt	1	30.0	0.679	1	50.4	0.625	1	91.2	0.500
		2	30.1	0.695	2	49.6	0.635	2	90.0	0.503
		3	30.1	0.686	3	50.0	0.642	3	89.6	0.529
		4	30.0	0.688	4	49.7	0.633	4	90.2	0.511
		5	30.0	0.684	5	50.0	0.636	5	90.1	0.484
UK4	polished concrete	1	30.0	0.529	1	49.3	0.454	1	89.8	0.354
		2	30.0	0.533	2	50.0	0.456	2	89.3	0.349
		3	30.0	0.525	3	49.9	0.466	3	89.8	0.361
		4	30.5	0.527	4	50.0	0.460	4	89.8	0.357
		5	30.0	0.525	5	49.6	0.458	5	90.1	0.348
		1			1			1		
		2			2			2		
		3			3			3		
		4			4			4		
		5			5			5		
		1			1			1		
		2			2			2		
		3			3			3		
		4			4			4		
		5			5			5		

Figure 2.2 Example of a completed data sheet for one device from a trial results spreadsheet (in this case, Device F13 at Trial 1,1).

2.1.5 The trials – Round 1

2.1.5.1 Trial 1,1 – UK

The first trial was based at the private research track of *TRL Limited*. This provided an initial test for the operating procedures and a basic model for the subsequent trials in this round in the Netherlands (1,2) and Spain (1,3).

Eight test sections were chosen. These included asphalt surfacings of a type widely used, but specific to, the UK, brushed and grooved cement concrete and a smooth epoxy surface laid for the purpose. The track layout meant that it was not possible to test all of the sections in turn in a single pass, so the testing was arranged to cover them in three “routes”. The tests were controlled from a central part of the test track (Figure 2.3).



Figure 2.3 Test vehicles waiting at the control area, trial 1,1

Initially, it had been planned to provide lines on the track as guides for the crews to follow to when testing. Unfortunately, wet weather at the time meant that the marker tape used would not adhere satisfactorily to the road surface. However, because the surfaces were on a test track, and therefore not subject to the concentrated polishing that would occur on an in-service road, this was not considered critical. To take account of the mixture of left-side, right-side and centrally-mounted test wheels, crews were instructed to operate with their test wheel in the centre of the lane. Marshals positioned close to each group of sections checked that each device followed the correct line.

The original concept required organisers to allow for sufficient time to enable water from one device to drain from the surface before the next device followed. However, this proved to be unrealistic for sites of this type given the number of devices taking part and the number of tests to be made. Therefore, a nominal two-minute interval between devices was planned. The marshals ensured that there was sufficient time for any excess water to drain from the test sections between each participating device.

Overall, in spite of delays due to heavy rain when the surfacings became waterlogged, the full programme of tests was completed. Device F11 developed a fault just prior to the main test runs. This prevented it recording its measurements at the planned fixed *slip ratio* and so it ran with a lock-and-release cycle, interpreting a value equivalent to the standard 18% slip subsequently.

2.1.5.2 Trial 1,2 - Netherlands

The second trial in the first round (1,2) was held in the Netherlands. The trial had been brought forward by a day so that work could be completed before a public holiday that affected some of the visiting crews. Therefore, there was little time between Trial 1,1 (which finished on the Thursday) and Trial 1,2 (with the briefing scheduled for the following Monday afternoon) to enable lessons learned in the first trial to be applied. Nevertheless, it was possible to take some points into account, which assisted the smooth running of the second trial.

There were six test sections, which were divided between two locations: four on the A6 motorway near Joure and two on a privately operated test track at Lelystad. Five devices took part in this second exercise. Crews were accommodated and the main briefing was held in a hotel approximately mid-way between the two locations and about half an hour's drive from each of them. The tests on the motorway (Figure 2.4) were controlled from a depot at Joure, close to the end of the motorway section. Devices were required to return to the depot for despatch at the appropriate time and sequence.



Figure 2.4 Device F01 approaches the end of the test section on the A6 at Joure

An interval of five minutes was allowed between devices to give time for water drainage and for vehicles that needed to stop to set up. In theory, this could have been shortened but the lengthy run between motorway junctions to go from the depot to the site and return to the depot meant that there was a natural interval of about four or five minutes between the machines.

Some crews commented on the need to return to the depot between passes once the test pattern was established because this required negotiating two roundabouts and an awkward turn. However, this was necessary since the co-ordinator could not know what was happening on the road and the crews would be unaware of any problems with other devices or changes in running order that could affect them.

The tests at Lelystad (Figure 2.5) were more easily controlled, although there were constraints resulting from shared use of the track. This prevented, for example, closer observation of some of the sections on foot during the testing. Heavy-duty adhesive tape markers were placed to identify the sections and indicate the test line. Unfortunately, as was found in the UK, the tape did not adhere well in the wet conditions and the strips were removed for safety reasons.



Figure 2.5 Control area on the Lelystad test track

2.1.5.3 Trial 1,3 - Spain

The third trial (1,3) was held in Spain and organised by *CEDEX*. Test sites were identified in the Valencia region and the base for the trials was the Road Maintenance Centre at El Rebollar, alongside the motorway section of the A3 route from Valencia to Madrid. The briefing meeting was held here, following a similar form to the previous occasions.

The test sections were on sites at two locations, both on in-service roads: part of the A3 motorway section on the Valencia side of El Rebollar (Figure 2.7) and four on the old non-motorway N-III route about 30km west of this base. On the first day, tests were made on the old road. Having been relieved by the motorway, this was now very lightly trafficked and so traffic management was considered unnecessary. The test vehicles were able to operate freely along the route (Figure 2.6). The tests were co-ordinated from an area of ground near a service area, with devices operating generally at about four-minute intervals.

On the second day, tests were made on the motorway sections. For this work, the test lane and hard shoulder were closed to normal traffic by a line of cones. "Guards" from the traffic management team prevented unauthorised traffic from entering the closed section where it began.

The machines were all filled with water after the initial briefing, from a large tanker that was filled from a well at the Maintenance Centre. This was towed to the more remote site by an agricultural tractor to provide additional water supply at the roadside. Fewer re-fills of water were needed during the tests on the motorway site because there were only two test sections. Any re-fills that were necessary were made at the Maintenance Centre.



Figure 2.6 Rural section on the old N-III in Spain



Figure 2.7 Device F02 on the Motorway site in Spain

As with the earlier trials, good planning ensured that the work went smoothly and most tests were completed satisfactorily, in spite of the generally cold and wet conditions, particularly on the first day.

2.1.6 The trials – Round 2

2.1.6.1 Trial 2,1 – Belgium

The trials in the second round were held in February and March 2002. These built on the experience gained in the first round.

Trial 2,1 was held in Belgium. The tests were organised through *MET* at their base in Nivelles. The seven test sites were all on public roads and as in the Netherlands and Spain, were located in two distinct areas. Five were on a stretch of the A25 main dual carriageway east of Nivelles and two were on rural single carriageways near Borders. The sites in the two areas were tested on the successive days.

In addition to the main *HERMES* participants, additional Belgian devices also tested the sites. For operational convenience and to avoid conflict with the main trial, these devices operated in a separate group.

For this exercise, the tests on the main road route were organised slightly differently. Meeting points were arranged in lay-by areas close to the turn-around point at one end of the circuit. However, rather than requiring all vehicles to report back after each pass, as had been the case at trials 1,2 and 1,3, crews were instructed to complete a set of replicates. They would only report back if there were problems or at the end of a set of measurements at one speed. Although the devices completed their replicates in a sequence, the trial was organized so that the order of the devices was randomised for the different speeds.

On the rural roads, both sites were controlled from parking areas that also served as turn-around points. One of the sites needed informal traffic management to keep the section clear for devices that had to travel on the wrong side of the road in order to follow the test line.

As with the Round 1 trials, the weather was wet for part of the time, with heavy rain falling for the final test site. This, however, was a well drained, coarse textured surface dressing so build-up of water was not a problem. It was possible for all devices to complete at least the minimum number of runs required.

2.1.6.2 Trial 2,2 - France

Trial 2,2 was held at the Nantes centre of *LCPC* in France and the test sections were all on the *LCPC* test track. As at *TRL* and *Lelystad*, some test sections were on parallel lanes, but at *LCPC* they were all on the same straight length (Figure 2.8). It was therefore possible to test parallel sections in sequence, with one device following another on the alternative line at a shorter interval than would have been possible with the normal interval to allow the road to drain. This made testing very efficient and, combined with the fine weather during the week, led to a very smooth trial.



Figure 2.8 Device F08, preceded by its tanker, on the track at LCPC

2.1.6.3 Trial 2,3 - Netherlands

Learning from their experience in the first round, the *DWW* team decided that Trial 2,3 should be held at a different location to Trial 1,2. This would simplify the operational aspects and provide a wider range of surface characteristics than had been possible at the earlier meeting. It is not a requirement of the Friction Index calibration concept that

calibration meetings should always be in the same place and on the same surfaces, so this provided a useful opportunity to test the procedures over a wider range of circumstances.

The sections for this exercise were all on motorway standard public roads, near Cuijk. The test sections were closed to normal traffic for the tests, but the traffic management organisation limited the amount of time that the devices could have on site. Also, for one site there was some traffic congestion approaching the lane closure that also affected the test vehicles.

As a result there was insufficient time to complete a full set of five replicates at all speeds but all devices achieved the minimum of three runs at each speed.

2.1.7 The trials – Round 3

The third round of trials were all repeat exercises from the earlier rounds and all were held in the same locations in their respective countries.

Both Trial 3,2 in Belgium and Trial 3,3 in France used the same sections and followed the same patterns as they had in Round 2, but with different combinations of devices. However, at *TRL* there had been some changes to the test track since Round 1 and several of the surfacings or test lines were changed for Trial 3,1. The trial programme and procedures were otherwise unaltered from Trial 1,1.

2.1.8 The test surfacings

A wide range of surfacings was eventually included in the *HERMES* exercises. These included examples of purpose-made surfaces on test tracks and ordinary road surfaces. The material types included smooth epoxy resins (on the test tracks at *TRL* and *LCPC*) as well as cement concrete and different types of asphaltic material, including modern thin layers and porous asphalt. On most of the in-service roads it proved difficult to find a wide range of materials in a convenient location or a range of levels of skid resistance and texture depth.

Nevertheless, sufficient surfacings were available to provide a robust test of the *CEN* friction index and device calibration proposals. Initial measurements of friction and texture depth were made by the host organisations to provide a guide to the surface characteristics. Table 2.6 gives a summary description of the different test surfaces, as provided by the organisers. Illustrative friction and *MPD* values have been included in the table to show the range and combinations of levels at each trial; for convenience, the sections are grouped by host country in this table.

Table 2.6 List of the test surfacings used at the trials

Section Code*	Brief description of surfacing	Illustrative levels		Trial
		Friction (Device _{speed}) [†]	MPD [‡]	
BE1/BE08	Brushed Cement Concrete	0,60	1,7	2,1 3,2
BE2/BE09	Bituminous Concrete	0,84	1,3	
BE3/BE10	Epoxy-bound Surface Dressing	0,97	1,0	
BE4/BE11	Asphaltic Concrete	0,55 (F04 ₅₀)	0,9	
BE5/BE12	Asphaltic Concrete	0,81	1,1	
BE6/BE13	Asphaltic Concrete	0,67	0,8	
BE7/BE14	Surface Dressing	0,66	2,4	
ES1	Stone Mastic Asphalt	0,89	2,1	1,3
ES2	Stone Mastic Asphalt	0,87	2,0	
ES3	Asphaltic Concrete	0,83 (F03 ₆₀)	0,9	
ES4	Asphaltic Concrete	0,89	0,8	
ES5	Porous Asphalt	0,61	2,0	
ES6	Porous Asphalt	0,63	2,2	
FR1/FR07	Surface Dressing	0,52	0,6	2,2 3,3
FR2/FR08	Asphaltic Concrete	0,39	0,7	
FR3/FR09	Very Thin Asphalt Layer	0,69	0,9	
FR4/FR10	Smooth Epoxy	0,04 (F02 ₆₀)	0,1	
FR5	Sand-Asphalt	0,41	0,3	
FR6/FR11	Porous Asphalt	0,47	1,5	
FR12	Very Thin Layer Asphalt, Polished	0,62	0,5	
GB1	Grooved Cement Concrete	0,53	1,1	1,1
GB2	Brushed Cement Concrete	0,49	0,6	
GB3	Fine Cold Asphalt	0,63	0,5	
GB4	Polished Cement Concrete	0,46 (F13 ₅₀)	0,5	
GB5	Stone Mastic Asphalt “ENCAP”	0,69	1,5	
GB6	Thin Layer “MARS” 14mm	0,69	2,2	
GB7	Smooth Epoxy	0,08	0,2	
GB8	Hot Rolled Asphalt	0,68	1,7	
GB9	GB1 in opposite direction	0,66	1,1	3,1
GB10	GB2 in opposite direction and shorter	0,63	0,6	
GB11	As GB5	0,81 (F13 ₅₀)	1,9	
GB12	As GB6 but different line	0,79	2,4	
GB13	As GB7	0,13	0,3	
GB14	As GB8	0,83	1,7	
GB15	Epoxy Bonded Pea Shingle	0,63	1,4	
GB16	White aggregate on dense asphalt	0,80	1,1	
NL1	Stone Mastic Asphalt 0/1 New	0,67	0,9	1,2
NL2	Dense Asphaltic Concrete 0/16	0,64	0,5	
NL3	Emulsified Asphaltic Concrete	0,47 (F01 ₅₀)	0,4	
NL4	Stone Mastic Asphalt 0/11 Old	0,56	0,6	
NL5	Cement Concrete	0,56	0,6	
NL6	Dense Asphaltic Concrete 0/16	0,62	0,9	
NL7	Dense Asphaltic Concrete	0,64	0,7	2,3
NL8	Dense Asphaltic Concrete	0,54	0,6	
NL 9	Porous Asphalt	0,62 (F01 ₅₀)	1,5	
NL10	Porous Asphalt	0,69	1,9	
NL11	Brushed Cement Concrete	0,56	0,6	
NL12	Brushed Cement Concrete	0,49	0,5	
NL13	Dense Asphaltic Concrete	0,55	0,7	
* Several of the sections were used at at more than one trial: where this occurred, separate numbers are used later in the report to allow for the possible change in friction or texture over time between the two meetings.				
† The illustrative friction values are averages for the “home” device operating at its normal domestic test speed at one of the trials at which the section was used.				
‡ Illustrative MPD values are shown rounded to 1 decimal place. More precise measurements are given later in Section 2.3.				

2.1.9 Discussion of practical technical issues

Overall, the trials process ran very successfully. A high level of co-operation between the various teams, both organisers and participants, ensured that the required data were gathered. As the organisers and teams gained experience, so the processes became more efficient.

Nevertheless, as would be expected, a number of technical issues emerged and lessons were learnt that have implications if the *CEN* procedure is to be revised and implemented in practice.

2.1.9.1 Reliability and number of devices at a meeting

Most participating devices successfully attended and completed a trial in each round. However, there were some mechanical or electrical problems with the equipment that did affect some devices.

It might be expected that before attending a trial of this type, devices would be thoroughly checked and arrive in a fully working condition. There is no reason to think that this was not the case and it appeared that most of the faults actually occurred by chance at the trial meetings. The problems are summarised below here and have been taken into account in the data analysis.

- At trial 1,1, after its initial warm-up, F11 could not measure in the standard fixed-slip mode it would normally use. Although measurements were made using a wheel-lock cycle and values for 18% slip were interpolated from the friction/slip curve, these data were less reliable and not necessarily the same as true fixed-slip values.
- F07 developed a wiring problem during Trial 1,2 that put it out of action for the rest of the project.
- F06 had problems during two of the trials but it managed to complete three trials. At Trial 1,2 the device had to operate with its alternative test wheel.
- F05 had limited water flow settings and could not test at speeds over 30km/h at trial 1,2, but this was resolved for later trials. (A similar device owned by a Spanish operator was also to take part but at Trial 1,3 it failed early the testing and took no further part in that exercise or subsequent trials).
- F09 successfully completed Trials 1,1 and 2,1 but developed a serious electrical fault during the first test pass of 3,1 and was unable to gather any data on that occasion (the problem was later traced to the knock-on effect of a failed water valve causing a circuit overload).

This experience would suggest that there is always a risk that equipment will develop problems during the trials that can cause delays to the procedures or result in devices having to withdraw. Therefore, it is suggested that although the *CEN* procedure requires just three devices for a calibration meeting, it is probably better to have more in case a failure invalidates the entire trial. However, with three or four reference devices needed for a valid calibration meeting, and the possibility of other devices attending for secondary calibration, the overall number of devices to be included in any future meetings also needs to be considered.

Almost all of the *HERMES* trial meetings ran with more than the minimum of three devices attending. This was mostly due to the addition of local devices at individual trials. Practically, it was found that up to eight devices could be accommodated depending on the site.

However, the presence of more machines introduced delays in completing the required number of passes. This was most significant on the public road sites because of the time taken for each device to complete a circuit. It was also relevant on the test tracks where conflicting paths could occur, which meant that all devices would have to complete a pattern of tests before beginning the next. It is therefore recommended that for any future exercises the number of devices in any single calibration exercise should be limited to six.

2.1.9.2 Choice of trial sites and test surfaces

As anticipated the outset of the project, this proved to be one of the most difficult aspects of the whole process. The host organisations who had access to their own test tracks found it easier to plan and control the exercises, but they were constrained by the layout and availability of surfacings on their particular tracks and the sections could be shorter than ideal.

Hosts who had to use public roads had problems in finding a sufficient range of material types and skid resistance or texture levels within a practical distance of their chosen operating base. This was particularly apparent in the first trial in the Netherlands, where the range of surfacings proved to be more limited than had been first thought, and hence the need to change location for the second trial in that country. This was also a major issue in Spain where the sections proved to be very similar to one another in character.

The range of surfaces in the trial overall was good, but was limited in some individual meetings. This is likely to be the most difficult part of organising such exercises in the longer term.

2.1.9.3 Test line

It was recognised that it would be important to identify the test line clearly. Various methods were tried to define the test line. On the test tracks, adhesive tape placed at intervals on the track to mark the width of the test path was proposed. This was tried initially at *TRL* and at *Lelystad* but failed in wet conditions. The technique was more successful at *LCPC*, having been laid in warmer and dry conditions. Special reflective studs (as used for temporary lane markings during road works) were later used successfully at *TRL*.

On in-service roads it was not possible to put marks on the roads, so the organisers had to depend on natural features such as the normal wheel path or edge marking lines to act as guides to the drivers.

However, whichever method is used, the range of approaches to the position of the test wheel relative to the vehicle can cause difficulties or create potential safety hazards. Some devices use trailers with one, two or three wheels and the test wheel can be in a vehicle wheel path (some right, some left), offset or central. Others are mounted on the back of a test truck, right or left. Yet others have an inboard test wheel that can be in line with either the left or right wheel path of the vehicle. Test or towing vehicles can range from saloon cars to large trucks, which means a variety of vehicle widths. This variety caused some practical problems at different meetings, for example:

- At the UK trials, the epoxy section was deliberately laid with a narrow width to enable test devices to keep two wheels on the normal track surface. However, establishing a safe test line was problem for a device with a centrally towed test wheel. In this situation it was difficult for the driver to keep two vehicle wheels on the higher-friction surface and the test wheel on in the centre of the section. (Figure 2.9).
- In the Netherlands, the public road sites were arranged so that vehicles with a left-mounted wheel could use the hard shoulder if necessary to gain the correct line, but this created a hazard with other maintenance vehicles stopped on the shoulder, even in the coned area. Even so, some vehicles had initial difficulty in following the wheel path.
- In Belgium one of the test sections was on the hard shoulder itself, which was relatively narrow. That made it rather difficult for drivers of the left-wheeled machines both to find the correct track and to stay on the road, especially at the higher speeds.



Figure 2.9 Device F12 on the narrow epoxy section at TRL

2.1.9.4 Other practical issues

It became apparent at the first trial that there was a clear need for a dummy run to familiarise operators with the section layout in addition to any preliminary visits to see the test sections. This important principle was applied in all subsequent trials.

Another point that emerged in the first two trials was that certain devices needed to stop and set up before a test run. This had not been fully appreciated beforehand and this caused some initial concerns for following devices. This problem was most noticeable on the main road sites where devices were running at timed intervals. In this situation, a device about to make a slow run at the end of a group could be stopping to set up on site immediately ahead of a following device leading the next group at a higher speed. Once aware of this problem it could be managed, and this information was specifically sought ahead of the later trials.

A further operational issue came to light in the first trial that affected devices that use servo systems to develop a fixed *slip ratio*. Problems can occur when changing from high- or medium-friction surfacings to low- friction surfacings during a test run. The servo system applies a certain force to the brakes to control the slip on the higher-friction surface. However, that is then too great for the low-friction surface and so the control

system enters a lock-and-release cycle to re-adjust the brakes to find the correct slip. As a result, stable conditions may not be established in time to gather meaningful data.

This has possible implications for minimum test section length. The limited length of some sections also meant that locked wheel devices could perhaps only conduct one or two measurements on these sections particularly at the higher test speeds required.

2.1.9.5 Weather conditions and water build up

A concern at the beginning of the project was that significant build up of water on the surface from repeated running could mean that the effective water depth might be rather greater than the theoretical depth for each device.

The original plan for allowing a fixed interval between devices proved impractical, particularly where larger numbers of devices were involved. Careful observation of the sites suggested that there was no significant water build-up that would be likely to significantly affect the results with normal testing. Even where a longer interval was possible, such as in the Netherlands, it was found that where the test section road was not open to normal traffic, the road did not drain or dry significantly more than with the shorter test intervals. There was some evidence of slight rutting on some of the test sections, but this was not sufficient to cause significant water build-up.

Although water build-up was not a general problem when the weather was dry, this was not always the case during continuous heavy rain and at almost every meeting this proved to be a problem for some of the time. One of the sections in Spain was on a slight downhill stretch that tended to drain along the line of the road, so water from successive test vehicles tended to build up towards the end of the section. There were some concerns that the water depths were getting too great on this length, particularly when it was raining.

It was found that, generally, the issue of water build-up can be managed by suspending testing during the worst weather and by making regular close observations of the surface condition.

As well as rain, the weather conditions during the testing on the tracks were windy. A line of trees screening the side of the track meant that one of the sections on the Lelystad track suffered from noticeable leaf fall in the wind, with leaves sticking to the wet road surface (Figure 2.10). However, the frequent passage of the test devices (particularly SCRIM, with its relatively high water flow rate and heavy test wheel) kept the test line clear and the results are unlikely to have been affected.



Figure 2.10 Leaf fall on the track at Lelystadt

It is likely that calibration meetings would always need to be held in the autumn or spring, to avoid the main testing seasons for most devices. The issue of adverse weather is therefore inevitable. Experience in these trials has shown that this can be managed, but some flexibility in planning may be necessary, particularly in periods with prolonged heavy rain.

2.1.9.6 Water supply

There were some concerns over water supply. This had been anticipated and every effort was made by the local trial organisers to ensure that water was available. However, in spite of attempts to resolve these in advance, there were inevitable problems with fittings not matching. In the more remote locations, large tankers were used to supply water to the devices.

In Spain, the tanker (figure 2.11) was fed from a well. It was noticed that it had picked up some leaves and other detritus in the water, some of which was transferred to the device tanks. There were concerns that this material could impede the water flow on some machines, although there was no evidence of this occurring during the tests. It was difficult to estimate precise water requirements and the final filling on the first day drained the tank completely.

In the second Netherlands trial, the *DWW ROAR* tanker was used as a remote source. However, with three SCRIMs joining in this exercise, the demand for water and the time taken to transfer it to the test devices were rather greater than elsewhere and therefore supplementary sources had to be found, including drawing water from a nearby canal.

Clearly, the issue of water supply is one that is important to consider in planning any trial location. It may be worthwhile compiling a set of connectors that could be used to link any of the devices to local hydrants or other water sources, but this is probably impractical. It is also important to take account of local difficulties regarding water supply in countries or areas where water is limited, as illustrated by the need to use a tanker fed from a well in Spain.



Figure 2.11 Tanker used for remote water supply in Trial 1,3

2.1.9.7 Device selection

The selection of devices for the *HERMES* experiment was simplified by limiting the number that were involved and because the procedures were being followed for a known period.

In future, calibrations being carried out on a regular basis, this aspect of planning will require careful attention. In particular, it will be important to avoid developing sub-sets of devices that meet together frequently. This could happen because operators may be reluctant to travel too far for calibration exercises and therefore geographical groups could emerge. Provision will also need to be made for the inclusion of devices for secondary calibration. It is recommended that for the full operation of the *CEN* procedures, the co-ordination of trial meetings and the allocation of devices to them should be the responsibility of a single overseeing body.

2.2 Non-technical issues

2.2.1 Use of questionnaires

Task 2.2 was included in the project specifically to address those aspects of organising and carrying out the trials that do not directly affect the technical or practical running of the exercises but are nevertheless important in the overall scheme of the harmonised calibration procedure. These would include issues such as the logistics of getting the devices together, traffic management and other safety aspects and the costs of the exercises.

At each trial, a member of the Steering Group (or a representative) was present to observe the operation of the trial and to take note of any non-technical issues that arose. The non-technical assessor was provided with a checklist to assist in this. In addition, questionnaires were used to gauge the opinions of the operating crews and operating organisations regarding their experience in attending the trials, and of the trial hosts regarding the organising of their particular exercises.

The information gathered in this way from the early trials was used to advise the organisers on ways of improving the later trials in the programme. Some of the important issues that emerged are discussed in sections 2.2.2, 2.2.3 and 2.2.4. The commitment and co-operation of the device crews were of considerable value in the success of the experimental programme. The experience that they gained contributed particularly to the smooth running of the later trials as they become more familiar with the processes involved, even though they may have been visiting new sites. This experience could also be of some value in any future calibration exercises where these teams are involved. Overall, the information from the questionnaires and the experience gained were used to prepare the advice regarding organising the trials to be included in the separate Guidelines developed as part of this task as a stand-alone document.

2.2.1.1 Questionnaire for participants

This questionnaire was designed to enable the crew and operating organisation of each device to record their impressions of each trial that they attended. Apart from standard information to identify the particular trial, the device and contact details, the participants were asked to provide some outline information on the costs to them of joining the

exercise and to comment on various aspects of the trial, either by ranking them on a scale or by adding their own remarks.

The main questions asked (shown here as bullet points for brevity) were as follows:

- What were your approximate costs in attending the calibration exercise? (These were broken down by staff time, travel and accommodation costs).
- Did the participation in the calibration exercise have any influence on your routine test programme in your country?
- What time period of the year is the most suitable for your organisation to participate in this type exercise, should future exercises be conducted?
- Did you have sufficient time to prepare your participation in the exercise?
- Did you have to make any special arrangement or changes to your device in order to be able to travel through foreign countries to reach the place for the exercise?
- What did you think of the traffic management on the sites?
- How was the access to the site?
- How did you find the safety of following the required test lines?
- How did you find the safety of test speeds at the test sites?
- Were you asked to carry any action you consider unsafe while testing?
- How do you rate the organisation of the test runs?
- How do you rate the clarity of instructions for the tests?
- How do you rate the completeness of the instructions?
- Did you meet any language problems while testing?
- How do you rate the marshalling throughout the tests?
- How do you rate the signing on the test sites?
- How do you rate the communication during the tests?
- How do you rate the assistance from the organisers?
- How was the assistance from other teams?
- How do you rate the quality of the initial instructions?
- How was the information for travel between the sites?
- How was the timing of the exercise?

2.2.1.2 Checklist for the non-technical assessor

The checklist that was provided for the non-technical assessor stressed that the assessor should “observe” and not interfere with the running of the trial (the Task Leader or his representative liaised with the organisers if it was felt that something should be changed). The questions addressed all the issues (except costs) covered in the participants’ questionnaire but also included more specific comments or observations on aspects that individual crews might not be in a position to notice, such as:

- The test section surfacing, etc.
- Whether there were any conflicts between testing vehicles.
- Accommodation.
- Whether test lines were followed properly.
- Any build-up of water on the test sections.
- Whether texture measurements were completed (on dry road).

2.2.1.3 Questionnaire for the host organisers

This much shorter form addressed issues specific to the organising of the local trial. As with the participants, the organisers were asked for an estimate of their costs, in terms of cash and staff time, in hosting the calibration exercise. They were also asked to comment specifically on:

- The site selection process.
- The planning of the trial runs.
- Whether the sites meet the requirements of the *prEN* and if not, whether non-technical problems were the reason.
- Any problems relating to use of foreign devices.
- Their perception of the performance of the teams.

The organisers were also asked whether they had been able to perform *MPD* texture measurements according to the *ISO* standard, and to describe any logistics (such as arranging hotels and transportation) that they had carried out.

2.2.2 Logistics

2.2.2.1 Local co-ordination

The individual trials were co-ordinated by a host country representative from the Steering Group. In the UK, the trials were hosted and organised by a team from *TRL*; in the Netherlands by *DWW*, in France by *LCPC* and in Spain by *CEDEX*. In Belgium, the local organisation was carried out by *MET* working with advice from *BRRC*.

The difficulties with the organisation depended largely on the type of site that the host intended to use. *TRL* and *LCPC*, for example, were able to use their own test tracks and this greatly simplified the arrangements because all the work took place on one site that was under the host's control. A disadvantage of this approach was that the operations were constrained by the layout of the particular test sections on the tracks and in some cases it was difficult to meet all the requirements of the standard. However, these problems were offset by the ease with which the test runs could be controlled.

The tests on public roads introduced additional problems, mostly relating to the time taken to carry out the tests as a result of the greater distances involved travelling along a site and then returning to the start for a replicate run. In some cases, where teams had to return to a central control point between passes, there was a time penalty as a result of having to leave the main road. Conversely, it was more difficult to maintain contact with the teams, especially those who were having problems, where they were not returning to a central point between passes. As experience developed over the groups of trials, this process improved so that marshals were stationed at contact points that were directly on, or very close to, the route to be followed.

The use of a private test track for some sections for the first trial in the Netherlands was of mixed success in that it provided a degree of control and some test efficiency, but constraints placed upon the operation by the track authorities caused some potential difficulties, such as water supply and ease of movement on and off the track.

Another aspect of local co-ordination that involved considerable work on the part of the hosts was the arrangement of accommodation for the teams. In some places a centrally located (compared with the test sites) hotel was used and in others the teams were dispersed among a number of local hotels. This then involved provision of overnight parking for the larger test vehicles and local transport to get teams to and from their hotels. This will always be an issue for organisers and can only be dealt with in a localised way. Overall, however, there were no significant problems for the test programmes from this.

The timing of the tests and the provision of meal breaks and rest facilities was a problem on some sites, particularly those using public roads where the working sites were some distance from the rest area. In some cases, the time taken to complete a pattern of tests proved longer than anticipated and this had a knock-on effect on the timing, resulting in fewer tests than planned being completed.

2.2.2.2 Travel to and from the trial Locations

Generally, there were no major problems in getting the devices to or from the main trial locations. However, for those teams that needed to use ferries (to/from the UK for instance, or from Norway/Denmark) there were additional time constraints. This could mean that participant crews had significant downtime before or after the trial where ferries were infrequent. Conversely, some teams were short of time because they found that in the event the test site was actually some distance from the publicised “location” and they were much further from their embarkation point than had been anticipated.

This indicates that as much advance information as possible should be provided. However, in some cases the forward plans had to be made before the location of sites was finalised. Although the participants knew in advance that they might be needed for an extra “contingency” day, those that needed to book ferries usually, and understandably, chose the earliest possible.

In some cases some effort was required by both the participants and the local co-ordinator in order to gain permissions from the appropriate authorities for some of the devices to operate outside their own country’s borders. Some of the potential problems of getting to what might have been perceived as the more difficult locations were avoided simply by participants declining to attend trials in those countries.

Another issue affecting longer-distance travel that had not been considered in advance but that affected some teams, was the constraint in some countries that prevents heavy goods vehicles travelling on Sundays.

All of these points emphasise that any future calibration system will need to have a number of centres, positioned such that devices can reach them comparatively easily. This does, however, have implications for the *EFI* which depends on the calibration meetings being managed to involve different combinations of devices wherever possible: there might be a trend for certain devices to “favour” particular locations and so create local sub-sets of devices.

2.2.2.3 Travel between test sites

In the countries where some or all of the test sites were located on public roads, the test sites were usually in groups at two or three different locations, sometimes many kilometres apart and not always close to the central hotel where the teams were staying. This also imposed a time penalty in collecting the devices together and then driving in convoy to the new location.

Experience showed that keeping to a convoy over long distances (especially where the driver of the lead vehicle did not appreciate that some of the test devices could not or were not permitted to run at car speeds) was difficult and placed added strain on the crews. Provision of good maps and clear instructions will be important if this situation is likely to occur in future.

2.2.3 Safety issues

Some specific safety issues have already been discussed in Section 2.1.9.3. This Section discusses some more general matters that emerged during the trials.

2.2.3.1 Traffic management

Traffic control on the tests tracks owned by the hosts was generally straightforward to arrange, with test vehicles generally circulating in one direction. The problem of some devices needing to stop and set up (Section 2.1.9.4) was catered for in the later trials by specifically asking participants to tell the organisers in advance that this was necessary.

The management of the public-road sites varied from full formal lane closures on motorways and main roads through local organiser's staff directing traffic or no control at all on quiet rural routes.

Some other potential safety risks were identified that should be taken into account in future planning, for example:

- Limitations of higher-speed testing in a closed lane alongside slower-moving traffic.
- Risk of live traffic following test vehicles into the closed lane.
- Risk of traffic management or organisers' vehicles being parked in or very close to the test lane.
- Lightweight cones being flicked by passing traffic into the test lane.
- Difficulty with test teams immediately communicating with marshals to resolve these kinds of issues.

Another consequence of the need for traffic management was that of serious delay to the programme when the management was not in place in time for the scheduled start of the test programme. In one case, there were delays to the test teams because the devices had to join the traffic queue created by the closure in order to get to it or to get back to the control point. These effects combined to reduce the test programme to three replicates only in one of the exercises.

2.2.3.2 Positioning of test sections

Although the test tracks were generally easier to manage, there were safety issues, particularly relating to the higher-speed tests, as a result of the positioning of test sections, either near the edge of the track (affecting right- or left-side test wheels) or close to run-out points. The organisers generally had little control over where the sections were (because in most cases they were already in existence).

Allowance had been made for the potential risks by the organisers, but in the event, there were some concerns expressed by team members that needed attention for subsequent visits, for example, Trial 1,1 at *TRL*, where it was necessary to brake and steer into a curve immediately after a test section. At Lelystad the test runs were interspersed with other users of adjacent lanes of the track.

The positioning of test sections on the carriageway or hard shoulder on the public roads has already been mentioned (Section 2.1.9.3). There was a further safety issue relating to traffic management at one location, where the test vehicles entered a closure protecting the hard shoulder, but then had to leave it and rejoin traffic and cross straight over an exit road. There was a risk of potential conflicts here particularly in the higher-speed test runs where there was no opportunity to reduce speed after the test section before crossing the live lanes and then to regain speed for the subsequent section.

2.2.4 Financial aspects

Clearly, if the proposed calibration system for *EFI* is to be taken up in the longer term, then the relative costs of the exercise should be considered. This section summarises in broad terms the costs indicated by the various hosts and the participants.

2.2.4.1 Costs of organising individual trials

The costs of organising the trials varied considerably from country to country and the make-up of the costs also varied, depending upon whether public roads, private test tracks or host's test tracks were to be used.

On test tracks, there was no need to fund traffic management on the highway, but usually there was a charge for the use of the facility of the test track that had to be borne by the project. The staff involvement also varied, with the number of marshals needed being different in different locations.

Broadly, arranging and running a calibration meeting involved general costs in the range 3 000 to 5 000 euros and around 150-200 hours of staff time.

2.2.4.2 Costs to participants

The costs to the participants (which were not part of the main project budget and were funded separately by the various *FEHRL* members involved) comprised two main components – travel to and from the trial location and time spent at the trial itself. As with the organisation of the trials, there was a wide range. Clearly, costs were lowest for participants from the host countries because they were usually based at or relatively near the test location, although in some cases they also travelled and stayed with the other teams during the trial. As expected, costs were usually highest for those with some distance to travel, especially where sea crossings were involved.

Typically, the costs of attending a calibration meeting were in the range 1 500 to 2 000 euros for devices with short distances to travel, such as those based in the host country or close to the borders of a neighbouring country, or 2 000 to 5 000 euros for devices with significant distances to travel or if ferries were involved.

The staff time could vary from 50 to 150 hours depending upon the travelling time and how many people were in the crew (typically two). These hours could also include some time for preparation, post-processing of data, booking ferries and other administrative tasks associated with attending the trial.

There were also additional, perhaps hidden, costs (such as hire charges for the test devices or loss of revenue-earning work) that varied widely and cannot be included easily in general estimates such as these.

2.3 Summary of the harmonisation process

2.3.1 Calculation of the *IFI* using the *PIARC*-model

As explained earlier, the first attempt to harmonise skid resistance measurements was the *IFI* (International Friction Index), developed as part of the 1992 *PIARC* experiment. The *IFI* uses two parameters: F_{60} (the common friction value at a slip speed of 60 km/h) and S_p (the speed constant, which is based on a texture measurement). Using these two parameters, a friction value can be predicted for any device at any test speed using a process described here as the “*PIARC*-model”.

Equations 2.1 – 2.4 show how the calculation is performed. Given a skid resistance measurement F , made with a certain device at a slip speed S and a texture measurement T_x , the following steps have to be carried out to calculate the *IFI*:

- transform the measurement result at a slip speed S to a friction value at a slip speed of 60 km/h;
- apply a correction for the specific device, to give a device-independent friction value at a slip speed of 60 km/h.

The transformation to a slip speed of 60 km/h, is done using equation 2.1.

$$F(60) = F(S) \cdot e^{\frac{S-60}{S_0}} \quad (2.1)$$

in which

$$S = \frac{\% \text{ slip}}{100} \cdot V \quad (2.2)$$

where V = the speed of the device and

$$S_0 = a + b \cdot T_x \quad (2.3)$$

From equation 2.3 it can be seen that the texture measurement is used for the speed correction. The parameters “ a ” and “ b ” in this equation are specific to the device used for the texture measurements.

The correction from the calculated value for the specific device ($F(60)$) at the reference speed of 60 km/h to a device-independent general value at the reference speed (F_{60}) is achieved by linear regression (equation 2.4):

$$F_{60} = A + B \cdot F(60) + C \cdot T_x \quad (2.4)$$

where “ A ”, “ B ” and “ C ” are device specific parameters for the friction measuring device. Parameter “ C ” is set to zero for devices using a smooth (blank) tyre.

In principle, when the *IFI* parameters F_{60} and S_0 are known, the friction value of a road surface at any other slip speed can be predicted. The intention of the *IFI* was to allow an easy comparison of measurements made with different skid testers through their conversion to a common scale.

2.3.2 From *IFI* to *EFI*

The Belgian research project used the *PIARC* experiment database together with additional data to optimise the parameters in the *IFI* definition and to focus more on the results of the devices operated in Europe. This included recalculating texture depth values in accordance with the new *ISO*-standard for the calculation of the Mean Profile Depth (*MPD*) [4]. (Throughout this report, the term *MPD* refers to values calculated following this standard). A second objective of the Belgian work was to extend the validation of the *IFI* to road surfaces that were either not included or insufficiently represented in the *PIARC* experiment and to this end additional test measurements were made on these surface types with devices used in Belgium. The final goal was to make a proposal for calibration of skid resistance and texture devices based on the revised index that would prevent devices drifting away from the common standard (which might occur over time).

This work led to the definition of what had become known as the European Friction Index. An important difference between the *IFI* and the *EFI* is that *EFI*, as well as being calibrated to devices used in Europe, uses a reference slip speed of 30 km/h rather than 80km/h. In that respect, it had been shown that a reference speed of 30 km/h instead of 60 km/h was better adapted to the fleet of European devices. The results of the Belgian work were incorporated into an informative annex to the draft *CEN* standard for the determination of skid resistance of a pavement surface (*prEN* 13036-2) [3]. It is the calibration procedures in this document that are being assessed by the *HERMES* project⁵.

2.3.3 Determination of the *EFI*

EFI is defined as:

$$EFI = A + B \cdot F_{30} \quad (2.5)$$

in which

$$F_{30} = F \cdot e^{(S-30)/S_0} \quad (2.6)$$

giving the general equation

$$EFI = A + B \cdot F \cdot e^{\frac{S-30}{S_0}} \quad (2.7)$$

Here, F_{30} is the measured friction coefficient, F , brought to the 30km/h reference slip speed using the predicted value of S_0 given by equation (2.8).

$$S_0 = a + b \cdot MPD \quad (2.8)$$

⁵ As explained previously, the Draft *prEN*-13036-2 [3], proposes the term Skid Resistance Index (*SRI*) to describe the harmonised scale, instead of European Friction Index (*EFI*). However, because *EFI* has been used in several previous publications, and in order to avoid confusion in readers' minds, *EFI* is also used in this report. A change to using the term *SRI* may be eventually necessary if the *prEN* retains that terminology and when it is used as a standard.

In practice, “A” and “B” are parameters specific to the friction measuring device used. The coefficients “a” and “b” of the original *PIARC*-model have been replaced by fixed values, either for a laser texture measurement (*MPD*) or a patch test (*MTD*), as in equations (2.8) and (2.9):

$$S_0 = 57 + 56 \cdot MPD \quad (2.9)$$

or

$$S_0 = 43 + 70 \cdot MTD \quad (2.10)$$

It should be noted that, with these formulae, S_0 is only an estimate of the real speed constant for different sections. Further, as will be seen later, by using these equations, an initial source of inaccuracy might be introduced into the calculations, depending on how well the real speed constant is estimated by the general formula.

2.3.4 The calibration procedure

In the draft *CEN*-standard, initial “A” and “B” values are given for the so-called “reference devices” that were in the original *PIARC* experiment. It is necessary to check that these “A” and “B” values for the reference devices remain stable over time. This is achieved by a periodic calibration of subsets of reference devices. In this “Type-1 calibration procedure”, as it is known, new values for “A” and “B” are calculated for the reference devices.

The calibration procedure also provides for the inclusion of “new” devices. This is achieved by means of a “Type-2 calibration” in which a new device runs alongside existing reference devices and initial “A” and “B” values are calculated for the new device. Once this has happened for a device, it joins the set of reference devices and will be included in a Type-1 calibration in the next round.

The calibration friction tests in any particular meeting are carried out on a range of surfaces (usually at least six) for which *MPD* has been measured. Friction tests are performed at least three times at each of three operating speeds. The speeds must include the speed that is standard for the device when operating in its own country and two others so that the range from 30 to 90 km/h is covered.

If a device needs to apply corrections to the results (for temperature for example), these should be made according to the standard procedure for that device and only the corrected results should be reported and used in the subsequent calculations. Speed corrections, of course, should not be made. The data from these measurements are then used in a series of calculations as follows.

Initially, value of *EFI* is calculated for each individual measurement using equations (2.7) and either (2.9) or (2.10), depending on the texture measurement method. Through most of the analyses in this report, equation (2.9) is used since the texture measurements in the various exercises determined *MPD*. The values for *A* and *B* used are those established for the device from the previous calibration exercise. In the case of the first trial where a “reference” device takes part, these would be the appropriate value provided in the draft standard.

Having calculated the individual EFI values, the next step is to apply tests to the data to check for outlying tests and devices. For each device (i) and for each surface (j), calculate the average of the r measured values (normally, $r=9$ for three runs each three speeds) of the EFI , which yields EFI_{ij} ($i=1,\dots,N$; $j=1,\dots,n$). N is the total number of friction devices taking part in the calibration exercise and n is the total number of surfaces used.

The standard deviation s_{ij} of each measurement series is calculated by means of the following equation:

$$s_{ij} = \sqrt{\sum_m \frac{(EFI_{ij} - EFI_{mij})^2}{r-1}} \quad (2.11)$$

where m is the run number ($m=1,\dots,r$).

If $s_{ij} > 0,04$, the measurement which has the largest deviation from the mean is discarded and the average is calculated again to give EFI_{ij} and s_{ij} with $m=1,\dots,r-1$. If, again, $s_{ij} > 0,04$, the whole measurement series of device (i) on surface (j) should be discarded.

For each surface, the “Grand Average” EFI_j of the N_R average values of EFI reported by the “reference devices” only should be calculated. (In later sections of the report the form “ $\langle\langle EFI \rangle\rangle$ ” is also used as shorthand to represent the grand average of all the reference device EFI values.)

For each device, the linear regression of EFI_j versus EFI_{mij} is calculated by the least squares method, which gives

$$EFI_j = a_i + b_i \cdot EFI_{mij} \quad , \text{ with } i = 1,\dots,N \quad (2.12)$$

The residual standard deviations with respect to the regression lines, s_i , are then calculated using the following formula:

$$s_i = \sqrt{\sum_m \sum_j \frac{(EFI_j - a_i - b_i \cdot EFI_{mij})^2}{(r \cdot n - 2)}} \quad (2.13)$$

If $s_i > 0,07$, device (i) should repeat the whole series of measurements after having taken steps to fix the problem with the device.

Having established that the devices have provided valid results following the calibration exercise, new values for “A” and “B” are determined. To do this for each device (i), the value for EFI_{mij} in equation (2.12) is replaced by its expression using the old values, i.e.:

$$EFI_j = a_i + b_i \cdot (A_{i,old} + B_{i,old} \cdot F_{30}) \quad \text{with } i = 1,\dots,N \quad (2.14)$$

and hence,

$$A_{i,new} = a_i + b_i \cdot A_{i,old} \quad (2.15)$$

$$B_{i,new} = b_i \cdot B_{i,old} \quad (2.16)$$

It would normally be expected that, assuming that the equipment is unchanged, changes in these parameters would be small. Clearly, if large differences appear between the old and the new values, the device should be checked to verify that it is producing proper friction values. It is also important that a device is maintained and calibrated according to the instructions of the manufacturer and should be in proper working order before it is sent to a calibration exercise. When a device that is not working properly is sent to a calibration exercise, it could introduce a problem for other devices because the *EFI* is based on the grand average of all the measurements in a calibration exercise.

2.4 Experimental results

2.4.1 Introduction

This section presents the results of the measurements carried out in the nine calibration trials. It also includes an initial analysis of the data following the process set out in the *CEN* draft standard and explained in 2.3.4 above.

2.4.2 Characteristics of the test surfaces

As Table 2.7 shows, the test sections covered a wide range of types of surfaces including dense materials, porous surface courses and open-textured thin layers, as well as different binders (such as asphalt, cement or epoxy resin).

Table 2.7 Tested surface types and Mean Profile Depths in mm.

Code	Type	MPD	Code	Type	MPD
BE01	Brushed Cement Concrete	1,69	GB01	Grooved Cement Concrete	1,09
BE02	Asphalt Concrete	1,31	GB02	Brushed Cement Concrete	0,57
BE03	Epoxy-Bound Surface Dressing	1,03	GB03	Fine Cold Asphalt	0,48
BE04	Asphalt Concrete	0,89	GB04	Polished Cement Concrete	0,54
BE05	Asphalt Concrete	1,13	GB05	Stone Mastic Asphalt "Encap"	1,54
BE06	Asphalt Concrete	0,79	GB06	Thin Layer "Mars" 14 Mm	2,23
BE07	Surface Dressing	2,42	GB07	Epoxy	0,19
BE08	Brushed Cement Concrete	1,71	GB08	Hot Rolled Asphalt	1,66
BE09	Asphalt Concrete	1,60	GB09	Grooved Cement Concrete	1,06
BE10	Epoxy-Bound Surface Dressing	0,98	GB10	Brushed Cement Concrete	0,62
BE11	Asphalt Concrete	0,90	GB11	Stone Mastic Asphalt "Encap"	1,85
BE12	Asphalt Concrete	1,00	GB12	As GB06 But Different Line	2,41
BE13	Asphalt Concrete	0,94	GB13	Epoxy	0,25
BE14	Surface Dressing	3,03	GB14	Hot Rolled Asphalt	1,73
ES01	Stone Mastic Asphalt	2,13	GB15	Epoxy Bonded Pea Shingle	1,43
ES02	Stone Mastic Asphalt	1,99	GB16	White Aggregate on Dense Asphalt Concrete	0,86
ES03	Asphalt Concrete	0,92	NL01	Stone Mastic Asphalt 0/11 (new)	0,86
ES04	Asphalt Concrete	0,79	NL02	Dense Asphalt Concrete 0/16	0,52

Code	Type	MPD	Code	Type	MPD
ES05	Porous Asphalt	2,02	NL03	Emulsified Asphalt Concrete	0,36
ES06	Porous Asphalt	2,23	NL04	Stone Mastic Asphalt 0/11 (old)	0,56
FR01	Surface Dressing	0,57	NL05	Cement Concrete	0,62
FR02	Asphalt Concrete	0,73	NL06	Dense Asphalt Concrete 0/16	0,91
FR03	Very Thin Asphalt Concrete	0,90	NL07	Dense Asphalt Concrete	0,66
FR04	Epoxy	0,09	NL08	Dense Asphalt Concrete	0,62
FR05	Sand Asphalt	0,34	NL09	Porous Asphalt	1,76
FR06	Porous Asphalt	1,54	NL10	Porous Asphalt	1,87
FR07	Epoxy-bound Surface Dressing	0,76	NL11	Brushed Cement Concrete	0,55
FR08	Asphalt Concrete	0,84	NL12	Brushed Cement Concrete	0,47
FR09	Very Thin Asphalt Layer	1,13	NL13	Dense Asphalt Concrete	0,70
FR10	Epoxy	0,16			
FR11	Porous Asphalt	1,78			
FR12	Very Thin Asphalt Layer. Polished	0,54			

The texture depths (measured as *MPD*) ranged from 0,09 to 3,03 mm. Two sections (FR04/FR10 and GB07/GB13) were made from epoxy resin, both having an extremely smooth surface. When more than one texture measuring device was used on a section (see Section 2.3.3), the average of the reported values has been given in Table 2.7.

2.4.3 Texture measurements

Texture measurements with the participating devices were carried out on each test surface at the start of the first day of friction testing. The device crews were asked to report the Mean Profile Depth averaged over the whole length of the section. At some trials, more than one texture profiler was used and this has provided an opportunity to evaluate the reproducibility of the measurement of *MPD* by different devices claimed to comply with ISO 13473-1 [4]. Table 2.8 lists the values reported by each individual device on each section.

Table 2.9 provides some statistics derived from the data in Table 2.8. The standard deviation (s_R) of reproducibility between pairs of devices (1 & 2) has been calculated using the following formula:

$$s_R = \sqrt{\frac{1}{2n} \sum_i^n (MPD_{1i} - MPD_{2i})^2} \quad (2.17)$$

where subscript *i* denotes the tested surface. Its overall value is 0,11 mm.

The linear regressions between pairs of devices, illustrated in Figures 2.12 to 2.20, have been calculated with the intercept forced to zero. The reason for this is that when doing so, the intercepts are generally of the order of the deviations from the regression line, which means that they are not significant. The resulting slope (*a*) is generally close to unity as expected. Its estimated relative standard deviation (s_a) is 4,7% on an average.

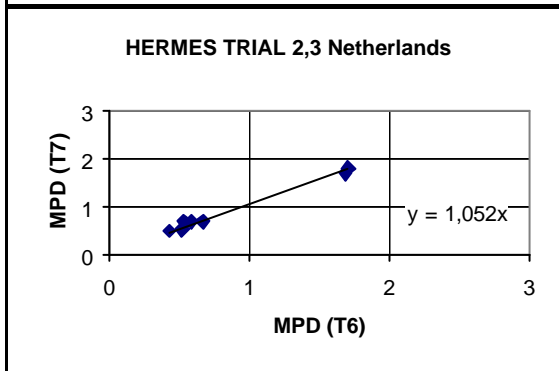
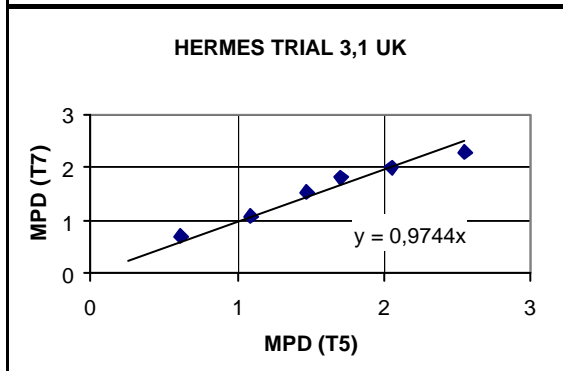
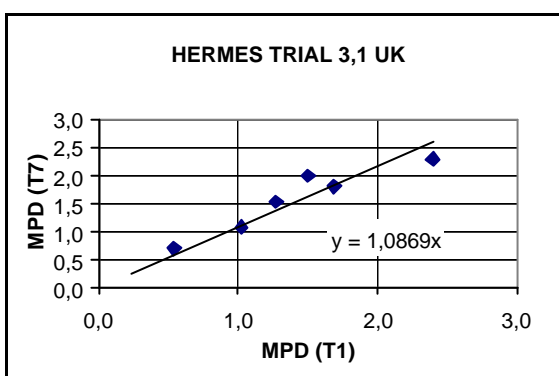
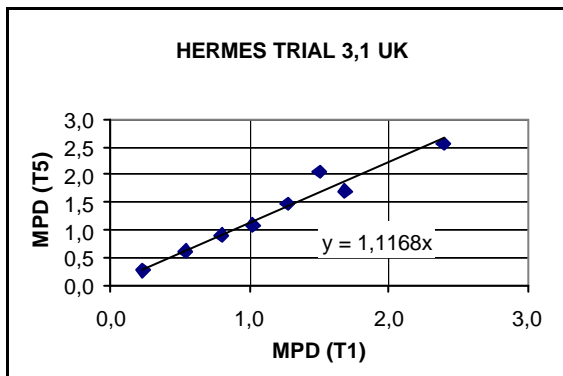
In the subsequent analyses, the average reported values of *MPD* (as in Table 2.7) have been used.

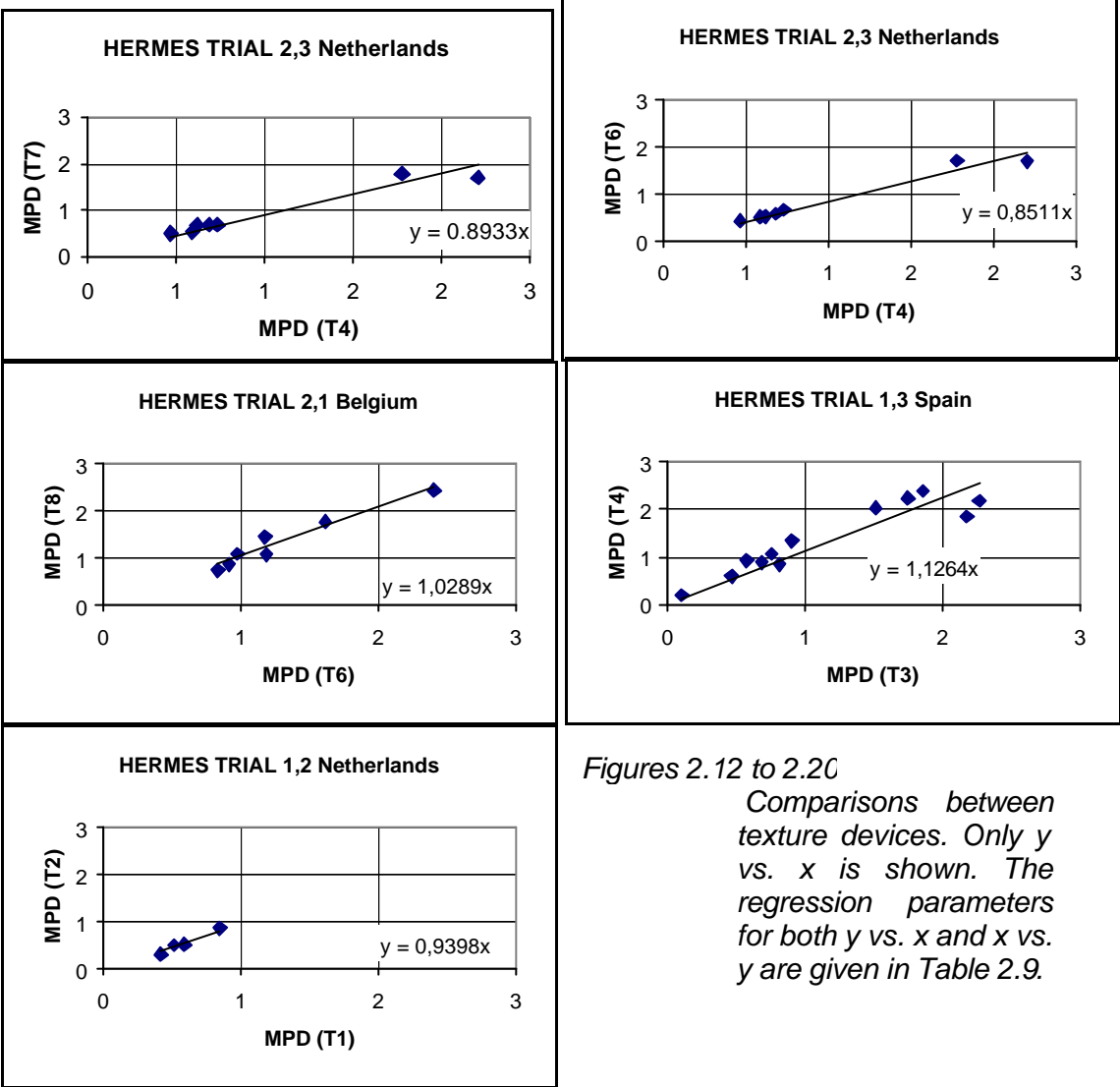
Table 2.8 Comparison of MPD(mm) values reported by different texture devices on a given section.

Section		Texture device							
Code	Type	T1	T2	T3	T4	T5	T6	T7	T8
BE01	Brushed cement concrete						1,62		1,76
BE02	Dense asphalt concrete						1,18		1,44
BE03	Epoxy-bound surface dressing						0,98		1,08
BE04	Dense asphalt concrete						0,92		0,86
BE05	Dense asphalt concrete						1,19		1,07
BE06	Dense asphalt concrete						0,84		0,74
BE07	Surface dressing						2,41		2,43
ES01	SMA			1,86	2,39				
ES02	SMA			1,75	2,23				
ES03	Dense asphalt concrete			0,76	1,07				
ES04	Dense asphalt concrete			0,69	0,89				
ES05	Porous asphalt			2,18	1,86				
ES06	Porous asphalt			2,27	2,19				
FR07	Surface dressing			0,58	0,93				
FR08	Dense asphalt concrete			0,82	0,85				
FR09	Very thin asphalt layer			0,91	1,34				
FR10	Epoxy			0,11	0,20				
FR11	Porous asphalt			1,52	2,03				
FR12	Very thin asphalt layer. Polished			0,47	0,60				
NL01	SMA 1 year old	0,85	0,86						
NL02	Dense asphalt concrete 0/16	0,52	0,51						
NL03	EAB Emulsified A Concrete	0,42	0,30						
NL04	SMA 0/11 Old	0,60	0,52						
NL07	Dense asphalt concrete				0,69		0,59	0,70	
NL08	Dense asphalt concrete				0,62		0,54	0,70	
NL09	Porous Asphalt				1,78		1,71	1,80	
NL10	Porous Asphalt				2,21		1,69	1,70	
NL11	Brushed cement concrete				0,59		0,52	0,53	
NL12	Brushed cement concrete				0,47		0,43	0,51	
NL13	Dense asphalt concrete				0,73		0,67	0,70	
GB09	Grooved concrete	1,02				1,09		1,08	
GB10	Brushed concrete	0,54				0,62		0,70	
GB11	SMA "ENCAP"	1,50				2,05		2,00	
GB12	Thin layer "MARS" 14 mm	2,40				2,55		2,29	
GB13	Epoxy	0,24				0,26			
GB14	HRA	1,68				1,71		1,82	
GB15	Bonded Pea Shingle	1,27				1,47		1,53	
GB16	White Stone Asphalt	0,80				0,91			

Table 2.9 Statistical comparison between MPD values reported by different devices (n: number of measurements; σ_R : standard deviation of reproducibility; a: slope of the linear regression of y vs. x; σ_a : estimated relative standard deviation of the slope)

Trial	x	y	n	a	σ_a	σ_R
1,2	T1	T2	4	0,940	5,7%	0,05
1,2	T2	T1	4	1,053	6,4%	
1,3 & 3,3	T3	T4	12	1,126	6,5%	0,24
1,3 & 3,3	T4	T3	12	0,857	4,9%	
2,1	T6	T8	7	1,029	3,7%	0,09
2,1	T8	T6	7	0,964	3,5%	
2,3	T4	T6	7	0,851	3,6%	0,15
2,3	T6	T4	7	1,162	4,9%	
2,3	T6	T7	7	1,052	2,8%	0,06
2,3	T7	T6	7	0,947	2,5%	
2,3	T4	T7	7	0,893	5,1%	0,14
2,3	T7	T4	7	1,098	6,3%	
3,1	T1	T5	8	1,117	4,3%	0,16
3,1	T5	T1	8	0,886	3,4%	
3,1	T5	T7	6	0,974	3,0%	0,09
3,1	T7	T5	6	1,021	3,2%	
3,1	T1	T7	6	1,087	6,3%	0,18
3,1	T7	T1	6	0,905	5,2%	
Average :					4,7%	0,11





Figures 2.12 to 2.20
Comparisons between texture devices. Only y vs. x is shown. The regression parameters for both y vs. x and x vs. y are given in Table 2.9.

2.4.4 Friction device-specific parameters

Table 2.10 lists the participating devices, together with the initial values ($A = A_0$ and $B = B_0$) of their specific parameters to be used in the calculation of EFI (Section 2.4.10). The values are derived from the *PIARC* International Experiment 1992 database but restricted to the devices in use in Europe [2]. The shading denotes devices that did not participate in the *PIARC* experiment and so were not initially regarded as reference devices. Their initial parameters were set to $A_0 = 0$ and $B_0 = 1$.

Device F09 did not participate in the experiment itself, but it is identical to one that did and so has been treated as a reference device at this stage. Although device F08 did actually participate in the *PIARC* experiment, it is not regarded as a reference device here because the test wheel yaw angle was changed from 15° to 20° in the period between the *PIARC* experiment and the *HERMES* trials.

Table 2.10 List of friction devices along with their initial specific parameters

Friction device		Lab, Country	Tyre	Measurement Principle	Slip Ratio	A ₀	B ₀
Code	Name						
F01	DWW Trailer	DWW, NL	PIARC Blank	BFC	0,86	0,100	0,751
F02	ADHERA	LCPC, FR	PIARC Blank	BFC	1,00	0,203	0,700
F03	SCRIM	CEDEX, ES	AVON Blank	SFC	0,34	0,115	0,815
F04	SCRIM	MET, BE	AVON Blank	SFC	0,34	0,006	0,992
F05	GripTester	MET, BE	Findley-Irvine Blank	BFC	0,15	0,190	0,779
F06	ROAR	DRI, DK	ASTME1551 Blank	BFC	0,20	0,000	1,000
F07	ROAR	DWW, NL	ASTME1551 Blank	BFC	0,86	0,000	1,000
F08	Odoliograph	BRRC, BE	PIARC Blank	SFC	0,34	0,000	1,000
F09	PFT	TRL, GB	ASTME524 Blank	BFC	1,00	0,264	0,574
F10	OSCAR	NRRL, NO	ASTME524 Blank	BFC	0,18	0,000	1,000
F11	ROAR Mk2	NRRL, NO	ASTME1551 Blank	BFC	0,18	0,000	1,000
F12	SRT-3	IBDIM, PL	Patterned	BFC	1,00	0,104	0,886
F13	SCRIM	TRL, GB	AVON Blank	SFC	0,34	0,006	0,992
F14	Odoliograph	MET, BE	PIARC Blank	SFC	0,34	0,291	0,514
F15	IMAG	STBA, FR	PIARC Blank	BFC	0,15	0,000	1,000

2.4.5 The database collected

In total, 4 231 measurements were made. The following data were discarded:

- Device F05 in Trial 1,2 because the device made measurements at only one speed.
- Device F11 in Trial 1,1 because the device did not operate at a fixed *slip ratio*.

This left 4 084 measurements to take forward to the analysis. Table 2.11 gives the number of measurements, broken down by device and by trial.

2.4.6 Repeatability of F

The repeatability standard deviation of the friction coefficient, F , reported from repeated runs by a given device at a given speed on a given surface was calculated. No correction was made for actual speeds being slightly different between repeated runs as those deviations from the specified speed must be considered as one of the factors affecting repeatability of the measurement in this context.

It was found that, in the event, the speed variations were generally rather small, as can be seen in Annex B. Table 2.12 gives the average values of repeatability of F for each device at each trial along with the averages per trial over all devices and the averages per device over all trials and finally the grand average over the whole measurement campaign. i.e. $\sigma_r(F) = 0,025$.

Table 2.11 Number of measurements carried out per device and per trial

Trial® Device -	1,1	1,2	1,3	2,1	2,2	2,3	3,1	3,2	3,3	Total
F01		90	90	81		75	120			456
F02			90		90				90	270
F03			90			75			90	255
F04		90		87		75		57	90	399
F05				80	90			87	90	347
F06		66		76			120			262
F07		70								70
F08			90		90			85		265
F09	103			78						181
F10	115			77					90	282
F11						73			89	162
F12	120				90				90	300
F13	120					75	120	84		399
F14				87				86		173
F15					90	75		98		263
Total	458	316	360	566	450	448	360	497	629	4084

Table 2.12 Repeatability of F for each device at each trial. Averages are weighted according to the number of measurements from Table 2.11.

Trial® Device -	1,1	1,2	1,3	2,1	2,2	2,3	3,1	3,2	3,3	Average
F01		0,011	0,015	0,017		0,018	0,018			0,016
F02			0,018		0,020				0,017	0,018
F03			0,030			0,032			0,023	0,028
F04		0,061		0,022		0,029		0,013	0,020	0,035
F05				0,025	0,035			0,033	0,025	0,030
F06		0,025		0,026			0,029			0,027
F07		0,017								0,017
F08			0,027		0,027			0,022		0,026
F09	0,029			0,029						0,029
F10	0,023			0,036					0,023	0,027
F11						0,024			0,018	0,021
F12	0,015				0,016				0,016	0,016
F13	0,012					0,038	0,023	0,037		0,028
F14				0,026				0,017		0,022
F15					0,017	0,017		0,013		0,016
Average	0,020	0,036	0,023	0,026	0,024	0,027	0,024	0,025	0,021	0,025

2.4.7 Reproducibility of F

In some trials, similar devices were participating and this permits an assessment of the reproducibility of their measurement of F . This was possible with the two Odoliographs, devices F08 and F14, and with the three SCRIM's, devices F03, F04 and. The reproducibility for the means of repeated runs is calculated by the following formula comparing two devices:

$$s_R = \sqrt{\frac{1}{2n} \sum_i \sum_j (F_{1ij} - F_{2ij})^2} \quad (2.17)$$

in which the sums are over the speeds and the surfaces.

Equation 2.17 includes both the systematic and the random deviations; for this reason the values for reproducibility given by equation 2.17 cannot be directly compared to the reproducibility of a single measurement. The results of this analysis are given in Table 2.13, with graphical comparisons in Figure 2.21 for the Odoliographs and Figures 2.22, 2.23 and 2.24 for the SCRIMs.

Incidentally, it can be seen in Table 2.13 that the relationship between pairs of similar devices varies from one round of calibration exercise to the next. This suggests that some characteristics of the devices can vary significantly in a six-month period. This is not surprising since, in spite of their apparent similarities, there are known differences between the machines. Regarding the SCRIMs, for example, F13 had a left-side test wheel whereas the other two machines had right-side test wheels. This could lead to differences in test line, especially on sites where there was limited room for manoeuvre. Further, it is known that, without careful control, differences can develop between machines of the same type and none of these machines had been cross-checked with one another in the way in which machines in a common fleet might be, such as occurs annually with the UK SCRIM fleet.

Figures 2.25 & 2.26 compare the locked-wheel devices. In this case, it must be noted that they differ in respect to the type of tyre used: F02 and F09 use a blank tyre while F12 uses a patterned tyre.

Table 2.13 Reproducibility standard deviation for the means of repeated runs

Device type	Devices compared	Trial	Reproducibility standard deviation	Number of measurements
Odoliograph	F08-F14	3,2	0,041	75
SCRIM	F03-F13	2,3	0,056	75
	F03-F04	3,3	0,051	85
		2,3	0,120	63
	F04-F13	2,3	0,171	84
		3,2	0,059	76
	Overall		0,103	383

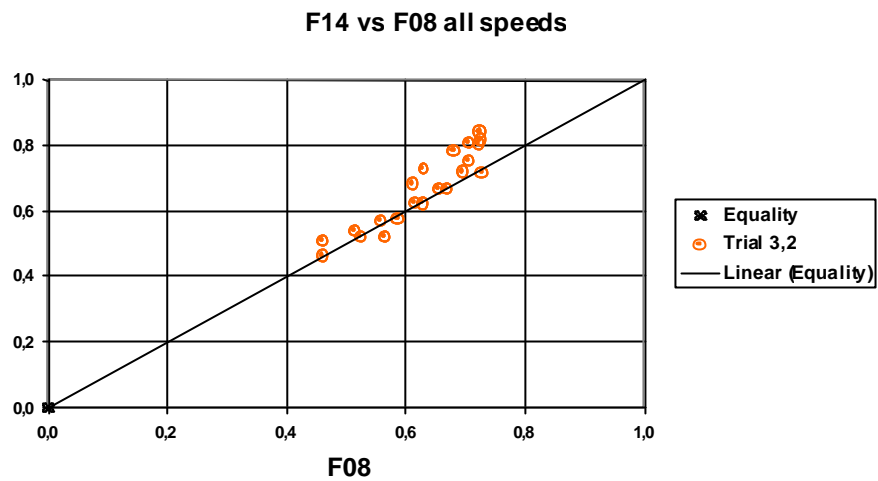


Figure 2.21 Comparison between the friction values reported by the two Odoliographs in Trial 3,2

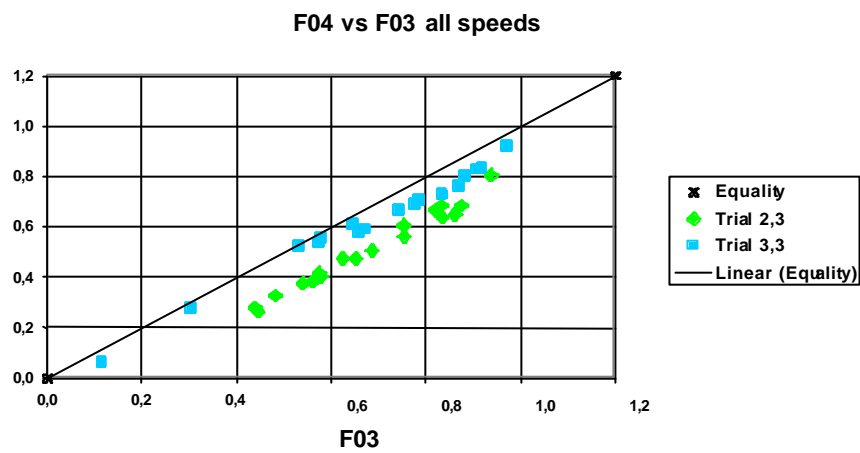


Figure 2.22 Comparison between the friction values reported by two SCRIMs in Trials 2,3 and 3,3

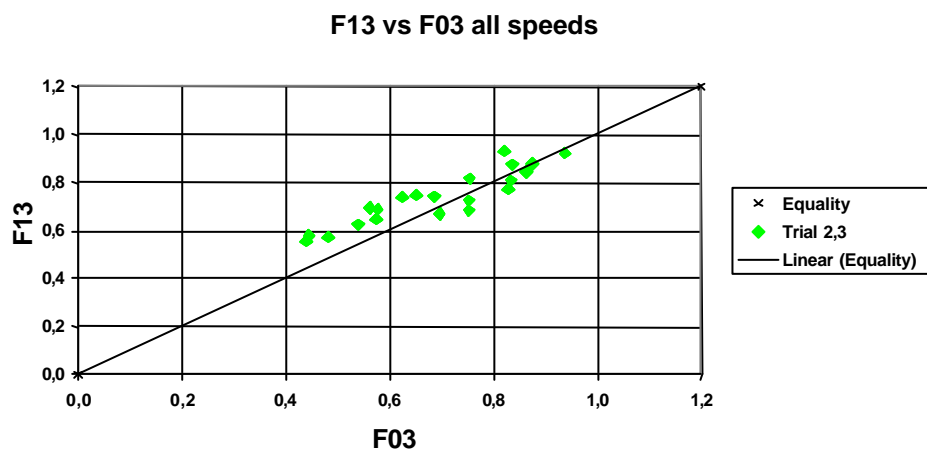


Figure 2.23 Comparison between the friction values reported by two SCRIMs in Trials 2,3

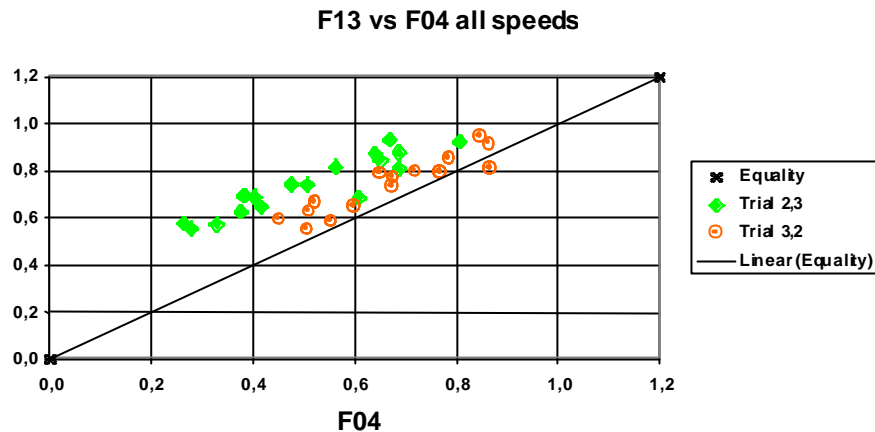


Figure 2.24 Comparison of friction values reported by two SCRIM's in Trials 2,3 and 3,2

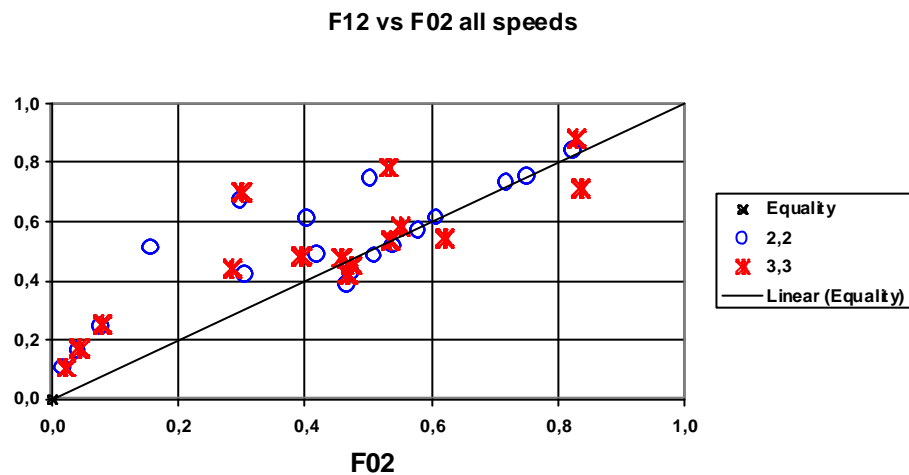


Figure 2.25 Comparison of friction values reported by two locked-wheel devices in Trials 2,2 and 3,3. As both trials took place on the same site (LCPC, in Nantes), several surfaces were the same. Note that they use different types of tyre.

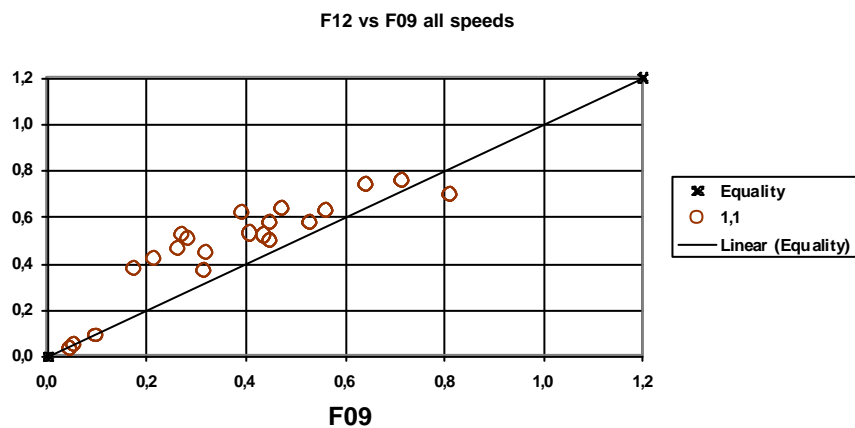


Figure 2.26 Comparison between the friction values reported by two locked-wheel devices in Trial 1,1 (note that they use different types of tyre).

2.4.8 Curve fitting on $F(S)$

The first step of the analysis was to determine the parameters for the speed correction for each device. Initially, values of S_0 for each device were determined from the test data by fitting the exponential curve

$$F = F_0 e^{-S/S_0} \quad (2.19)$$

to the reported values of the friction coefficient (F) versus the slip speed (S), the latter being calculated as the reported operating speed (V) multiplied by the *slip ratio* listed in Table 2.10. A least-squares linear regression was calculated on the logarithmic form of the equation:

$$\ln F = \ln F_0 - S/S_0 \quad (2.20)$$

A few measurement series where S_0 was negative (that is, where friction *increased* with increasing speed) were discarded from the analysis: an example of this is shown in Figure 2.27.

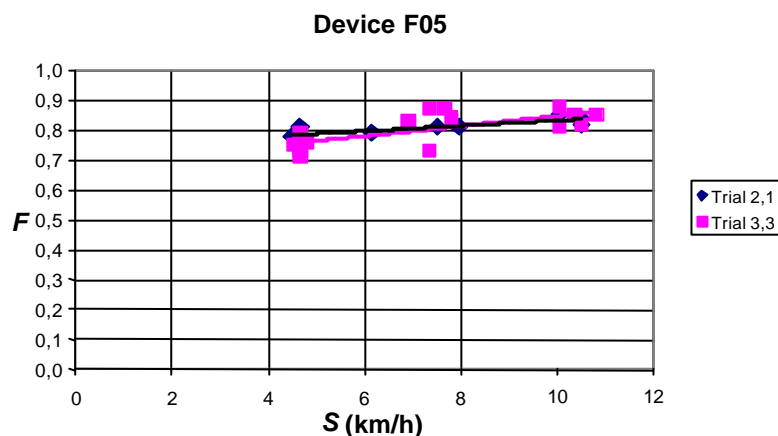


Figure 2.27 Examples of exponential curve fitting on $F(S)$ yielding negative S_0 values

In addition, some zero - or close to zero - values reported for F on the smooth epoxy surfaces were discarded because they did not fit in the calculation of the exponential regression. In total, less than 0,9% of the measurements were discarded for either of these reasons (Table 2.14). Annex B presents all the graphs of F versus S .

Table 2.14 Number of measurements discarded per trial.

Trial®	1,1	1,2	1,3	2,1	2,2	2,3	3,1	3,2	3,3	Total
$F < 0,01$	0	0	0	0	9	0	0	0	3	12
$S_0 < 0$	0	0	0	9	0	0	0	0	15	24
Total	0	0	0	9	9	0	0	0	18	36

2.4.9 Deriving S_0 from MPD

According to the “PIARC-model” specified in the CEN standard [3], S_0 is predicted from the texture depth using the linear equation (2.8). When, as here, texture has been measured using MPD method, the version of this formula in equation (2.9) is used, with the constants set so as to give S_0 in km/h from MPD in mm.

When plotting all the values of S_0 versus MPD from the nine trials, as shown in Figure 2.28, it was found that the formula fitted the data reasonably well. However, the scatter was rather wide. Annex C presents all the graphs of S_0 versus MPD per device and per trial.

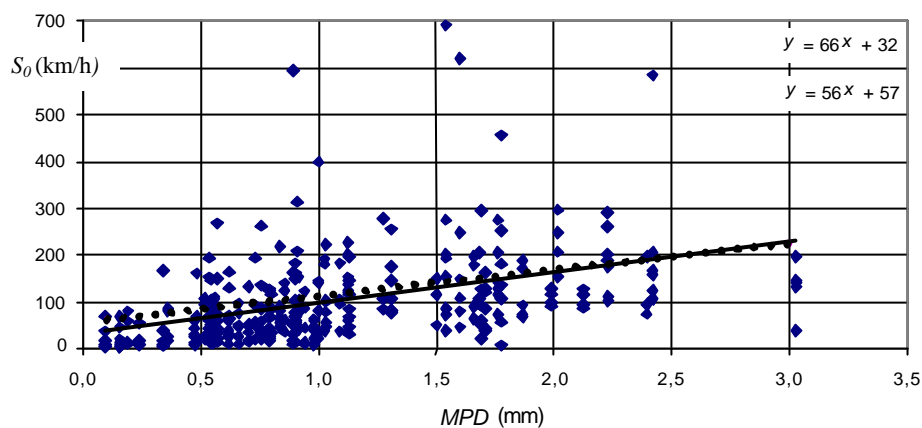


Figure 2.28 General correlation between S_0 and MPD , all measurement results plotted together. The solid line is the actual regression; the dotted line is the equation proposed in the CEN standard [3].

2.4.10 Applying statistical tests to the EFI measurements

Values of EFI were calculated as explained in Section 2.3.3, together with the grand average $\langle\langle EFI \rangle\rangle$ for all the reference devices (see Table 2.10). As explained in 2.3.4, two statistical tests are used to identify outlying measurements.

The first test is applied to the values of EFI obtained from repeated runs at the three speeds by a given device on a given surface. When the repeatability standard deviation (s_r) of the series is larger than 0,04, the value that has the largest deviation from the mean is discarded. If the test fails again, the whole series is discarded. When this test was applied to the *HERMES* data it was found that, in all cases, eliminating the most deviating value did not bring the standard deviation for the device and surface below the threshold and the whole series had to be discarded. Table 2.15 shows how many measurements had to be discarded per trial.

The second test (see Equation 2.10) is applied to the reproducibility of EFI . When the residual standard deviation of the linear regression between $\langle\langle EFI \rangle\rangle$ and all the individual EFI -values reported by a given device in a given trial (Equation 2.11) is larger than 0,07, the whole measurement series for that device is discarded and the calibration of that device is declared invalid in that trial. When applied to the *HERMES* results after

the repeatability test had been made, the reproducibility test never failed. However, for devices F06 and F07 in Trial 1,2, the repeatability test left results from less than two surfaces, in which case the regression (Equation 2.11) could not be calculated.

Table 2.15 Number of measurement data discarded after the repeatability test.

Trial	Number of discarded measurements	Percentage of discarded measurements
1,1	199	43%
1,2	229	72%
1,3	112	31%
2,1	156	28%
2,2	208	46%
2,3	234	52%
3,1	0	0%
3,2	41	8%
3,3	96	15%
Total	1275	31%

In view of the unacceptable severity of the repeatability test, the data were processed again, but this time applying only the reproducibility test. In this case, only one measurement series was flagged, namely from device F10 in Trial 1,1, and those particular results were not used in the analysis that followed. Device F10, which was not initially in the reference group, gained its first valid calibration parameters values (A , B) after its participation in the second round, at Trial 2,1.

This second stage of processing will be referred to as “Scenario #1” because, later in this report, different variants for the data processing are considered with a view to finding ways that might improve the reliability and precision of the calibration procedure. In that context, the strict application of the standard that was the first to be considered will be referred to as “Scenario #0”.

2.4.11 Calibration results

New values of “ A ” and “ B ” were determined as explained in Section 2.3.4, using Equations 2.13, 2.14 and 2.15. This was repeated for each trial meeting, with those devices that at first had not been defined as “reference devices” gaining their initial values of “ A ” and “ B ” after their first trial and then being included as reference devices in subsequent trials.

The way in which “ A ” and “ B ” for each device evolved from trial to trial using the “Scenario #1” analysis is shown in Tables 2.16 and 2.17 and is represented graphically in Figures 2.29 and 2.30. In these graphs, dotted lines are used to represent the devices that initially were not “reference devices”. Table 2.18 and Figure 2.31 show the evolution of the residual standard deviation (s_{EFI}) of EFI . The overall average value of s_{EFI} is 0,032. Its average value over the last trial only is 0,024.

Table 2.16 Evolution of calibration parameter “A” for each device according to Scenario #1

Device® Trial ⁻	F01	F02	F03	F04	F05	F06	F07	F08	F09	F10	F11	F12	F13	F14	F15
Last-5	0,100			0,006											
Last-4	0,535			0,421	0,190								0,006		
Last-3	0,402	0,203	0,115	0,374	0,451	0,000		0,000				0,104	0,186		0,000
Last-2	0,396	0,366	0,334	0,506	0,405	0,444		0,454	0,264	0,000	0,000	0,185	0,403	0,291	0,432
Last-1	0,384	0,421	0,461	0,469	0,560	0,345	0,000	0,445	0,195	0,431	0,514	0,407	0,386	0,332	0,544
Last	0,372	0,504	0,460	0,464	0,513	0,413	0,383	0,437	0,401	0,488	0,489	0,482	0,455	0,475	0,541

Table 2.17 Evolution of calibration parameter “B” for each device according to Scenario #1

Device® Trial ⁻	F01	F02	F03	F04	F05	F06	F07	F08	F09	F10	F11	F12	F13	F14	F15
Last-5	0,751			0,992											
Last-4	0,066			0,320	0,779								0,992		
Last-3	0,354	0,700	0,815	0,399	0,319	1,000		1,000				0,886	0,818		1,000
Last-2	0,317	0,449	0,417	0,252	0,437	0,256		0,392	0,574	1,000	1,000	0,589	0,333	0,514	0,401
Last-1	0,368	0,338	0,265	0,275	0,159	0,468	1,000	0,405	0,738	0,358	0,198	0,281	0,355	0,454	0,169
Last	0,369	0,182	0,256	0,276	0,248	0,364	0,287	0,350	0,381	0,287	0,258	0,186	0,276	0,268	0,171

Table 2.18 Evolution of s_{EF} for each device according to Scenario #1

Device® Trial ⁻	F01	F02	F03	F04	F05	F06	F07	F08	F09	F10	F11	F12	F13	F14	F15
Last-5															
Last-4	0,056			0,034											
Last-3	0,025			0,031	0,016								0,048		
Last-2	0,026	0,025	0,015	0,020	0,036	0,049		0,026				0,063	0,028		0,053
Last-1	0,023	0,042	0,021	0,012	0,016	0,020		0,044	0,066	0,040	0,023	0,053	0,015	0,014	0,024
Last	0,020	0,024	0,010	0,011	0,032	0,021	0,050	0,012	0,039	0,015	0,017	0,026	0,015	0,011	0,020

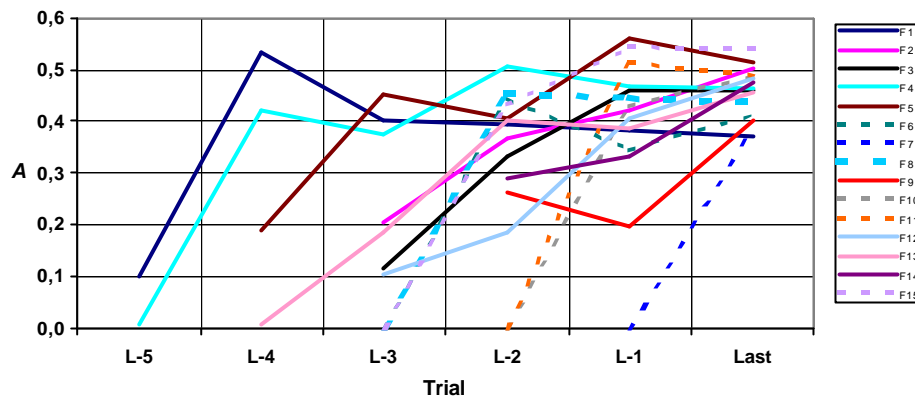


Figure 2.29 Evolution of calibration parameter “A” for each device according to Scenario #1. Devices that were “non-reference” initially are shown by dotted lines. (Last) is the last trial in which the device took part.

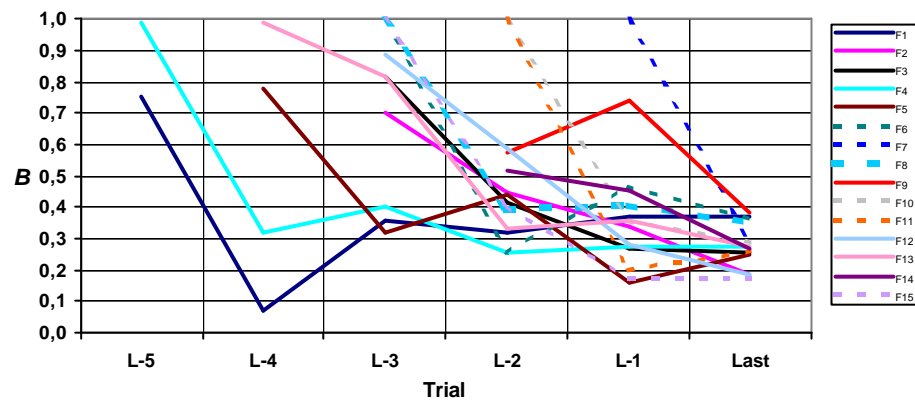


Figure 2.30 Evolution of calibration parameter “B” for each device according to Scenario #1. Devices that were “non-reference” initially are shown by dotted lines. (Last) is the last trial in which the device took part.

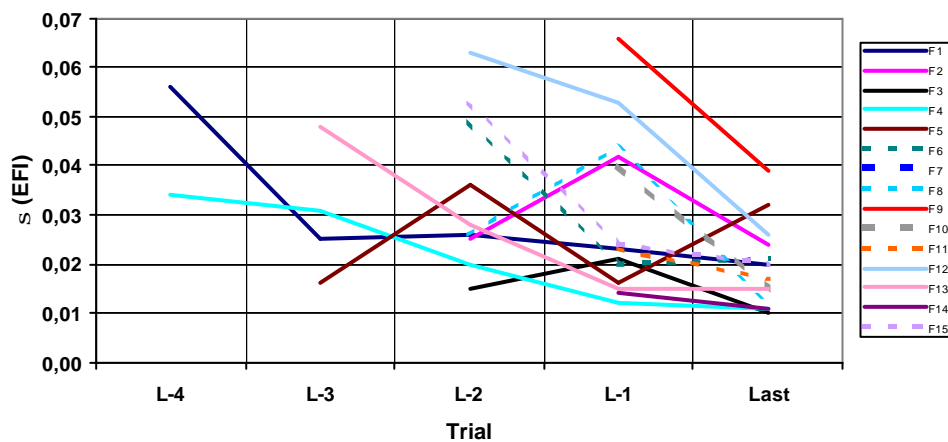


Figure 2.31 Evolution of s_{EFI} for each device according to Scenario #1. Devices that were “non-reference” initially are shown by dotted lines. (Last) is the last trial in which the device took part.

2.4.12 Discussion

The analysis of the results of the test programme has revealed a number of drawbacks in the draft CEN standard [3]. This section discusses the main areas where improvement is needed.

The statistical tests are obviously inappropriate. An alternative approach would be to apply a standard procedure, considering the different devices as different laboratories and the measured object as the $\langle\langle EFI \rangle\rangle$ value of a given surface. Then, consistency tests could be applied to the repeatability and reproducibility standard deviations following an established standard for assessing the precision of test methods such as ISO 5725-2 [5].

The prediction of S_0 from MPD exhibits considerable scatter that can affect the precision of EFI to a large extent, particularly when the measurement speed and equipment principles are such that the slip speed is far from the reference speed of 30 km/h. The more the predicted S_0 departs from its actual value, the more EFI depends on speed as the extrapolations of $F(S)$ to F_{30} from different speeds diverge, as illustrated for one device and trial in Figure 2.32.

In view of Annex D, it seems that some improvement could be gained by considering the relationship $S_0(MPD)$ as device-dependent. Then, not only “A” and “B” but also “a” and “b” would be device-specific parameters requiring calibration.

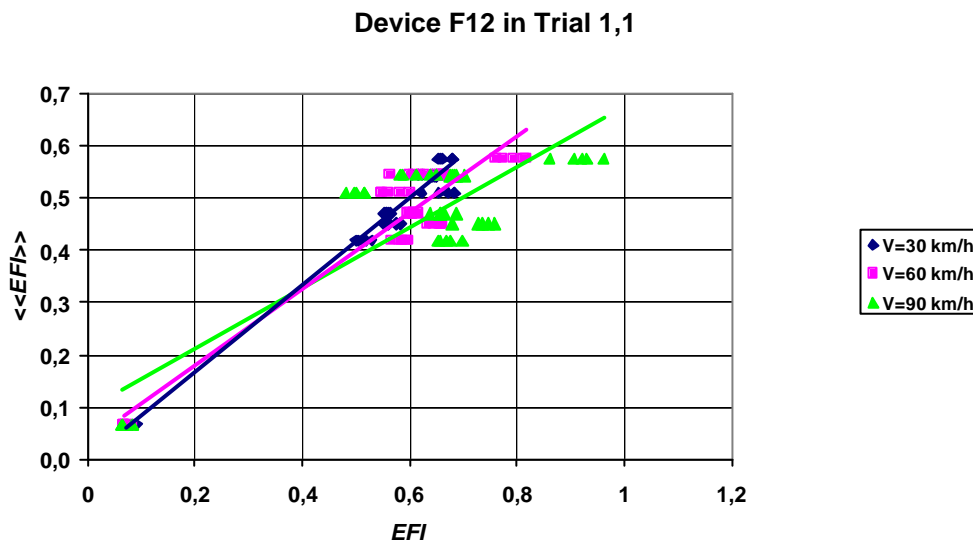


Figure 2.32 Example of operating speed (V) influence on EFI

In eight cases, occurring in Trials 1,1, 2,2 and 3,3, the predicted S_0 has a small, negative value for some low- MPD surfaces (see Annex D). This is not acceptable because it leads to absurd values for F_{30} . To avoid this, a non-linear model for $S_0(MPD)$ should be used, which would also better fit most data sets.

Moreover, in view of some of the graphs in Annex D, in several cases, some S_0 values depart markedly from the general trend. In order to prevent such outlying values to have too much influence on the curve fitting, it would be advisable to use a weighting that gives less weight to S_0 values derived from poorly-correlated $F(S)$ data.

From another viewpoint, even if S_0 were accurately predicted, measurement series not fitting the exponential model could also affect the precision of EFI to some extent. That is what happens in number of instances in the *HERMES* tests, of which Figure 2.33 shows an example. Therefore, a better model could be needed for $F(S)$.

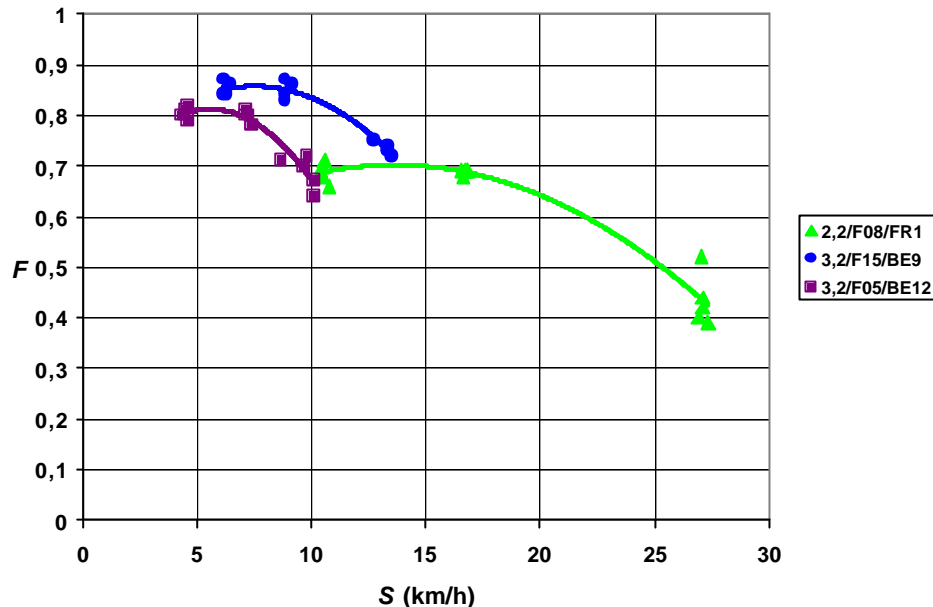


Figure 2.33 In these examples, the data exhibit a negative curvature, which is opposite to the exponential model

As a given device undergoes successive calibrations, there is a general tendency for its “A” parameter to increase and its “B” parameter to decrease, which has two undesirable consequences. Firstly, “A” is effectively the EFI -value that would be obtained on a zero-friction surface. That being so, values higher than 0,5 (see Table 2.16) are hardly acceptable values for a very slippery surface, such an icy one, for example. Secondly, “B” reducing to a range of 0,18–0,38 means that if the difference in friction coefficient between two surfaces at a given speed is ΔF , their difference in terms of EFI will decrease to 18–38% of ΔF , which would be a dramatic loss of sensitivity of EFI in comparison with the skid resistance of the surface.

Moreover, the apparently good precision of the calibration, namely $s_{EFI} = 0,024$ in the last round of tests, is an artefact of the low “B” values. Indeed, for it to be compared to the precision of EFI , the precision of actual measurements of F must be multiplied by B , which is generally much lower than one.

The development of “A” and “B” over successive trials is considered to be mainly due to a bias arising from the least squares linear regression method being used in a situation where both the independent variable and the dependent variable have measurement errors. This tends to pull the slope towards low values all the more because the scatter is large. The effect is amplified as the procedure is repeated over successive trials, as Figures 2.29 & 2.30 show.

A possible way to prevent that behaviour could be to calculate the regression of EFI against $\langle\langle EFI \rangle\rangle$ and then to reverse the equation to get back $\langle\langle EFI \rangle\rangle$ against EFI . From a statistical viewpoint, this is a better approach than the original regression. However, the

project was already at an advanced stage when this approach was first introduced. An initial attempt to analyse the data in this way was made (see 4.6) but this was inconclusive and there was insufficient time to fully re-work the data. Another possibility might be to force “A” to zero. Then, by a new definition, *EFI* would just become proportional to F_{30} :

$$EFI = B \cdot F_{30} \quad (2.21)$$

This is a logical and practical approach, since *EFI* would then vanish on a zero-friction surface. Moreover, for the data from the *LCPC* and *TRL* test tracks that included low-friction epoxy surfaces, the regression lines (Equation 2.12) pass close to the origin (Trials 1,1; 2,2; 3,1; 3,3 in Annex D). This supports the idea that model (2.21) should be applied in all cases. However, there might be individual situations where the form is not linear through the whole friction range (compare, for example, the first two graphs in Annex G).

3 Revision of the friction model

3.1 Introduction

In the Belgian study [2] that followed up the 1992 *PIARC* experiment, the reproducibility and the repeatability of the *EFI* were calculated. The standard deviation describing the repeatability over all the devices and sections was 0,08 and the standard deviation for the reproducibility of the *EFI* by different devices was 0,14.

This means that, in the situation where one device is used to predict the measurement results of another device, the confidence interval is very large. Therefore, the use of the *EFI* in its present state is very limited and improvement of the model is desirable.

In this Chapter, the work carried out in the *HERMES* project to improve the model will be presented. This work was carried out mainly by *DWW* and *LCPC*, with a contribution from *TRL*.

3.2 Further improvements to the model

In the process of investigating ways of improving the *EFI*, three databases were used: the *HERMES* database; a small database containing the results of an experiment carried out by *BASf*, *DRI* and *DWW* in 1996, and the original database from the *PIARC* experiment in 1992. From the *PIARC* database, only data from friction devices with blank tyres were included. For the texture devices, only the Belgian data processed according to the *ISO* standard were used. Three possible improvements were tested:

- a specific relation between the speed parameter S_0 and MPD for every device, instead of the general relation according to Equation 2.9;
- a non linear relation between S_0 and MPD with specific coefficients for every device;
- a model based on the lubrication theory developed in tribology (the Stribeck formula).

3.2.1 Calculation of S_0 vs. MPD_{ISO} per device

In Section 2.3.3 the comment was made that inaccuracies might occur in calculating the *EFI* because the speed constant is estimated from a general formula, independent of the friction device. It was found that the “real” speed constant, calculated from the measurement results, was not independent of the friction device. Therefore, an attempt was made to derive a device-dependent relation to calculate S_0 from a texture measurement.

As a first step, a linear regression line was fitted for each device and site combination, with

$$x = S - 30 \quad (3.1)$$

and

$$y = \ln(F) \quad (3.2)$$

The results of this analysis (the regression coefficients and their standard deviations) were saved and from this dataset, the following parameters were calculated:
 S_0 , from the slope of the regression line as:

$$S_0 = \frac{-1}{slope}.$$

Note that this is the “real” S_0 for the different devices and not an estimate as calculated with equation 2.9;
the standard error of S_0 as

$$se(S_0) = \frac{se(slope)}{slope^2};$$

a weighting factor as

$$w(S_0) = \frac{1}{se(S_0)^2}.$$

The next step was to determine the relationship between the S_0 and the texture parameter MPD . To find this relationship a weighted linear regression was fitted (for each device) with:

$$x = MPD \quad (3.3)$$

$$y = S_0 \quad (3.4)$$

with the weight $w(S_0)$.

With the introduction of a weighting factor, it is possible correct the influence that the accuracy of the parameter S_0 has on the regression. Values of S_0 with small standard errors will have a greater weight in the regression analyses than S_0 values with a large standard error. Together with this weighted analyses, the Cook’s distance was used to check for outliers. The Cook’s distance is a method to indicate whether deletion of a particular value will have a large influence on the regression coefficients.

For each device, the following graphs were drawn in order to judge the regression analysis:

- the standardised residuals versus the fitted values;
- the Cook’s distances versus the fitted values;
- standardised partial residual plots (plots in which the effects of the other dependent variables are eliminated).

When performing a linear regression with $y = S_0$ and $x = MPD$ and $weight = w(S_0)$, then what actually is done, is to fit a linear regression without an intercept and with:

$$x_1 = \sqrt{w(S_0)} \quad (3.5)$$

$$x_2 = \sqrt{w(S_0)} \cdot MPD \quad (3.6)$$

$$y = \sqrt{w(S_0)} \cdot S_0 \quad (3.7)$$

In the situation where a weighted linear regression is used, no direct estimate is made of the intercept of the regression line. The regression coefficient belonging to x_1 represents the intercept, and the regression coefficient belonging to x_2 stands for the effect of the *MPD*. In subsequent analyses (maximum 5 repetitions) the measurements with the largest Cook's distances were deleted from the regression analysis.

The analysis resulted in a specific relation between S_0 and *MPD* ($S_0 = a + b \cdot MPD$) for every friction device instead of the general relation $S_0 = 57 + 56 \cdot MPD$ derived from the data from the *PIARC* experiment. The coefficients for the different devices are listed in Table 3.1.

Table 3.1 Coefficients by device (Device reference numbers refer to the *PIARC* experiment)

Device	a	b	Device	a	b	Device	a	b	Device	a	b
B1 LKD	81	43	B5 LKD	94	34	C5	49	93	D 3	47	32
B1 SLP	33	6	B5 SLP	28	22	C6E	35	39	D 4	106	9
B2 LKD	115	53	C1	83	55	C9	-9	46	D 5	52	26
B2 SLP	34	17	C10	-8	55	D1E	34	32	D 6	3	93
B3	35	19	C3B	61	32	D2	56	6	D 8	-4	53

With a specific relation established for each device, the original model was followed to calculate values for the *EFI* per site and per device. This calculation showed that the accuracy of the results was worse than the results from the original model. To demonstrate this, the standard deviations for the reproducibility and the repeatability of the new model and the original model are listed in Table 3.2. In fact, this is a very strange result: by improving the model for the relationship between slip speed and texture, the overall result worsens. The only explanation for this is that *MPD* alone is not the right explanatory factor for the speed dependency of friction.

Table 3.2 Comparison of the standard deviation for the repeatability and the reproducibility of both models

	Standard deviation for	
	Repeatability	Reproducibility
Original model	0,08	0,14
New model	0,13	0,13

With the dataset available after this analysis it was possible to check the findings demonstrated at the SURF 2000 symposium [6] concerning a linear relation between the

slope in the relation S_0 vs. MPD and the *slip percentage* of the devices. Again a weighted linear regression was used, with a weighting factor

$$w = \frac{1}{se(slope)^2}.$$

Using this relation, an estimate was made for the coefficients “a” and “b”. In Table 3.3 these estimates are listed as (a^* and b^*), together with the values that were calculated from the weighted linear regression. Although most of the estimated “a” and “b” values were very close to the calculated values, the results of the analysis were not very satisfying. The percentage variance accounted for was 31%. The slope of the regression, however, was very significantly different from zero (Probability = 0,994).

Table 3.3 Coefficients estimated from slip percentage

Device	% slip	Calculated		Estimated from slip percentage		Device	% slip	Calculated		Estimated from slip percentage	
		a	b	a*	b*			a	b	a*	b*
B 1 LKD	100	81	43	68	56	C 5	86	49	93	79	53
B 1 SLP	14	33	6	25	14	C 6E	34	35	39	40	33
B 2 LKD	100	115	53	113	56	C 9	26	-9	46	2	27
B 2 SLP	20	34	17	30	21	D 1E	34	34	32	33	33
B 3	20	35	19	33	21	D 2	34	56	6	32	33
B 5 LKD	100	94	34	75	56	D 3	34	47	32	47	33
B 5 SLP	20	28	22	29	21	D 4	34	106	9	78	33
C 1	100	83	55	82	56	D 5	34	52	26	46	33
C 10	34	-8	55	6	33	D 6	100	3	93	28	56
C 3B	34	61	32	61	33	D 8	18	-4	53	17	19

When the values of the *EFI*, that were calculated with the new model were analysed, it was found that these values were still dependent from the slip speed. From the “real” relation between friction and slip speed, it was seen that some non-linearity exists in the relation “ln (friction)” versus slip speed. As a possible measure to eliminate this dependency, it was decided to perform a non-linear regression analysis for the relation between “ $y = \ln (F)$ ” and “ $x = S-30$ ”.

3.2.2 Quadratic regression analysis

As stated above, the new model with specific “a” and “b” values for every device, resulted in *EFI*-values that still depended on the slip speed. Therefore the possibilities of finding a better model to define the relation between “ln(friction)” and the slip speed were discussed, the idea being to remove, or at least reduce, the influence of the slip speed on the *EFI*.

As a result of this discussion, and based on the graphs from earlier calculations, a quadratic model was chosen to describe the relation between “ln(friction)” and the slip speed. It should be emphasized that a quadratic model was decided upon arbitrarily, based on the shape of the graphs of the real relation; there was no physical reason for the

choice. The quadratic model was chosen merely to demonstrate that a non-linear model for the relation between “ln(friction)” and slip speed would improve the standard deviation for the repeatability and reproducibility of the *EFI*. It was decided to determine a specific model for each device again. The following relation was used for the analysis:

$$\ln(F) = b_0 + b_1 \cdot (S - 30) + b_2 \cdot (S - 30)^2 \quad (3.8)$$

As a first step, this model was fitted for the devices that were used in the experiment with *BAST*, *DRI* and *DWW*, because this was a limited dataset. One of the results of the quadratic model is illustrated in Figure 3.1.

In this experiment, six sections, with the following surfacings, were tested:

- S1 Sheep foot rolled;
- S2 Cement concrete steel brushed;
- S3 Rolled mastic;
- S81, S82 Bituminous concrete;
- S4 Porous asphalt;
- S71-S76 Porous asphalt < 6 months.

The *MPD*-values measured on these sections are shown in Figure 3.2.

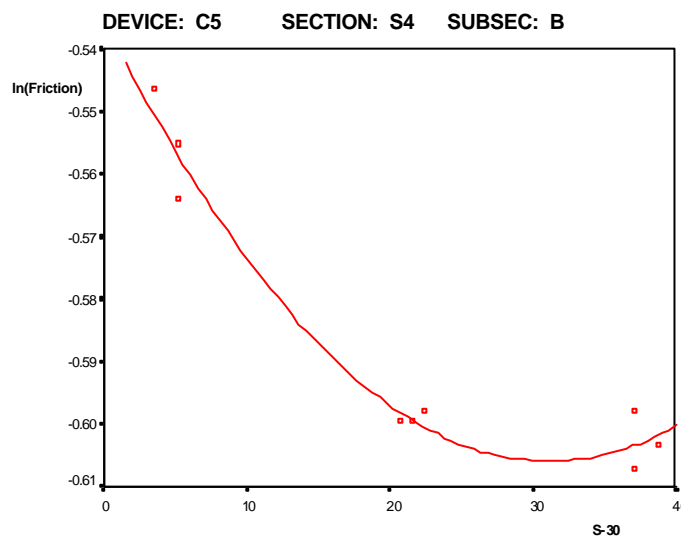


Figure 3.1 A quadratic function in the relation of ln(friction) and slip speed

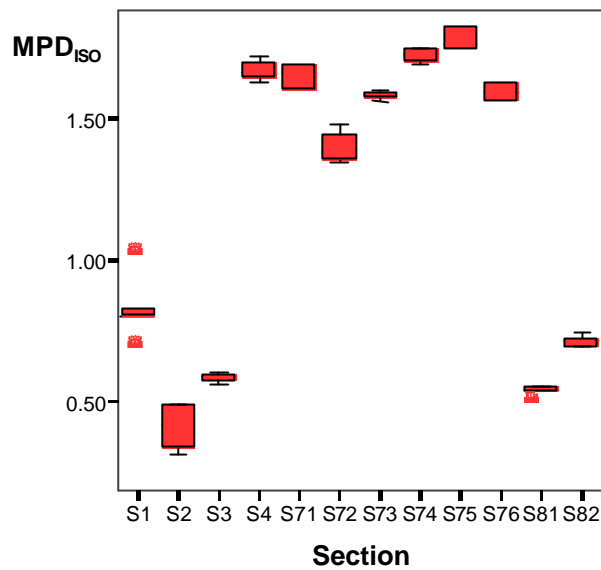


Figure 3.2 *MPD-values of the test sections in the experiment of BAsT, DRI and DWW*

Since the analysis of the limited database showed good results, the exercise was repeated for the *PIARC* database. When the coefficients b_0 , b_1 and b_2 were calculated, S_0 could be calculated. With this parameter, the F_{30} was calculated for each device, site and run. Then, the mean value over the runs per device was calculated for each site and the *EFI* was calculated as the mean value of F_{30} per site. With this data a linear regression was fitted per device with $y=EFI$ and $x=F_{30}$. From this linear regression the “A” and “B” values were calculated.

The next step was to use these “A” and “B” values to calculate the *EFI* per site for every device, from $EFI = A + B F_{30}$. A result of this calculation is shown in Figure 3.3, in which the relation between *EFI* and measured friction is broken down by site. Separate colours for every device identify the different devices. It can be seen that the speed dependency no longer exists. However, different devices still report different levels for the *EFI* on the same section.

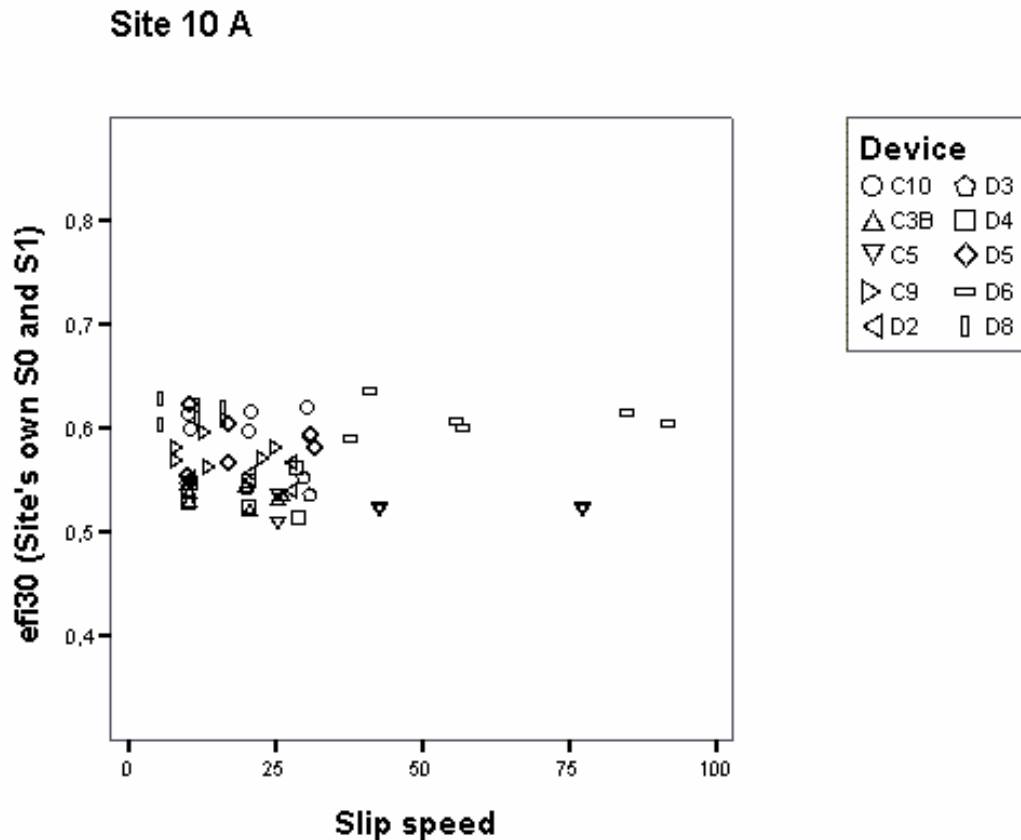


Figure 3.3 Relation between slip speed and EFI with a quadratic model and calculated S_0 and S_1

3.2.2.1 Quadratic model with estimation of S_0 and S_1

So far the coefficients S_0 and S_1 used in the calculations were the “real” S_0 and S_1 as calculated from the measurements at different vehicle speeds. In normal service practice it will not be possible to use calculated values for S_0 and S_1 , because measurement passes will usually only be made once and at only one test vehicle speed. Therefore, in order to calculate values for EFI routinely, the coefficients S_0 and S_1 have to be estimated, preferably from the texture of the road surface.

To investigate the relation between S_0 , S_1 and MPD , a regression was performed for the relations S_0 vs. MPD and S_1 vs. MPD . It was found from these regression lines that both S_0 and S_1 were almost independent of the texture. However, the estimates of S_0 and S_1 were implemented in the quadratic model and again EFI -values were calculated. From Figure 3.4 it can be seen that the results are very disappointing, because of the fact that the EFI -value is again dependent on the original friction value of the device (and with the vehicle speed of the device). This is further evidence that MPD alone is not the parameter that explains the speed dependency of friction. Some other influences are also playing a part in the tyre-road interaction.

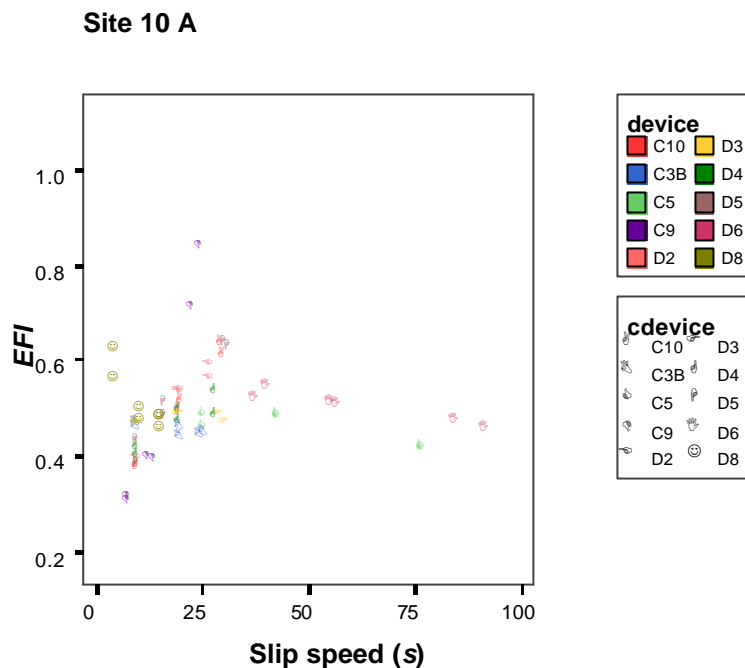


Figure 3.4 Relation between *EFI* and slip speed for the quadratic model with estimated S_0 and S_1

3.2.2.2 Conclusions regarding the quadratic model

From this analysis it can be concluded that a non-linear (quadratic) model in the relation “ln(friction)” – slip speed can result in *EFI*-values that are independent of the vehicle speed as long as the “real” values for S_0 and S_1 are used. The model using this relation shows an improvement compared with the previous models, as can be seen from the standard deviations for the reproducibility and the repeatability listed in Table 3.4, which makes a comparison with the models described earlier.

Table 3.4 Standard deviations for the reproducibility and the repeatability

	Standard deviation for	
	Repeatability	Reproducibility
Original <i>PIARC</i> -model	0,08	0,14
New linear model with “real” coefficients	0,13	0,13
New linear model with estimated coefficients	0,11	0,11
Quadratic model with “real” coefficients	0,01	0,06
Quadratic model with estimated coefficients	0,08	0,08

From these standard deviations, both the repeatability and the reproducibility of the *EFI* using the model with estimated coefficients were calculated to be 0,23. Although this is an improvement compared with the original model, the accuracy of the predicted *EFI* is poor and a device and speed dependency remains which has to be dealt with before accurate *EFI*-values can be calculated. Likely candidates for factors involved in these dependencies are the slip percentage, the measurement principle or influences like the contact area or the contact pressure.

In practice, the results of the latest analysis show that it is not possible to calculate a good value for the *EFI* that is independent of the vehicle speed and the device. This also means that the measurement values obtained with a particular device cannot be used to predict accurately the measurement values of another device.

More research is needed to describe the parameters that are responsible for the interaction between devices and sites and, with this, those leading to the speed dependency and the different levels of the *EFI* found on any one site.

3.2.3 The *LCPC*-model

In parallel with the work at *DWW*, research into the improvement of the original *PIARC*-model was carried out at *LCPC*. The *LCPC* approach was based on the lubrication theories developed in tribology (friction-related research). The idea is supported by the fact that many similarities exist between the lubrication mechanisms investigated in tribology and the nature of the contact system that occurs between the tyre and road in the presence of water.

Before a model based on tribology was developed, the limitations of the *PIARC* model in the description of the friction versus slip-speed curve were investigated. The second task was to propose a more general alternative model. The validation of the new model was based on two criteria:

- How the model fitted the experimental data;
- The correlation between the model constants and measurable parameters such as the road and vehicle characteristics.

3.2.3.1 Statistical analyses based on the original *PIARC* model

As with the work of *DWW*, the *LCPC* analysis started with some statistical analyses based on the original *PIARC*-model. For this work, the data from the *HERMES* calibration meetings were used. This database contained the following information:

- Device-related characteristics (*slip ratio*, *tyre type*);
- Surface characteristics (*MPD*);
- Friction values at various slip speeds.

From the friction values at various slip speeds, it is possible to derive S_0 values for each measurement series of *slip ratio* and *MPD*. Each meeting can then be treated as a factorial design experiment in which the *MPD* and the *slip ratio* are "the factors" and S_0 is "the response". Analyses of variance were then performed to establish how S_0 varied with *MPD* for different *slip ratios* or, conversely, how S_0 varies with *slip ratio* for different *MPD*.

Strictly speaking, each meeting was a factorial design experiment with unbalanced data, since the number of repetitions was not the same for all measurement series. In the analyses this was not taken into account. All data were treated as though they were sets of balanced data. Therefore, inaccuracies might occur in the results.

For the calculation of S_0 , a regression was performed for each device and for each surface. Firstly, to obtain S_0 , the exponential function $y = a \cdot e^{bx}$, where y represents the friction and x the corresponding slip speed, was fitted to the data. Then, S_0 was calculated as $-1/b$. As an example of the results from this analysis, two graphs using data from meeting 1,1 are shown in Figure 3.5.

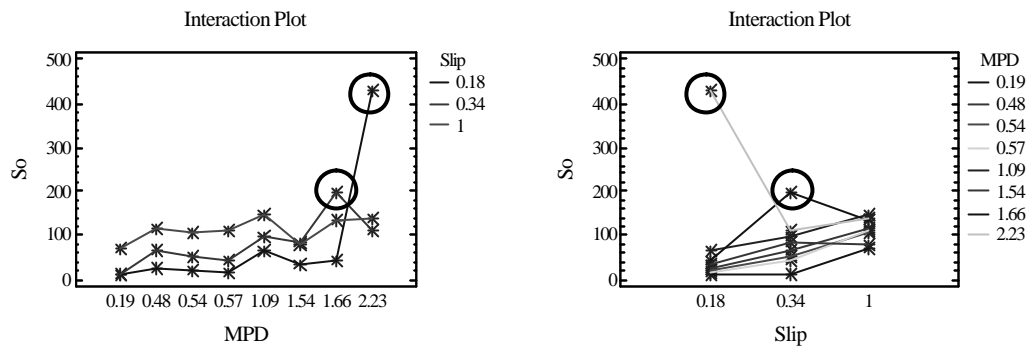


Figure 3.5 Example of the variation of S_0 with MPD and slip ratio

The graphs show that there is a general tendency for S_0 to increase for increasing values of both *MPD* and *slip ratio*. However, two unexpected points can be seen on the graphs: those for device F10 on section GB6 and for F13 on GB8.

Examples of the Friction versus Slip Speed graphs for these cases are shown in Figure 3.6. For device F10, friction is constant with slip speed, leading to a very high value of S_0 , while for F13, friction is steady for the first two speeds, decreasing for the highest speed.

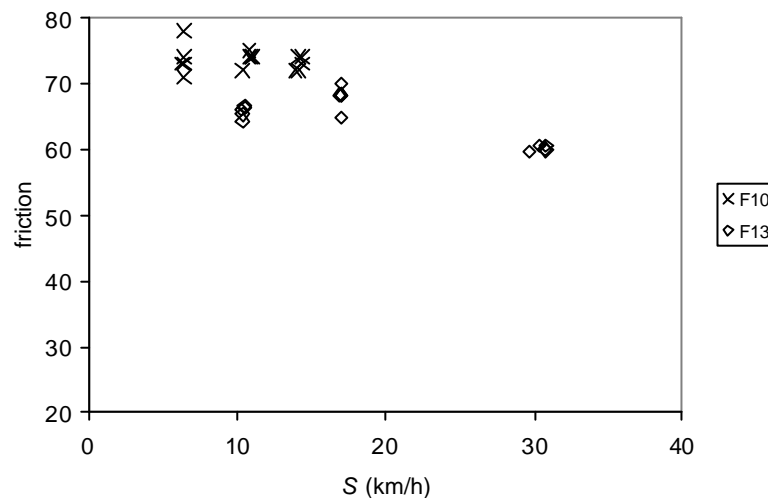


Figure 3.6 Friction – slip speed curves for F10 on GB6 and F13 on GB8

Overall, the analysis of variance generally showed a non-linear increase of friction for increasing values of both *MPD* and *slip ratio*. However there were twenty-eight measurement combinations of device and surface that did not respect this trend (representing about 9% of the whole *HERMES* calibration campaign). Since no apparent measurement error could be found, except that it was known that device F05 had reported the wrong results, any explanation must rely upon physical phenomena that are not properly described by the model used for the analyses. It was found that, typically, either:

- The friction did not vary with slip speed (referred to subsequently as “type I” behaviour, similar to F10 above), or;
- The friction remained stable for the first two speeds then decreased for the highest speed (referred to subsequently as “type II” behaviour, similar to F13 above).

For both type of behaviour, the exponential model cannot be fitted to the experimental data and the speed parameter concept does not have any physical meaning. Device behaviour is generally of “type I” on porous asphalt surfaces; that is why this type of surface is generally considered to be a “bad” surface in the context of model validation. The 28 measurement series that, unexpectedly, did not follow the general tendency are listed in Table 3.5.

Table 3.5 Summary of unexpected measurement series

Meeting	1,1	1,2	1,3	2,1	2,2	2,3	3,1	3,2	3,3
Measurement series	F10/GB6 F13/GB8		F01/ES5 F02/ES5 F03/ES5 F08/ES5	F01/BE7 F05/BE4 F09/BE4 F10/BE7	F05/FR1 F05/FR2 F05/FR3 F05/FR6	F11/NL9 F11/NL10	F01/GB15 F06/GB15 F13/GB9 F13/GB10	F05/BE9 F05/BE11 F08/BE9 B13/BE12	F05/FR7 F05/FR8 F05/FR9 F05/FR12

It should be noted that a high proportion (11 out of 28, roughly 40 %) of the “unexpected” measurement series related to device F05. However, this may have been caused by the “wrong” results for this device having been used in the analyses. (Correct data were eventually provided, but too late to be taken into account in this analysis.)

Another important comment that can be made is that, even though the different *MPD* devices quite well with one another in general (see Section 2.4.3), there was nevertheless considerable scatter between *MPD* values between different texture measuring devices. Differences of up to 30 % were observed between T3 and T4, for example (Table 2.9). This scatter could have a significant influence on the correlation between S_0 and the coupling of *MPD* and the *slip ratio*.

(1) *Regression analysis to derive the S_0 function*

In the general case, the interaction graphs show almost no interaction between *MPD* and *slip ratio*. Therefore, it was decided to derive S_0 from both *MPD* and *slip ratio* using a power function (this was an arbitrary choice; other non-linear functions should also work). The following expression was used:

$$S_0 = a_1 \cdot MPD^{a_2} \cdot (slipratio)^{a_3} \quad (3.9)$$

This formula can be transformed using the logarithm function:

$$\log(S_0) = \log(a_1) + a_2 \cdot \log(MPD) + a_3 \cdot \log(slipratio) \quad (3.10)$$

Where $\log(a_1)$, a_2 and a_3 are constants to be determined from multiple linear regression.

(2) *Regression with all data*

Multiple-linear regression was performed on the whole database (nine calibration meetings) to derive values of the constants. The comparison between measured and calculated (estimated) values of S_0 is shown in Figure 3.7. From this graph it can be seen that there is a large scatter around the line of equality, possibly due to the “unexpected” values described earlier.

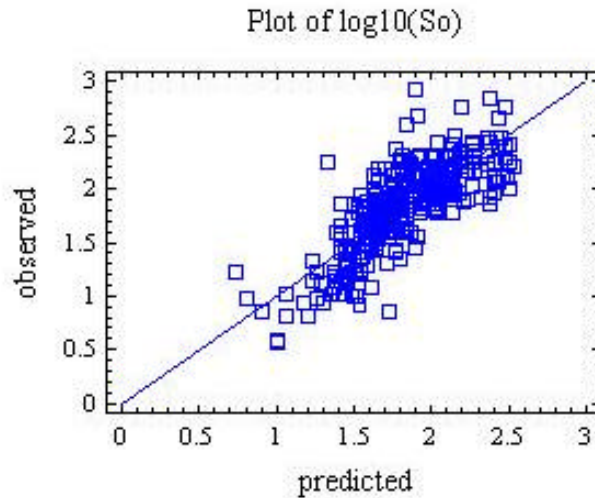


Figure 3.7 Validation of the regression from formula 3.10

(3) Regression with all data except “unexpected” measurement series

In order to reduce the effects of the scatter, the analysis was repeated, omitting the “unexpected” values listed in Table 3.5, to derive modified values for the constants. Comparison between measured and calculated values of S_o is shown in Figure 3.8.

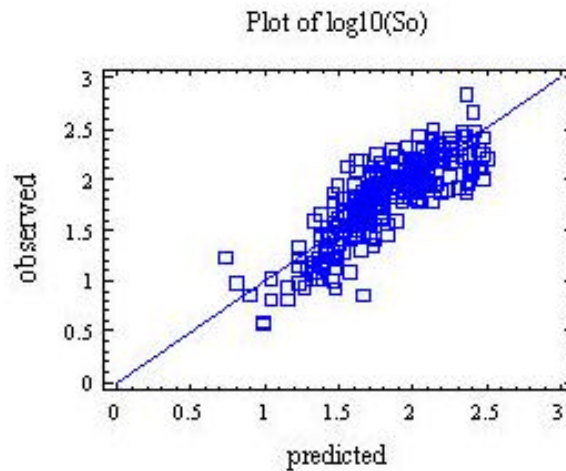


Figure 3.8 Validation of the regression from formula 3.10 excluding “unexpected” measurement series

The suppression of the “unexpected” measurement series improves the regression coefficient (R^2 increased from 0,63 to 0,69), confirming what can be seen in the graphs. However, it can also be seen that there is still a large scatter around the line of equality in Figure 3.8. Further, some curvature can be seen in the data points. Since it was shown that the “unexpected” measurements are due to specific behaviour for which the exponential model cannot be applied, it was decided to use the constants obtained after discarding those outlying measurements series for the ongoing analysis. The final formula relating the speed constant to the *slip ratio* and *MPD* is thus:

$$\log(S_o) = 2,22 + 0,73 \cdot \log(MPD) + 0,87 \cdot (\text{slipratio}) \quad (3.11)$$

Formula 3.11 can be rewritten as:

$$S_0 = 167 \cdot MPD^{0,73} \cdot (slipratio)^{0,87} \quad (3.12)$$

Based on the results from the *HERMES* calibration meetings, the relation in formula 3.12 explains almost 70 % of the variation of the speed parameter using the surface *MPD* and the vehicle *slip ratio*.

Additionally, a regression per device was investigated. From the individual regression plots it could be seen that there was both large scatter and a curvature in the graphs. Values of regression constants “a” and “b” for the device-specific relations are given in Table 3.6. The relation between the constant “b” (device dependent) and the *slip ratio* is shown in Figure 3.9.

Table 3.6 Constants for the regression $\log(S_0) = a \cdot \log(MPD) + b$ for each device

	F01	F02	F03	F04	F05
a	0,575	0,703	0,729	0,953	0,564
b	2,169	2,129	1,899	1,849	1,387
	F06	F07	F08	F09	F10
a	0,90	0,89	0,983	0,23	1,201
b	1,610	2,319	1,795	1,965	1,645
	F11	F12	F13	F14	F15
a	0,847	0,36	0,771	0,746	0,857
b	1,526	2,260	1,880	1,801	1,457

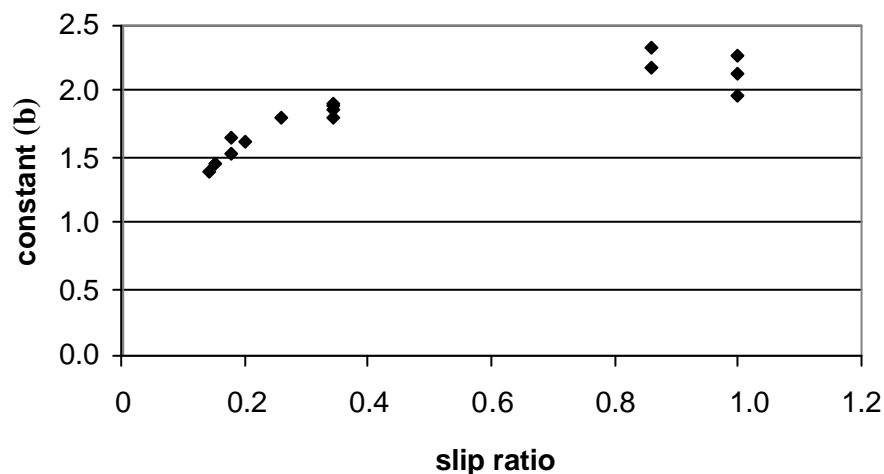


Figure 3.9 Relationship between constant “b” and slip ratio

It is of interest to note the close relationship between “b” and the *slip ratio*. Two types of curve were then investigated to fit these points: polynomial and logarithm. The regressions obtained were as follows:

$$b = -2,09 \cdot (slipratio)^2 + 3,17 \cdot (slipratio) + 1,05 \quad (3.13)$$

$$b = 2,21 + 0,84 \cdot \log(\text{slipratio}) \quad (3.14)$$

The first regression (3.13) has an R^2 of 0,93 and, for the second (3.14), R^2 was 0,88. The second regression is interesting since it is similar to the sum of the first and third terms of equation (3.11). Besides, the values are almost the same: 2,22 and 0,87 compared with 2,21 and 0,84 for equations (3.11) and (3.14) respectively.

To summarise, individual regressions lead almost to the same formula as does general regression. The only difference is the value of the *MPD* exponent (constant “a” in Table 3.6), which is now device-related.

Individual regressions were also performed using an exponential model, that is to say:

$$S_0 = a \cdot e^{b \cdot MPD} \quad (3.15)$$

or

$$\ln(S_0) = \ln(a) + b \cdot MPD \quad (3.16)$$

However, the regression coefficients were no better than those obtained with the power model. Since individual regressions do not significantly improve the correlation between S_0 , *MPD* and *slip ratio*, the general regression has been applied. The exponential model can be now written as:

$$F(S) = F_0 \cdot \exp \left[\frac{-S}{167 \cdot MPD^{0,73} \cdot (\text{slipratio})^{0,87}} \right] \quad (3.17)$$

The F_{30} values are calculated for each surface, each device and each run using the following formula:

$$F_{30} = F(S) \cdot \exp \left[\frac{S - 30}{167 \cdot MPD^{0,73} \cdot (\text{slipratio})^{0,87}} \right] \quad (3.18)$$

For many of the measurement series for individual device and surface combinations, it was observed that F_{30} (the friction measurement adjusted to the 30km/h reference speed) was speed-dependent. An example of this is shown in Figure 3.10 for the measurement series of device F02 on section FR1. In this graph, the data have been plotted in test run order, with five repeated runs at each of three speeds, with higher speeds for the later groups of runs and corresponding reductions in F_{30} .

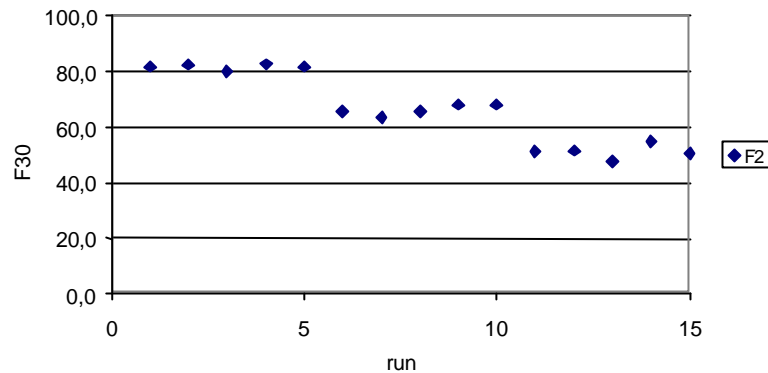


Figure 3.10 Dependence of F30 on slip speed (F02 on FR1)

In such cases, σ_{ij} will be high and the standard deviations for the repeatability and the reproducibility will be high also. The new formula for S_0 , therefore, is still not satisfactory. At this stage, it is worthwhile looking for other approaches that might provide a better description of the friction versus slip-speed curve.

(4) Validation limits of the exponential model

The exponential model was proposed almost 30 years ago to describe the decrease of friction for increasing slip-speed. The HERMES trial results have shown that this description is not complete. Depending on the device operating conditions and the surface, one of what has been described as the “Type 1” or “Type 2” patterns of behaviour can be observed. These different kinds of behaviour are frequent for porous asphalt surfaces and devices operating at low slip speeds.

A literature research showed that such behaviours correspond to actual physical phenomena or, more exactly, to the lubricated contact between the tyre and the road. Stribeck investigated a complete description of the friction versus slip-speed curve in 1902. The commonly observed friction – speed curve for tyre/road interaction can be regarded simply as a part of the general Stribeck curve. The next section of the report considers a new model based on this idea.

3.2.3.2 Investigation of a new model

In a Stribeck curve (Figure 3.11), friction between two surfaces separated by a lubricant is presented as a function of the parameter:

$$H = \frac{h \cdot S}{p} \quad (3.19)$$

Where:

- S is speed, which can be relative sliding speed depending on the authors;
- h is the lubricant viscosity;
- p is the apparent normal pressure.

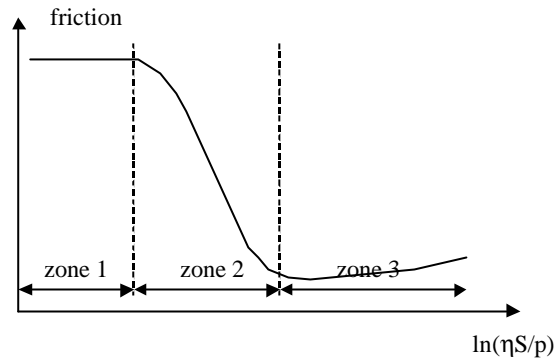


Figure 3.11 Example of the Stribeck curve

In Figure 3.11, three zones can be seen:

- Zone 1: the lubrication is called "boundary" because lubricant film is present at the interface, but its thickness is such that direct contact between the surfaces is possible without adhesion;
- Zone 2: the lubrication is called "mixed" because the lubricant supports part of the contact area;
- Zone 3: the lubrication is called "(elasto) hydrodynamic" because the lubrication film separates the surfaces.

In 1996, a Dutch working group proposed a modified H parameter for tire/road contact [7]:

$$H = \frac{h^a \cdot S^b}{p(h, V)^c \cdot h_t^d} \quad (3.20)$$

Where:

$p(h, V)$	is the effective contact pressure;
h	is water film thickness;
V	is vehicle speed;
h_t	is the texture depth;
a, b, c, d	are positive constants.

The main question is how to determine the shape of the effective-pressure function. Emmens [8] studied the mixed lubrication between two rough steel sheets, where friction is generated on isolated spots and reduced by the lubricant pressure at the sheet interface (Figure 3.12).

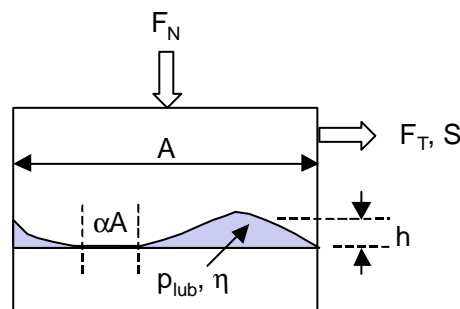


Figure 3.12 Pressure exerted by the lubricant at the interface between two sliding surfaces

According to Emmens, the lubricant pressure is given by:

$$p_{lub} = l \cdot \frac{h \cdot S}{h^2} \quad (3.21)$$

Where:

p_{lub} is the lubricant pressure;
 h is the lubricant viscosity;
 S is the relative sliding speed between the sheets;
 h is the average gap height created by surface roughness;
 l is a constant.

Due to surface roughness, the real contact area is a fraction aA of the total area “A” (Figure 3.12). The normal load is divided into two components:

$$F_N = F_m + F_{lub} \quad (3.22)$$

Where:

F_N is the normal load;
 F_m is a metal bearing component;
 F_{lub} is a lubricant bearing component.

Since $F_{lub} = p_{lub} \cdot (1-a) \cdot A$, the metal part is given by $F_m = F_N - p_{lub} \cdot (1-a) \cdot A$. The friction force is given by:

$$F_T = F_m \cdot m_m + t_0 \cdot (1-a)A \quad (3.23)$$

Where:

F_T is the friction force;
 m_m is the coefficient of friction at boundary lubrication ;
 t_0 shear stress in the lubricant.

Neglecting the lubricant shear stress in the case of water, the coefficient of friction is given by:

$$m = \frac{F_T}{F_N} = m_m \cdot \frac{F_m}{F_N} = m_m \left[1 - l \cdot \frac{h \cdot S}{h^2} \cdot (1-a) \cdot \frac{A}{F_N} \right] \quad (3.24)$$

Defining $p = \frac{F_N}{A}$ (normal pressure) and $H = \frac{h \cdot S}{P \cdot h^2}$, the coefficient of friction is then a linear function of H . Emmens found further that the gap height is best described by the R_{pm} parameter, which is the mean distance between the roughness profile mean line and highest peak.

It is of interest to note that the H parameter employed by Emmens is quite similar to that proposed by the Dutch working group, and that the standard definition of R_{pm} is similar to that of the MPD . This leads to the idea that, on the one hand, the effective pressure can

be approximated by the normal pressure and, on the other hand, the “ h ” parameter can be represented by the MPD . The H parameter (Equation 3.20) can then be written as

$$H = \frac{h^a \cdot S^b}{p^c \cdot MPD^d},$$

where p is the normal pressure. Before being able to applying this to the *HERMES* data, the major difficulty was to gather normal pressure values for the devices participating in the *HERMES* meetings. These values had been recorded in 1992 for the devices that took part in the *PIARC* experiment [1]. However, since H is quite sensitive to variations of p , current values of p would be preferable.

(1) *Similarity between Stribeck and Tyre/road friction curves*

A representation of friction as a function of slip speed for some of the devices participating in the *HERMES* exercises is provided in Figure 3.13.

For devices F05 and F08, it can be seen that the experimental points start from zone 1 of the Stribeck curve – where friction is almost constant – and go to zone 2, the intermediate speed being the transition point. For other devices, a linear tendency corresponding to zone 2 is observed. Actually, the “type I” and the “type II” behaviours mentioned in the statistical analyses correspond to the boundary lubrication and to the mixed lubrication conditions respectively.

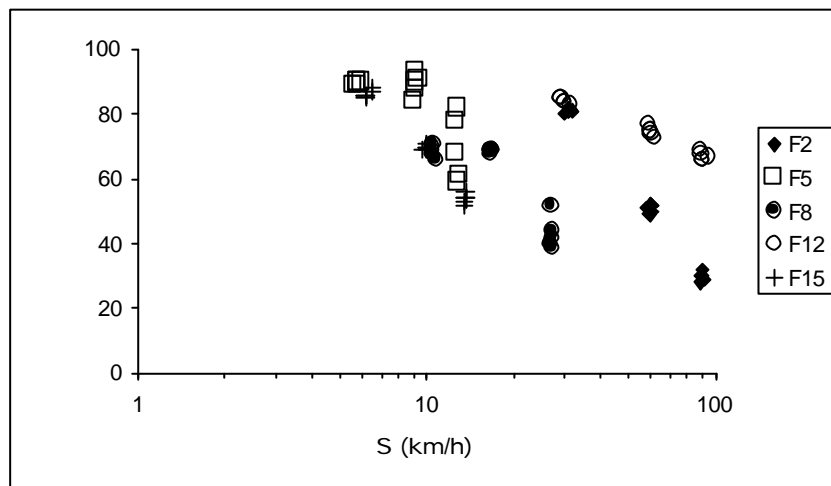


Figure 3.13 Example of friction – slip speed curves (Trial 2,2 – Surface FR1)

In the opinion of the authors of this report, the problems in relating the *speed parameter* to the MPD and the *slip ratio* that are caused by the measurement series for some device and surface combinations are not due to measurement errors. These have simply demonstrated that the exponential model is not always suitable for representing the variation of *friction* with *speed* and/or MPD is not sufficient to describe the road surface texture.

(2) *Application of the Stribeck presentation to tyre/road contact*

The question now is how to represent the inverse S-shape of the Stribeck curve. In the European collaborative project VERT (Vehicle Road Tyre interaction), the following function was proposed [10]:

$$m = m_{ref} \cdot \left(b_0 + \frac{b_1}{1 + b_2 \cdot e^{(b_3 + b_4 \cdot V)}} \right) \quad (3.25)$$

Where: m is the friction;
 m_{ref} is "reference" friction;
 V is test speed;
 b_i are constants ($i=1, \dots, 4$).

Emmens [8] proposed an arctangent function, which reproduces the first two zones well, even if zone 3, where friction starts to increase, cannot be represented. Van den Bol [9] proposed another logistic function called "the Gompertz function", which can be written in the following form:

$$F = a + g \cdot e^{-e^{-b \cdot (S-m)}} + e \quad (3.26)$$

Where: F is friction;
 S is slip speed in km/h;
 a, b, g, m are constants;
 e is an error term.

Values of the constant b must be strictly positive to obtain the required inverse S-shape variation. Since there are many constants to be estimated in this function, alternative functions were investigated. Studies related to failure phenomena such as fatigue usually employ the Weibull reliability function, which is written in the following form [11]:

$$R(t) = 1 - e^{-b \cdot t^a} \quad (3.27)$$

Where: R is the reliability function;
 t is time;
 a, b are constants.

Physically, the reliability function expresses the probability that an item will function up to a time (t) and will fail only after time (t). Example of variation of $R(t)$ with the time (t) is shown in the Figure 3.14 (the simulation represents $a = 3$, $b = 0,01$; time is expressed in arbitrary units). Since it has an S-shape, the appropriate function to give the inverted S-shape like a Stribeck curve is the complement, $1 - R(t)$.

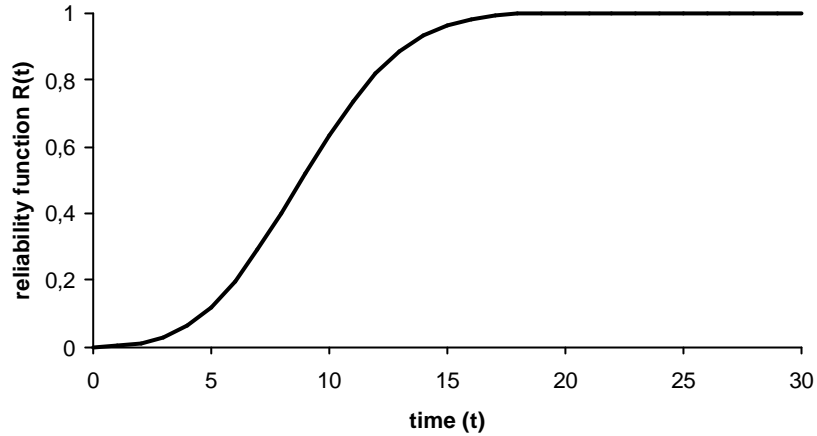


Figure 3.14 Example of the Weibull reliability curve

Among the various functions mentioned above, the complement of the reliability function proposed by Weibull, seems to be the most promising since it represents the inverse S shape, it is simple and its form is quite similar to the *PIARC*-model. For convenience, this will now be referred to as "the Stribeck function" (although it is only an approximation of the Stribeck Function).

Actually, equation (3.27) can be adapted and rewritten as :

$$F = F_0 \cdot \exp \left[- \left(\frac{S}{S_0} \right)^a \right] \quad (3.28)$$

With

$$S_0 = \left(\frac{1}{b} \right)^{\frac{1}{a}} .$$

In this form, formula 3.28 represents a generalization of the *PIARC*-model, which corresponds to the case where $a = 1$. The S_0 term still preserves its meaning and can be still called "the speed constant".

Thus, it was decided to adopt Equation 3.28 as a new friction model. It should be noted at this stage that no model can be used that is able to describe the small increase of friction for high slip speeds, because it is not possible to make an estimate of the coefficients of such a model (like the Gompertz function). At this stage, it was decided to use only the exponential term in order to simplify the calculations.

3.2.3.3 Fitting the new model to the *HERMES* data

Having arrived at a new model based on the Stribeck function, the next step was to fit this to data from the *HERMES* calibration trials. To simplify the calculations, the following equation was used to fit the data:

$$F = F_0 \cdot e^{-b \cdot S^a} \quad (3.29)$$

The following tasks were then performed:

- Fitting equation (3.41) to each measurement series of device and surface, giving the values of the constants F_0 , a and b ;
- Transformation of b into S_0 ;
- For the whole HERMES database, correlation between S_0 and physical parameters such as surface MPD or device slip ratio.

(1) Fitting constraints

In theory, for each measurement series of device and surface, there are between 9 and 15 values (3 slip speeds repeated 3 to 5 times) to fit a 3-constant function. In practice, however, the values are grouped around 3 slip-speed levels, which are very close to each other for low slip ratio devices. The major difficulty in fitting, then, is how to generate a realistic inverse S-shape curve from only 3 values.

The first tentative attempts at fitting showed that F_0 could be very high. Since this constant represents the friction at very low slip speeds and friction is actually measured on wet roads, it was thought that F_0 could be reasonably imposed to be less than 1.

For the constant b , in order to reproduce the decrease in friction, values were required to be positive.

It was noted that the relative widths of the zones 1 and 2 of the Stribeck curve depend on both a and b . Therefore, the value of a was adjusted by trial and error to obtain the observed zone 1 width from the HERMES data. It was found that a could be kept constant and that the best fit was obtained for $a = 3$.

In summary, the following constraints were imposed when fitting the new model to each measurement series for a surface and device combination, in order to reproduce an estimate of the Stribeck curve: $F_0 < 1$; $b > 0$; $a = 3$. It should be mentioned that these constraints are quite arbitrary and further investigation is needed, especially to derive eventually a physical meaning for the exponent a .

(2) Results of Fitting

Values of the constants F_0 , b and S_0 (recalculated from b) are reported in Annex E for Trials 1,1 to 3,3 respectively. Examples of the fitted curve are shown in Figure 3.15. On the left-hand graph, even though the fitted curve appears to be a good representation, uncertainties still exist, mainly in the right-hand part of the curve (corresponding to high slip speeds) due to the absence of experimental data. The graph on the right shows that the new model does not work as well as the exponential model in the case of locked-wheel devices. This is caused by the constraints that are imposed in the curve-fitting; the experimental data showed a clear S-shape.

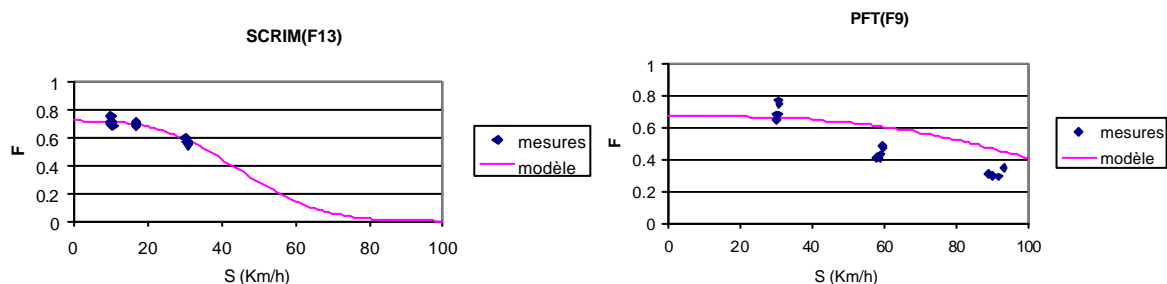


Figure 3.15 Examples of model fitting

It could be said at this stage that, with the exception of locked-wheel devices the new model fits the experimental data well. However, to be of practical use, the model constants must be related to physical parameters. Investigation was therefore focused on the relationship between the speed parameter S_0 , the surface *MPD* and the device *slip ratio*. The constant F_0 is ignored at first, since it is not required for the calculation of the *EFI* (F_0 disappears when expressing $F(30)$ as a function of $F(S)$).

3.2.3.4 Relationship between S_0 , surface *MPD* and device *slip ratio*

Two steps are required to establish a formula relating S_0 to *MPD* and *slip ratio*:

- Perform the analysis of variance for each *HERMES* meeting to derive the variation of S_0 with the *MPD* for different values of the *slip ratio* (and vice versa).
- Carry out the regression between S_0 , *MPD* and *slip ratio*.

(1) Analysis of variances

An example of graphs of variation of S_0 is shown in Figure 3.16 (for Trial 2,2). It can be said that S_0 varies non-linearly with the *slip ratio* and, to a lesser degree, with the *MPD*. The “unexpected” measurement series of device and surface are summarised in the Table 3.7.

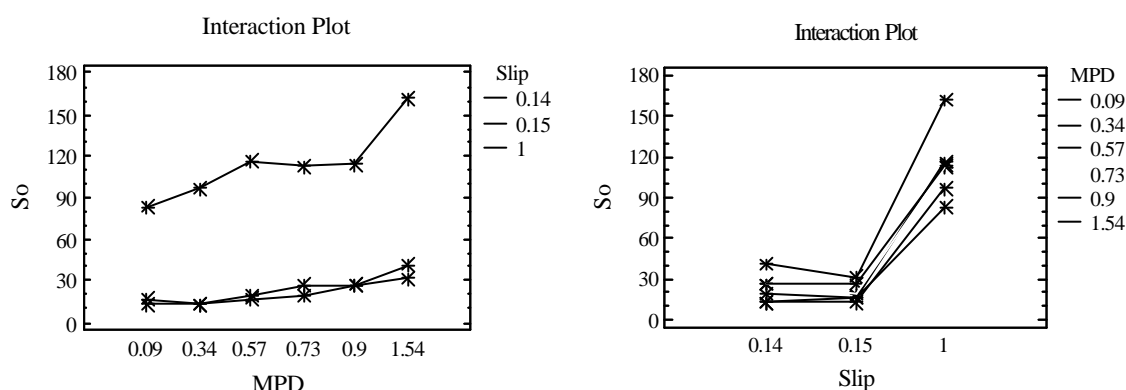


Figure 3.16 Example of the variation of S_0 with *MPD* and *slip ratio*

Table 3.7 Summary of unexpected measurement series

	Meeting								
	1,1	1,2	1,3	2,1	2,2	2,3	3,1	3,2	3,3
Measurement series				F05/BE3				F05/BE10 F05/BE11 F05/BE13	F05/FR12

No explanation has been found for these special cases. It can be noted that there are fewer unexpected measurement series with the new model (5 cases) than with the original exponential model (28 cases) and that some are different. This is further evidence of the fact that the unexpected behaviour is caused by inaccurate models and not by any physical problem. The most significant fact is that, this time, all the “unexpected”

measurement series were related to the F05 device, which might have been caused by the use of partially-incorrect data for this device.

(2) *Regression*

Next, it was proposed that S_0 should be related to the *MPD* and the *slip ratio* using Equation 3.30:

$$S_0 = a_1 \cdot MPD^{a_2} \cdot (slipratio)^{a_3} \quad (3.30)$$

Multiple-linear regression was performed on the logarithmic transformation of Equation 3.30 using the whole *HERMES* database except the special cases listed in Table 3.7. It was found that the regression coefficient was high ($R^2 = 0,91$), demonstrating the improved relevance of the model (a coefficient of 0,69 was obtained with the *PIARC*-exponential model).

The comparison between measured and calculated values of $\log_{10}(S_0)$ is shown in Figure 3.17. Again, a curvature and a large scatter around the line of equality can be seen in this graph.

The fitted relationship between S_0 , *MPD* and the *slip ratio* is then:

$$\log(S_0) = 0,27 \cdot \log(MPD) + 0,92 \cdot \log(slipratio) + 2,09 \quad (3.31)$$

This regression analysis led to a subsidiary question: would it be possible to further improve the prediction of S_0 when device-specific relationships between S_0 and *MPD* are developed?

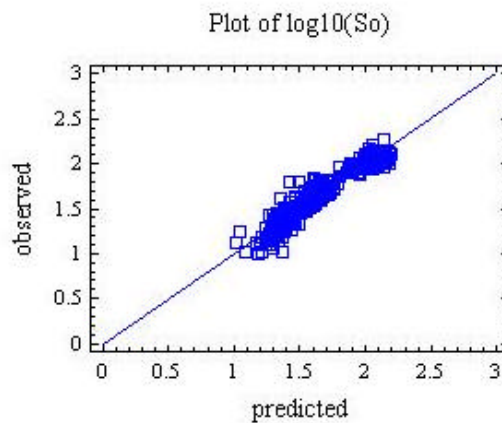


Figure 3.17 Validation of the regression $\log(S_0) = \log(a_1) + a_2 \cdot \log(MPD) + a_3 \cdot \log(slip ratio)$

(3) *Derive device-dependent constants by individual regression between S_0 and *MPD**

Data used to derive the relation (3.31) were divided into 15 sub-databases: each sub-database included all S_0 values obtained by one device from different *HERMES* meetings as well as the corresponding values of *MPD*. An example of the graphs describing the relation between S_0 and *MPD* is shown in Figure 3.18. The colours identify the different trials. It can be seen that the non-linear variation of S_0 with *MPD* is more or less pronounced, depending on the device.

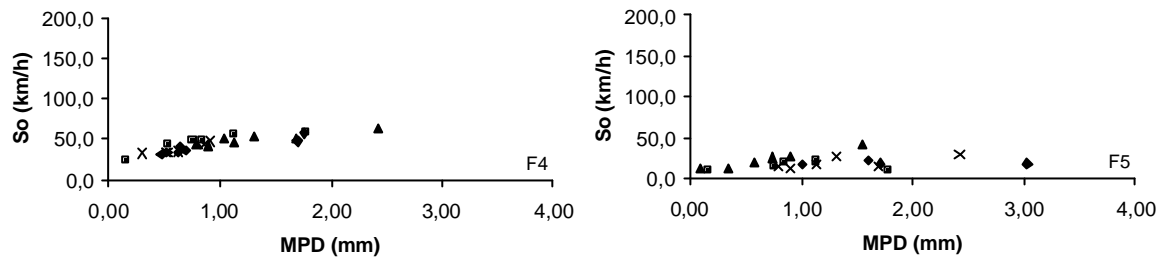


Figure 3.18 Example of S_0 – MPD graphs from different comparison meetings put together.

Linear regression was performed on $\log_{10}(S_0)$ (dependent variable) and $\log_{10}(MPD)$ (independent variable) to give:

$$\log(S_0) = a \cdot \log(MPD) + b \quad (3.32)$$

Values of the regression constants for each device are given in Table 3.8.

Table 3.8 Constants for the regression $\log_{10}(S_0) = a \log_{10}(MPD) + b$ for each Device

	F01	F02	F03	F04	F05
a	0,158	0,191	0,265	0,361	0,191
b	2,032	2,029	1,684	1,665	1,269
	F06	F07	F08	F09	F10
a	0,321	0,233	0,434	0,095	0,488
b	1,428	2,054	1,603	2,016	1,438
	F11	F12	F13	F14	F15
a	0,428	0,095	0,249	0,291	0,291
b	1,402	2,086	1,688	1,547	1,307

It is interesting to notice that again there was a very close relationship between the device-dependent constant “b” and the slip ratio (Figure 3.19).

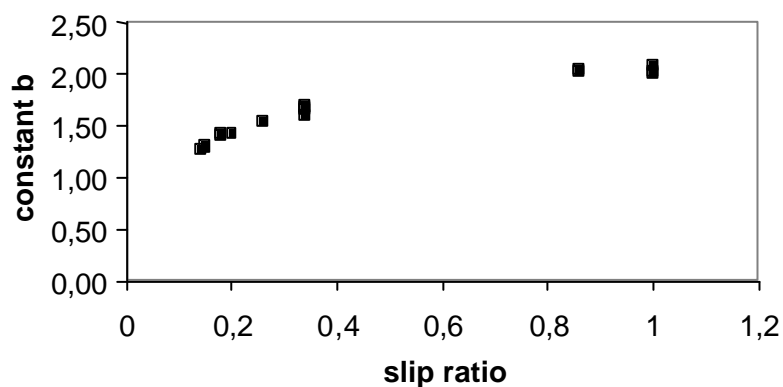


Figure 3.19 Relationship between device-specific constant (b) and slip ratio

Logarithmic fitting was performed, giving the following formula:

$$b = 0,90 \cdot \log(\text{slipratio}) + 2,07 \quad (3.33)$$

Formula 3.33 can now be written as:

$$\log(S_0) = a \cdot \log(MPD) + 0,90 \cdot \log(\text{slipratio}) + 2,07 \quad (3.34)$$

Where: a is a device-specific constant.

The formulae 3.31 and 3.34 are quite similar. It can thence be concluded that individual regression leads to the same formula as that given by the general regression. The only difference is that the value of the MPD exponent is now device- dependent.

The values of S_0 that emerged from fitting the physical data, called "observed values", were then compared to those calculated from equations 3.43 and 3.46. For each device, the relative difference between the observed and calculated values - the ratio $((S_0 \text{ observed} - S_0 \text{ calculated})/S_0 \text{ observed})$ - was determined (each ratio was related to a specific road surface on which the friction measurements had been carried out) and averaged. The mean ratios related to the general regression were then compared with those related to device-specific regressions (Figure 3.20). The prediction was good when the ratio was low. It can be seen that the prediction of the speed constant is slightly improved when device-specific constants, mainly the MPD exponent, are used. From the graph it can be seen that, for some devices this is more than a "improvement". On the other hand, the method chosen to compare both methods is not capable of determining systematic effects.

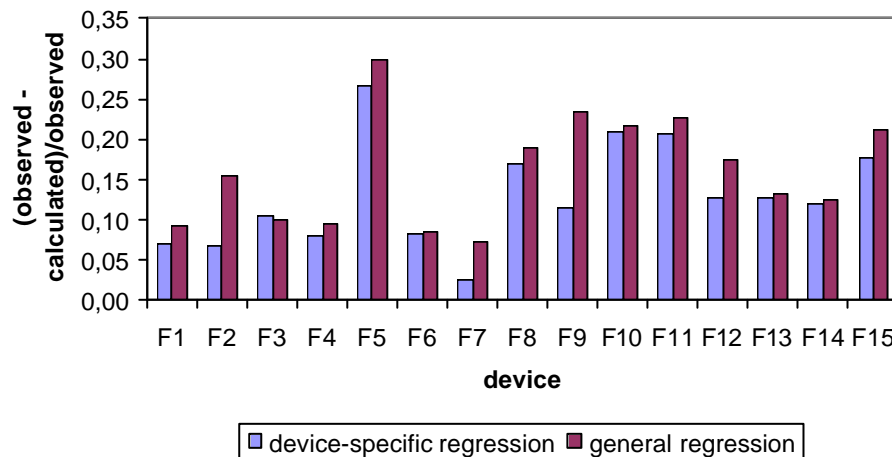


Figure 3.20 Improvement of the prediction of S_0 using device-specific parameters

3.2.3.5 Resulting friction model based on tribology approach

The following formula is proposed for the calculation of the friction at a slip speed S , based on the Stribeck function:

$$F(S) = F_0 \cdot e^{-\left(\frac{S}{117(MPD)^a \cdot (\text{slipratio})^{0,9}}\right)^3} \quad (3.35)$$

Where: F_0 is the “theoretical” friction at 0 km/h slip speed;
 S_0 is the speed constant, in km/h;
 a is a device-specific constant.

Since the Stricbeck curve shows a stable-friction zone for low slip speeds, the constant F_0 can be estimated from friction measured at low speeds; less than 20 km/h, say. Values of the constant “ a ” for the devices participating in the *HERMES* calibration trials are summarized in Table 3.9.

Table 3.9 Constant (a) of LCPC model for each *HERMES* Device

	F01	F02	F03	F04	F05
a	0,158	0,191	0,265	0,361	0,191
	F06	F07	F08	F09	F10
a	0,321	0,233	0,434	0,095	0,488
	F11	F12	F13	F14	F15
a	0,428	0,095	0,249	0,291	0,291

3.2.4 Investigation of alternative characteristics of surface texture depth

In earlier Sections, it has been shown that *MPD* alone is not necessarily the correct explanatory factor to use to predict the speed dependency of the friction devices. This observation prompted an additional analysis at *TRL* to attempt to determine whether other characteristics of the surface texture might be more successful.

For sites where the texture profile data were available, a number of additional characteristics of the texture depth were calculated. The texture profile data were filtered to pass wavelengths within octave bands centred at 2, 4, 8, 16, 31,5, 63, and 125 mm, as well as the 2 mm to 100 mm wavelength range used for the *MPD* calculation. The filtered profiles were then characterised by:

- the root mean square (RMS);
- ten percentile and ninety percentile measures of the filtered profile heights;
- the skewness of the distribution of profile heights.

A method similar to the *MPD* calculation was also applied at each of the different wavelength ranges. In this method, for each 100 mm length of the filtered profile, the highest profile point in each half of the 100 mm length was identified and the average of these two values was calculated. This method is referred to below by the shorthand “peak-pick” (i.e., choosing the highest point) to distinguish it from *MPD*, which requires a specified wavelength range. The *MPD* values from the *HERMES* database and the Sensor Measured Texture Depth (*SMTD*) method, a root mean square texture depth method used in the UK since the late 1970s, were also included.

For analysis, the friction devices were grouped into categories by their *slip ratio*, taking note of the observation that the speed dependency was influenced by the *slip ratio*. The devices grouped in each category are listed in Table 3.10.

For each category, the correlation coefficient for the linear regression between the “real” S_0 values and the values of each texture characteristic was calculated. The R^2 values for the most highly correlated texture characteristics are listed in Table 3.11.

Table 3.10 Device grouped by slip ratio

Grouping criterion	Friction device
Low slip ratio (<0,2)	F05 Grip Tester
	F06 ROAR
	F10 OSCAR
	F11 ROAR
	F15 IMAG
Intermediate slip ratio (0,34)	F03 SCRIM
	F04 SCRIM
	F08 Odoliograph
	F13 SCRIM
	F14 Odoliograph
High slip ratio (0,86 – 1,0)	F01 DWW trailer
	F02 ADHERA
	F07 ROAR
	F09 PFT
	F12 SRT3

Table 3.11 Texture characteristics most highly correlated with S_0 values

High slip ratio			Intermediate slip ratio			Low slip ratio		
Rank	Characteristic*	R^2	Rank	Characteristic	R^2	Rank	Characteristic	R^2
1	8 mm; 10 percentile	0,07	1	2-100 mm; peak-pick	0,29	1	2-100 mm; 90 percentile	0,23
2	4 mm; 10 percentile	0,07	2	2-100 mm; 90 percentile	0,25	2	2-100 mm; RMS	0,21
3	4 mm; 90 percentile	0,07	3	63 mm; peak-pick	0,22	3	2-100 mm; peak-pick	0,21
4	8 mm; 90 percentile	0,06	4	125 mm; peak-pick	0,22	4	UK SMTD	0,21
5	8 mm; peak-pick	0,05	5	63 mm; 90 percentile	0,22	5	16 mm; 10 percentile	0,21
7	MPD (HERMES)	0,05	7	63 mm; RMS	0,21	12	63 mm; RMS	0,20
13	2-100 mm; peak-pick	0,02	14	UK SMTD	0,18	13	16 mm RMS	0,19
22	UK SMTD	0,01	19	MPD (HERMES)	0,14	20	MPD (HERMES)	0,17
* Characteristic texture parameter listed as (wavelength range; method)								

In all cases, the low overall amount of variation explained by any individual texture characteristic was disappointing. Furthermore, the performance of the 2 to 100 mm peak-pick calculation performed for this analysis and the *MPD* values from the *HERMES* dataset (both highlighted in Table 3.11) were different. Since these methods are ostensibly the same, this again highlights problems with the definition of the *MPD* method.

As judged by the R^2 values, the 2 to 100mm peak-pick method is the best single texture parameter, or close to the best method, for both the intermediate and low *slip ratio* categories. The ninety percentile method using the same wavelength range ranks highly, as does the RMS-method for the low *slip ratio* devices. The ninety percentile method would be worth considering as an alternative to *MPD* because it uses at least 10 texture profile values to determine the texture.

For the intermediate and low *slip ratio* categories, the long wavelength features seem to be the most important in determining the speed dependency. In contrast, for the high *slip ratio* devices, the short wavelength texture characteristics are the most successful. However, the correlation, while significant at the 90% level, explains only a very small amount of the overall variation in S_0 values for the high *slip ratio* devices.

Although it would be desirable to study the individual friction devices separately, the large amount of variability in the measurements for individual devices in this dataset made it difficult to determine trends for the individual friction devices with confidence. (This was partly because texture profile data were not available for all the *HERMES* test sites). Therefore, two larger UK databases were investigated to see if the larger amount of data would make it possible to establish more robust relationships for the two UK friction devices.

The first database consisted of friction measurements at 20, 50, 80 and 100 km/h for device F09 (using the locked wheel method). These measurements were obtained from nearly 150 UK sites covering a wide range of surface types. These friction values were used to determine “real” S_0 values, as described above. However, the values obtained may not correspond exactly to those measured in the *HERMES* experiment because the speed range is different. Texture measurements were available as Sensor Measured Texture Depth (*SMTD*) values from the UK *SCRIMtex*, which, as well as participating in *HERMES*, also participated in the *PIARC* experiment. *MPD* data were not available for these sites, but *MPD* values are typically a factor of between 1 and 1,4 times larger than *SMTD* values, depending on the surface type.

Figures 3.21 & 3.22 show that, for these data, the S_0 values are highly correlated with the texture depth, through a linear or power relationship, but it can also be seen that a substantial scatter about the overall trend remains, particularly when porous surfacing materials are included. The overall standard deviation of the residuals, excluding porous materials, is 16,7, although this may be dependent on the *SMTD* value.

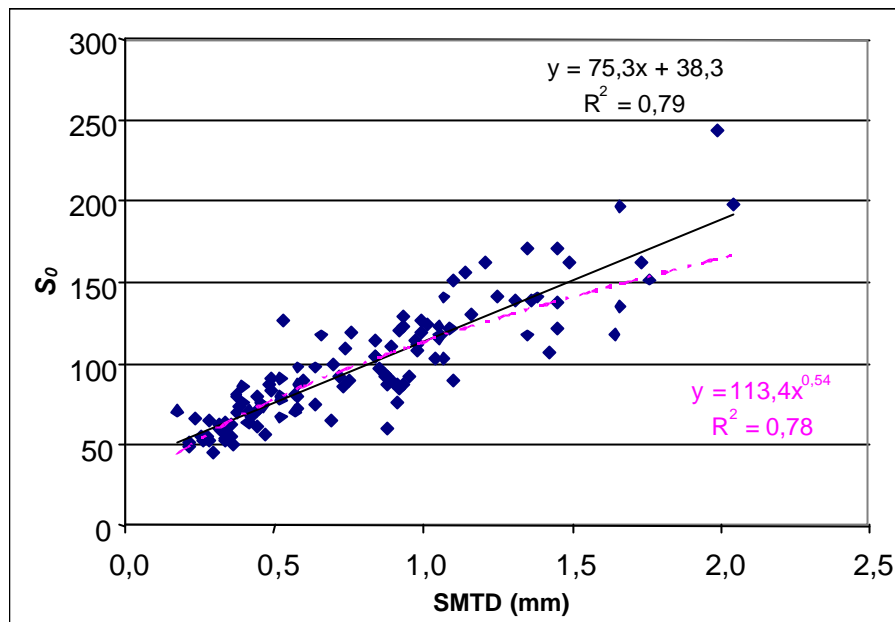


Figure 3.21 Relation between S_0 and texture depth for device F09 (UK dataset, excluding porous materials). Solid line: linear regression. Axis line: exponential regression.

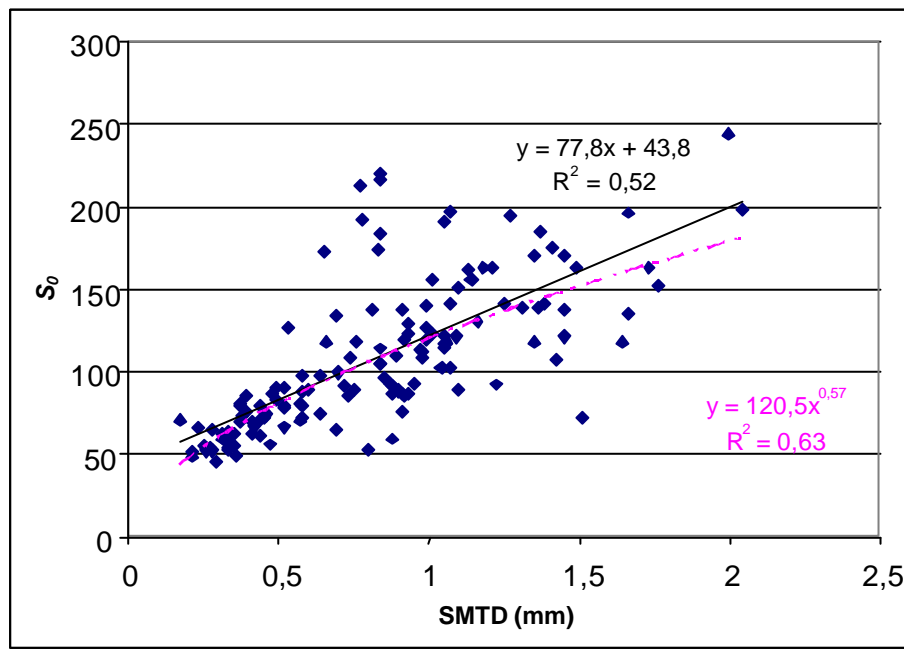


Figure 3.22 Relation between S_0 and texture depth for device F09 (UK dataset including porous materials). Solid line: linear regression. Axis line: exponential regression.

The choice of test tyre for device F09 (smooth or ribbed) also has a substantial influence on the value of S_0 , as indicated in Figure 3.23, which shows the distribution of values obtained on the same sites with different tyres. This is expected, because it is known that

measurements using ribbed tyres are less influenced by speed than measurements using smooth tyres. However, this result suggests that the different characteristics of the test tyres could be one reason for the need for S_0 values to be specific to the friction device.

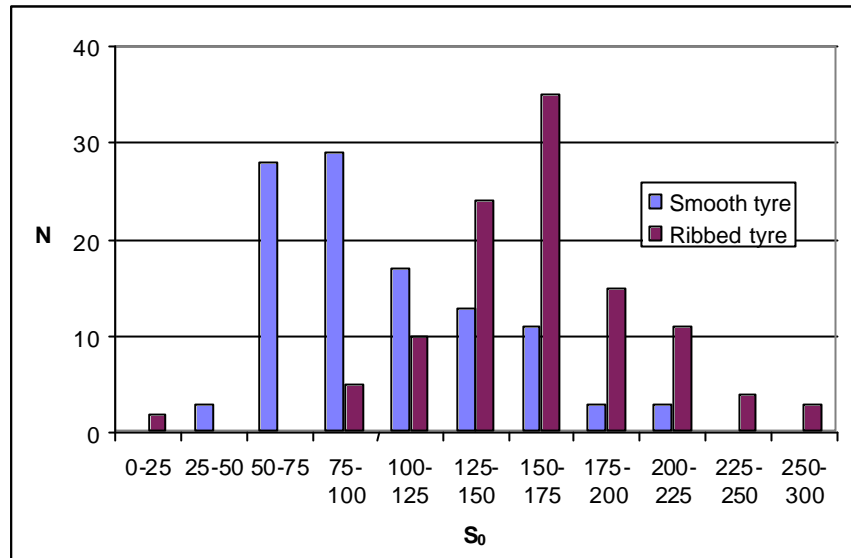


Figure 3.23 Comparison of S_0 values measured using smooth and ribbed tyres

The second dataset comprised measurements on over 45km of in-service roads made at two test speeds by device F13 (the UK SCRIM). For each 100 m section, the “real” S_0 value was calculated from these two measurements. Determining the S_0 value in this way (i.e., from only two points) will be less precise than in the earlier analysis but this is offset in the analysis by the large amount of data available. The relationship between S_0 and $SMTD$ is shown in Figure 3.24, by surface type. A small number of extreme S_0 values (those below zero or above 300) have been excluded from this analysis.

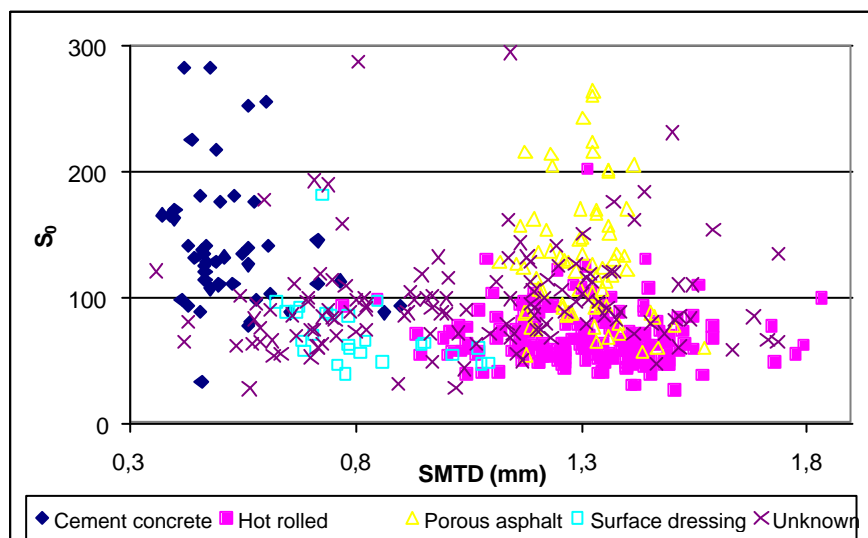


Figure 3.24 Relation between S_0 and texture depth for device F13 (UK dataset)

In contrast with device F09, where there was a clear trend with the texture depth, for device F13, the trend with texture depth is not significant at the 90% level. However, the data indicate that the surface type will be significant in determining the S_0 value for this device.

This additional analysis indicates that different features of the surface type and surface texture influence the speed dependency of the different friction measurement devices. The variability of the measurements exhibited by the two UK devices when examined on a larger dataset suggest that it may be necessary to determine the characteristics of the individual devices on a much wider scale than was possible within the *HERMES* experiment. Furthermore, should some devices be found to be more sensitive to effects that cannot be adequately measured using current technology then it may be necessary to consider whether they can be fully included in the harmonisation procedure.

3.3 Discussion

From the analyses in this chapter it can be concluded that, although the models can be improved, the accuracy of the *EFI* is still poor. Where individual devices show values for repeatability and reproducibility of about 0,03 and 0,04, the *EFI* has a repeatability of 0,23 and a reproducibility of 0,23 – 0,40 depending on the model that is used for the calculation. This means that the *EFI* (and a comparison between devices) is not sufficiently accurate for the purposes for which skid resistance measurements are normally used (assessment of skid resistance after accidents, acceptance of new works, and planning of maintenance works).

The inaccuracy can be understood by looking at the procedures for the calculation of the *EFI*. In Figure 3.25 a theoretical example of a friction curve is shown. In this graph, measurements are indicated for three devices with different slip percentages at three different speeds.

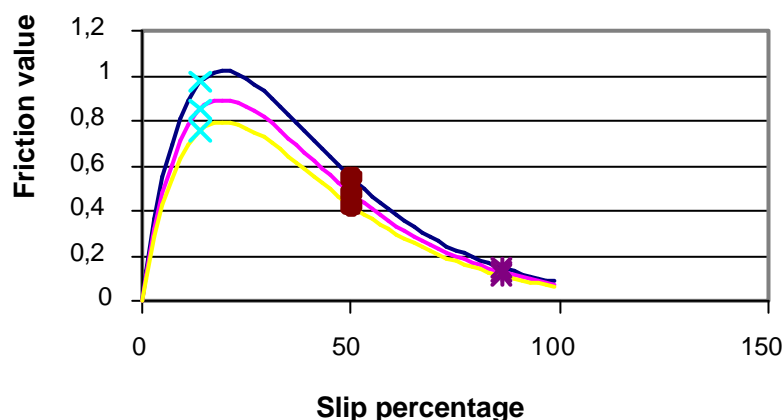


Figure 3.25 Theoretical friction curves at a site X for three different devices.

With this information, the figure can be transformed to a graph showing the relation between *friction value* and *slip speed*. This graph is shown in Figure 3.26.

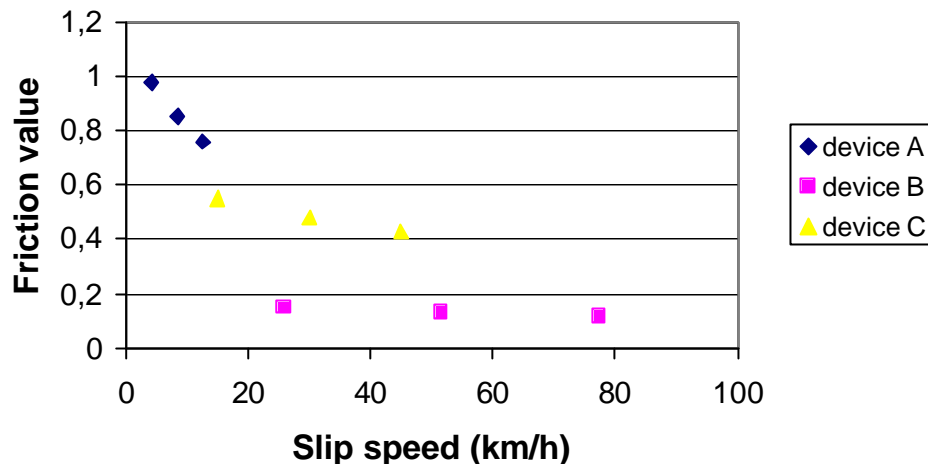


Figure 3.26 Relation between the friction value and slip speed for site X

From Figure 3.26, the reason why a reference slip speed of 60 km/h gives such poor results becomes apparent. Transforming a measurement value at a given slip speed to a slip speed of 60 km/h means an extrapolation for all devices with the exception of those with high slip percentages and devices with locked wheel. A reference speed of 30 km/h means less extrapolation, demonstrating that the decision to use 30 km/h as reference slip speed for *EFL* that was made in the Belgian study [2] was sound.

However, extrapolation is still necessary for devices with a low slip percentage and with this extrapolation a source of error is introduced. This can be shown in Figure 3.27, in which linear and quadratic regression lines are drawn for the three devices.

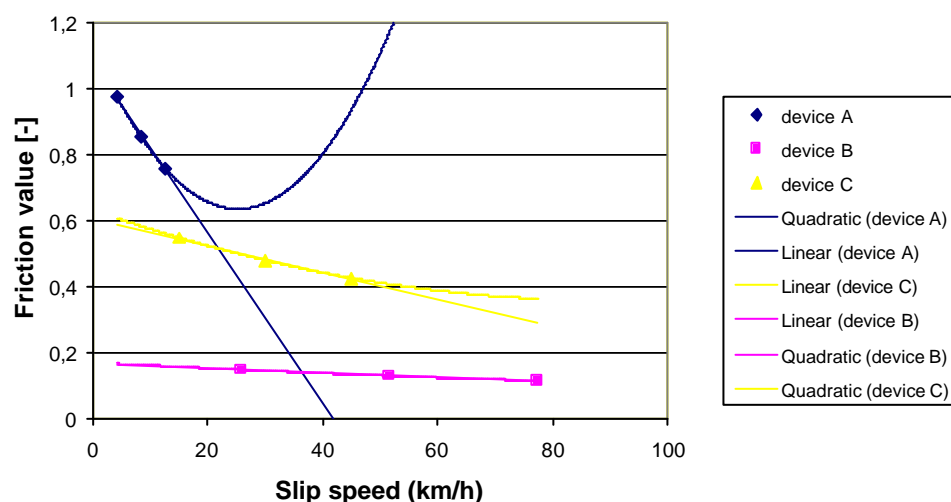


Figure 3.27 Example of different methods for the regression analysis

Devices with high slip percentages (and therefore a larger difference in slip speed with the three vehicle speeds used in the experiments) show only small influences of the model that is used. On the other hand, devices with low slip percentages (most of the devices in the experiments) show a large influence of the model used for the calculation of F_{30} . A way to overcome this problem would be to operate devices with low slip percentages at

other (higher) speeds than the devices with high slip percentages. This, however, introduces new problems such as traffic safety during calibration meetings and the water flow needed when measuring at higher speeds.

Since the different devices all measure on a different part of the friction/slip curve (before, around or after the peak of the curve), it is difficult to find a general model to describe the speed dependency of the friction measurement. New research into the interaction between devices and sites is necessary to develop better models for the calculation of a common scale for friction measurements. When new parameters are found or derived from existing data it might even be possible to use non-linear models, from which it has been shown that an improvement can be achieved. The practical problem at present that no, or at least insufficient, physical parameters are available to determine the constants of the more complex models.

Unfortunately, for the next few years, the normative Annex A [3] will be the best available for a standard regarding road surface friction. A lot of extra research into the interaction between devices and sites is necessary before an accurate harmonized friction value will be available.

For the short term, it might be a solution to use different relationships for devices operating at almost the same *slip ratio*. This, again, is far from a harmonised friction value. Another possibility is to define pairs of devices of which the measurement results at the normal operating speed of these devices show a good correlation against each other. The data from the *PIARC* experiment and the *HERMES* calibration exercises should give enough information to determine these relationships between devices.

The most important question to answer, however, is what level of accuracy is needed, either using models or by direct comparison of devices.

4 Alternative processing of experimental data

4.1 Introduction

Section 2.4 presented an initial analysis that followed the calculation procedures and used the models specified in the draft *CEN* standard. Chapter 3 has explored possible ways of improving the models. A further important part of the HERMES project, partly carried out in parallel with the model development work, was to use the data from the calibration meetings to explore ways of improving the reliability and precision of the calibration procedure.

This chapter presents successive attempts to improve the procedures by applying different treatment scenarios to the experimental data, including utilising the more promising of the ideas discussed in Chapter 3.

The two scenarios already considered in Section 2.4 and the twelve more considered in this chapter are brought together and summarised in a table at the end of this part of the report, in Section 4.14.

4.2 Improved model for S_0 vs. MPD

In Section 2.4.9, it was pointed out that when plotting S_0 vs. MPD the scatter is rather wide. Looking at the graphs presented in Annex C, it appears that the relationship between S_0 and MPD depends on the friction device. This means that “ a ” and “ b ” in equation (2.8) should be considered as device-specific. But then it is clear that a linear equation is no longer adequate, for two reasons.

Firstly, as illustrated by the example in Figure 4.1, back-calculating S_0 for small values of MPD can yield small, negative values of S_0 , which is not acceptable because it can lead to enormous, absurd, values of $F30$ and EFI . This happened eight times in the HERMES data, in Trials 1,1, 2,2 and 3,3 where very smooth surfaces were tested (Annex C).

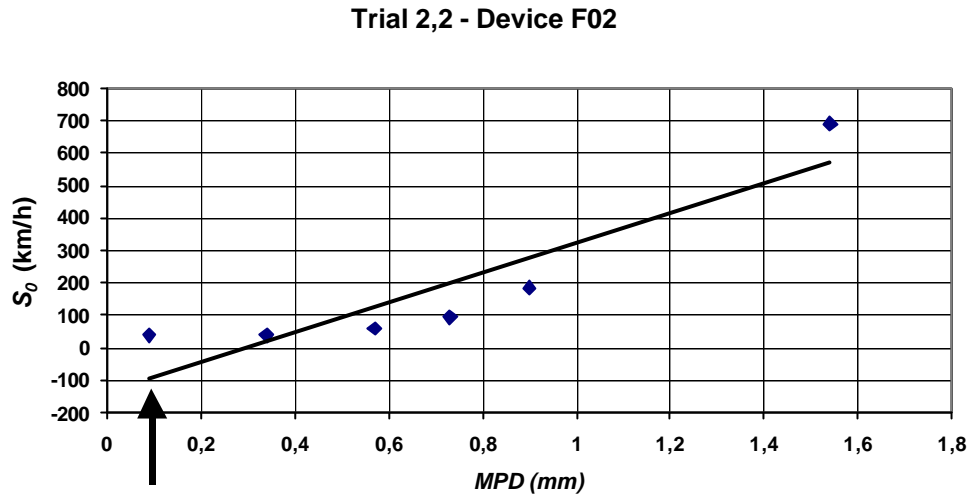


Figure 4.1 Example illustrating the need for a non-linear relationship between S_0 and MPD . The arrow points to a case where the predicted value for S_0 is negative.

Secondly, a non-linear curve provides a better fit to the data. It has been found (Section 3.4.3) that, in general, a power law offers the closest fit, i.e.:

$$S_0 = a \cdot MPD^b \quad (4.1)$$

where “a” and “b” are device-specific, as are “A” and “B”.

Values were determined for “a” and “b” using a least squares regression on the logarithmic form of (4.1), i.e.:

$$\ln S_0 = \ln a + b \cdot \ln MPD \quad (4.2)$$

As there were still many cases where the scatter was rather wide, a weighting was applied in the calculation in order to minimize the influence of less significant S_0 values. To that end, the weighting (w) was set to be inversely proportional to the squared relative standard deviation s_{S_0} of S_0 with respect to the regression line in equation (2.20). Then, the regression equation becomes:

$$w \cdot \ln S_0 = w \cdot \ln a + w \cdot b \cdot \ln MPD \quad (4.3)$$

with

$$w = (S_0 / s_{S_0})^2 \quad (4.4)$$

A good example of the effect of weighting is shown in Figure 4.2. Annex F presents all the graphs of S_0 vs. MPD with the fitted weighted and unweighted curves.

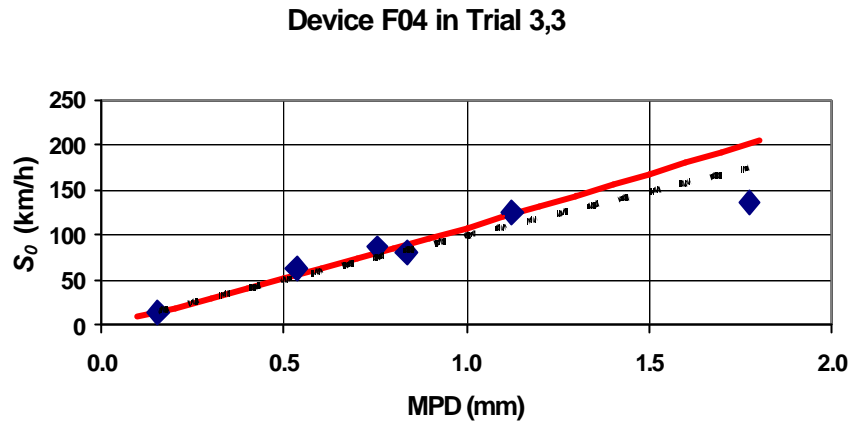


Figure 4.2. This is an example of the effect of weighting in the regression of S_0 vs. MPD. The solid and dotted lines represent the weighted and unweighted regressions respectively

In all subsequent processing of the experimental data, the new, weighted, model has been applied, except in Scenario #12 (Section 4.11).

4.3 Statistical tests

As suggested in Section 2.4.12, an attempt to improve the procedure by using different statistical tests has been made by applying the consistency tests described in ISO 5725-2 [5] while considering the different friction devices as different “laboratories”. The object of the measurement is the “true” EFI -value of a given surface. We call the 5 repeated runs at the 3 different speeds “a measurement series”. The “k-test” detects the measurement series made by a given device on a given surface that exhibits a repeatability standard deviation (s_r) excessively large in comparison with the average repeatability of all the devices on the surface being considered. The “h-test” detects those measurement series made by a given device on a given surface that exhibit an average EFI -value ($\langle EFI \rangle$) excessively deviating from the grand average ($\langle \langle EFI \rangle \rangle$) of EFI -values reported by all the devices on that surface. The latter test has, of course, to be applied after calibration, i.e. on EFI -values re-calculated using A_{new} and B_{new} .

When these tests were applied to the HERMES data, a probability level of 0,5% was used. The “k-test” was applied first and the measurement series that did not pass that test were discarded. The “h-test” was subsequently applied to calibrated EFI -values and those measurement series that failed were discarded. Then, $\langle \langle EFI \rangle \rangle$ had to be re-calculated, together with “A” and “B”, using the remaining data.

In addition to those standard tests, a test has been applied on the correlation coefficient (R_F^2) of the regression F against S . The measurement series with $R_F^2 < 0,5$ were discarded from the calculations.

A similar test was made on the correlation coefficient (R_{EFI}^2) of the calibration regression equation: $\langle \langle EFI \rangle \rangle = a + b \cdot EFI$. Cases where $R_{EFI}^2 < 0,5$ were flagged but not discarded.

4.4 Scenario #2: applying new statistical tests

In Scenarios #0 & #1 used in Section 2.4, the statistical tests proposed in the draft standard [3] were applied. As an alternative, in Scenario #2, the four statistical tests described in Section 4.3 were applied. Table 4.1 reports the percentage of measurements eliminated by the different tests.

Table 4.1 Percentage of measurements eliminated by the different tests

Test applied	Proportion eliminated at each trial									Total
	1,1	1,2	1,3	2,1	2,2	2,3	3,1	3,2	3,3	
$R_F^2 < 0,5$	3,3%	0,0%	0,0%	6,7%	8,0%	2,5%	4,2%	5,2%	4,8%	4,2%
$k > k_{0,5\%}$	14,0%	20,9%	12,5%	16,6%	16,7%	16,7%	25,0%	14,5%	14,3%	16,4%
$h > h_{0,5\%}$	16,2%	13,3%	12,5%	5,8%	3,3%	11,4%	20,8%	2,4%	0,0%	8,5%
Total	33,4%	34,2%	25,0%	29,2%	28,0%	30,6%	50,0%	22,1%	19,1%	29,1%

The test on R_F^2 appears to be both effective and useful since it eliminates really poor measurement series, as can be assessed by looking at the specific cases in Annex B. The cases of interest in this context are listed in Table 4.2. In all subsequent Scenarios, that test will be applied.

It appears that the consistency tests are again unacceptably severe. In some cases, the application of the “k-test” did not allow the analysis to move on to the calibration calculation because only the results from one surface were left. This happened for device F05 in Trial 2,1 and device F11 in Trial 2,3. Moreover, despite having discarded failing measurement series, in 33% participations (14 out of 42), devices were flagged because R_{EF}^2 remained lower than 0,5.

It was concluded that the “h- and k-tests” are helpful, but they cannot be used in practice with the linear models because of the inaccuracy of these models.

Table 4.2 Measurement series exhibiting a correlation coefficient of $F(S)$ lower than 0,5

Trial	Device	Surface
1,1	F10	GB06
2,1	F05	BE03
2,1	F05	BE07
2,1	F09	BE04
2,1	F10	BE07
2,2	F08	FR04
2,2	F08	FR06
2,2	F15	FR06
2,3	F11	NL10
3,1	F06	GB05
3,2	F08	BE09
3,2	F13	BE12
3,3	F10	FR09
3,3	F10	FR11

4.5 Scenario #3: applying simpler statistical tests

Here, only the test on R_{EFI}^2 is applied. But, in addition, a test is made on whether the coefficient of variation (CV_{EFI}) of the range of EFI values reported by the device being considered is larger than 10% (Scenario #3a) or 5% (Scenario #3b). This supplementary test is designed to prevent calibration regressions based on a very narrow range of EFI values, even with a high correlation coefficient, to be taken into account and spoil the whole procedure. The worst of such cases is shown in Figure 4.3.

With this scenario, the devices that did not pass either the test on R_{EFI}^2 or on CV_{EFI} in a given trial were not considered to be calibrated. In that event, for this analysis, the “old” values for “A” and “B” were kept until they next participated in a trial. If any reference devices were in this category, they were treated as though they were not reference devices in that trial and the calculations were repeated without including their EFI -values in the grand average $\langle\langle EFI \rangle\rangle$. (In practice, a device that was not calibrated would not be able to be used to provide EFI values until it had successfully participated in a future trial). The outcome of this approach is presented in Tables 4.3 and 4.4.

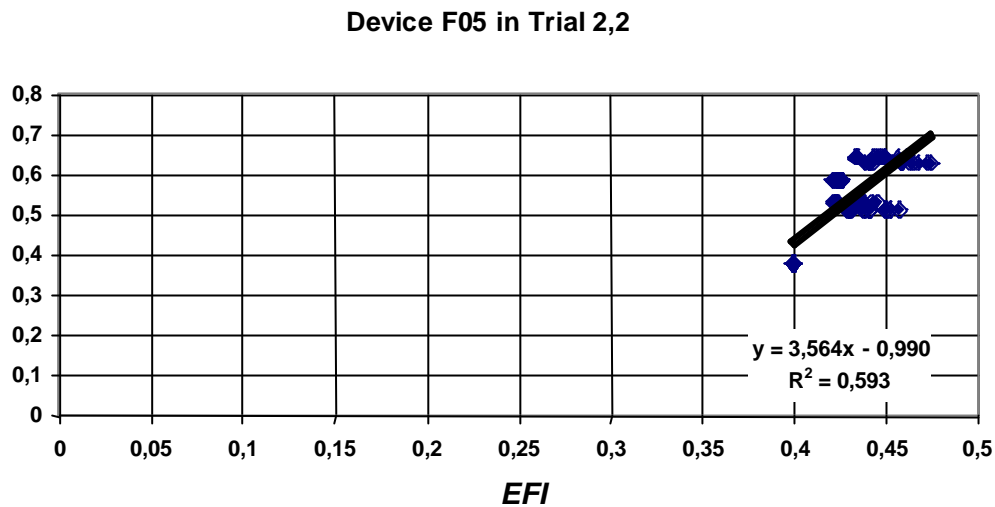


Figure 4.3 An example of a calibration regression based on a very narrow range of EFI values, while still exhibiting an acceptable correlation coefficient.

Table 4.3 The outcome of Scenario #3a. Superscript ^R means that the calculations have been repeated after the reference devices failing either test were discarded.

Trial	Device	Reference	R _{EFI} ²	CV _{EFI}
1,1	F09	YES	0,914	0,22
	F10	NO	0,638	0,68
	F12	YES	0,882	0,29
	F13	YES	0,941	0,41
1,2	F01	YES	0,020	0,06
	F04	YES	0,777	0,29
	F06	NO	0,798	0,29
	F07	NO	0,171	0,07
1,2 ^R	F04	YES	0,826	0,29
	F06	NO	0,701	0,29
	F07	NO	0,078	0,07
1,3	F01	YES	0,850	0,12
	F02	YES	0,792	0,10
	F03	YES	0,905	0,12
	F08	NO	0,285	0,24
2,1	F01	YES	0,709	0,14
	F04	YES	0,798	0,15
	F05	YES	0,945	0,19
	F06	YES	0,887	0,16
	F09	YES	0,333	0,14
	F10	YES	0,387	0,19
	F14	YES	0,788	0,09
2,1 ^R	F01	YES	0,812	0,14
	F04	YES	0,884	0,15
	F05	YES	0,868	0,19
	F06	YES	0,741	0,16
2,2	F02	YES	0,602	0,21
	F05	YES	0,596	0,05
	F08	NO	0,303	0,41
	F12	YES	0,940	0,27
	F15	NO	0,161	0,76
2,2 ^R	F02	YES	0,594	0,21
	F08	NO	0,260	0,41
	F12	YES	0,952	0,27

Trial	Device	Reference	R_{EFI}^2	CV_{EFI}
	F15	NO	0,132	0,76
2,3	F01	YES	0,444	0,07
	F03	YES	0,943	0,13
	F04	YES	0,947	0,24
	F11	NO	0,851	0,64
	F13	YES	0,612	0,07
	F15	NO	0,842	0,97
2,3 ^R	F03	YES	0,944	0,10
	F04	YES	0,946	0,10
	F11	YES	0,973	0,09
	F13	NO	0,537	0,09
	F15	YES	0,974	0,09
2,3 ^{RR}	F03	YES	0,960	0,10
	F04	YES	0,962	0,10
	F13	NO	0,578	0,09
3,1	F01	YES	0,892	0,21
	F06	YES	0,913	0,31
	F13	YES	0,956	0,26
3,2	F04	YES	0,877	0,07
	F05	YES	0,791	0,14
	F08	NO	0,692	0,12
	F13	YES	0,279	0,08
	F14	YES	0,671	0,07
	F15	YES	0,667	0,07
3,2 ^R	F05	YES	0,850	0,06
	F08	YES	0,702	0,06
3,3	F02	YES	0,775	0,22
	F03	YES	0,977	0,18
	F04	YES	0,978	0,16
	F05	YES	0,632	0,08
	F10	NO	0,798	0,47
	F11	YES	0,785	0,08
	F12	YES	0,910	0,20

Table 4.4 Outcome of Scenario #3b. Superscript ^R means that the calculations have been repeated after the reference devices failing either test are discarded.

Trial	Device	Reference	R_{EFI}^2	CV_{EFI}
1,1	F09	YES	0,914	0,22
	F10	NO	0,638	0,68
	F12	YES	0,882	0,29
	F13	YES	0,941	0,41
1,2	F01	YES	0,020	0,06
	F04	YES	0,777	0,29
	F06	NO	0,798	0,29
	F07	NO	0,171	0,07
1,2 ^R	F04	YES	0,826	0,29
	F06	NO	0,701	0,29
	F07	NO	0,078	0,07
1,3	F01	YES	0,850	0,12
	F02	YES	0,792	0,10
	F03	YES	0,905	0,12
	F08	NO	0,285	0,24
2,1	F01	YES	0,709	0,14
	F04	YES	0,798	0,15
	F05	YES	0,945	0,19
	F06	YES	0,887	0,16
	F09	YES	0,333	0,14

Trial	Device	Reference	R_{EFI}^2	CV_{EFI}
2,1 ^R	F10	YES	0,387	0,19
	F14	YES	0,788	0,09
	F01	YES	0,833	0,14
	F04	YES	0,878	0,15
	F05	YES	0,851	0,19
	F06	YES	0,767	0,16
2,2	F14	YES	0,821	0,09
	F02	YES	0,601	0,21
	F05	YES	0,593	0,04
	F08	NO	0,300	0,41
	F12	YES	0,941	0,27
	F15	NO	0,158	0,76
2,2 ^R	F02	YES	0,594	0,21
	F08	NO	0,260	0,41
	F12	YES	0,952	0,27
	F15	NO	0,132	0,76
2,3	F01	YES	0,442	0,06
	F03	YES	0,943	0,13
	F04	YES	0,947	0,20
	F11	NO	0,852	0,64
	F13	YES	0,613	0,07
	F15	NO	0,843	0,97
2,3 ^R	F03	YES	0,954	0,13
	F04	YES	0,959	0,20
	F11	YES	0,900	0,64
	F13	NO	0,607	0,07
	F15	YES	0,894	0,97
3,1	F01	YES	0,892	0,19
	F06	YES	0,910	0,28
	F13	YES	0,959	0,35
3,2	F04	YES	0,891	0,08
	F05	YES	0,754	0,13
	F08	NO	0,693	0,12
	F13	YES	0,289	0,09
	F14	YES	0,697	0,10
	F15	YES	0,628	0,09
3,2 ^R	F04	YES	0,845	0,08
	F05	YES	0,837	0,13
	F08	NO	0,579	0,12
	F14	YES	0,590	0,10
	F15	YES	0,747	0,09
3,3	F02	YES	0,770	0,22
	F03	YES	0,970	0,21
	F04	YES	0,981	0,17
	F05	YES	0,678	0,11
	F10	YES	0,845	0,09
	F11	YES	0,828	0,10
	F12	YES	0,880	0,20

With a 10% threshold on CV_{EFI} , the number of rejected measurement series is excessively large: in Trials 2,2 and 2,3, only two devices are kept and the whole of Trial 3,2 is cancelled. With a 5% level, only the worst case (the one shown on Figure 4.3) is detected. In either Scenario, the problem with “A” and “B” pointed out in Section 2.4.12 is not solved, as can be seen in Figures 4.4 to 4.7: “A” is still increasing and “B” decreasing unacceptably.

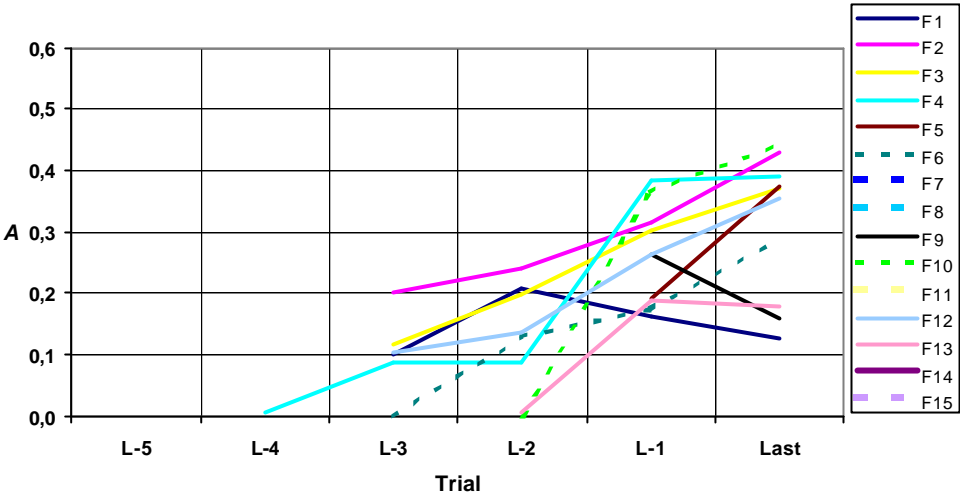


Figure 4.4 Evolution of “A” in Scenario #3a.

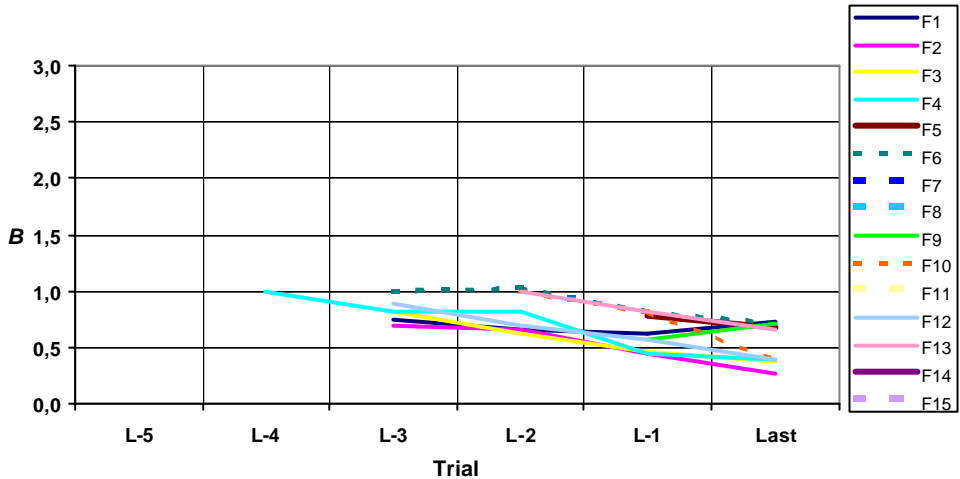


Figure 4.5 Evolution of “B” in Scenario #3a

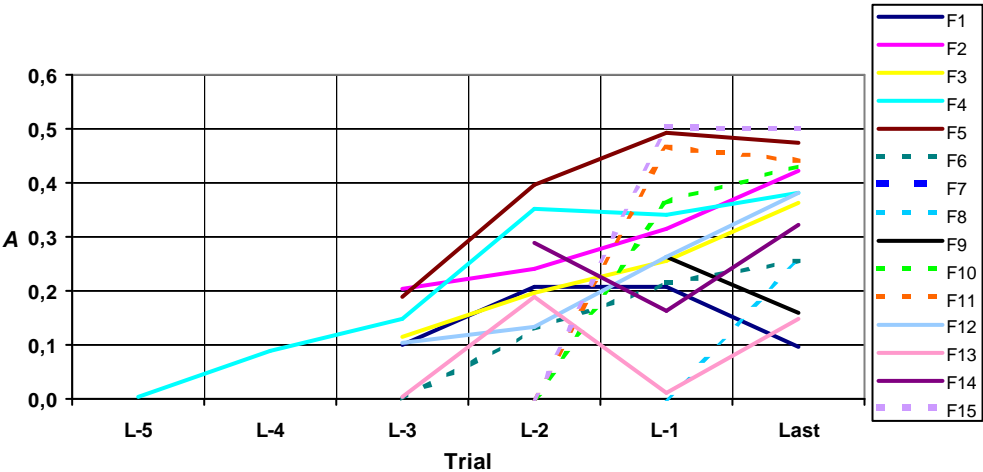


Figure 4.6 Evolution of “A” in Scenario #3b

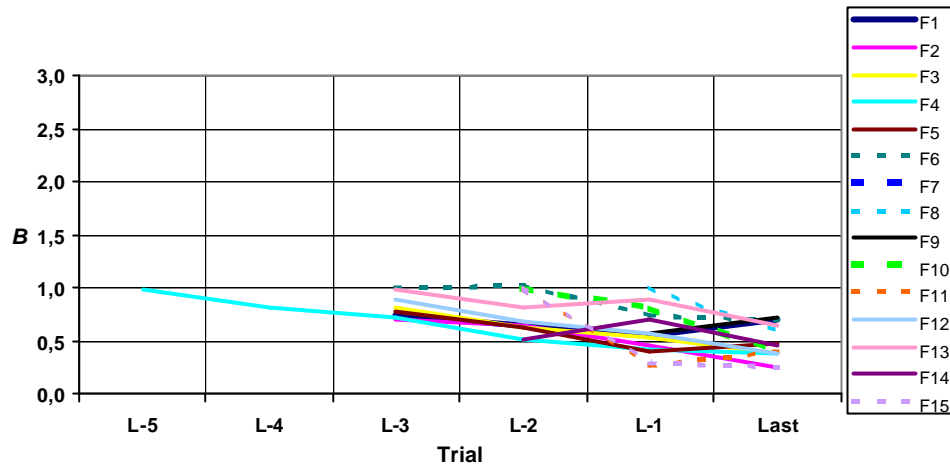


Figure 4.7 Evolution of “B” in Scenario #3b

4.6 Scenario #4: reversing the regression calculation

As suggested in Section 2.4.12, in Scenario #4, the calibration procedure was reversed by calculating first the regression of *EFI* (individual values) versus $\langle\langle EFI \rangle\rangle$ (grand average):

$$EFI = a' + b' \cdot \langle\langle EFI \rangle\rangle \quad (4.5)$$

and then calculating back $\langle\langle EFI \rangle\rangle$ against *EFI*:

$$\langle\langle EFI \rangle\rangle = a + b \cdot EFI \quad \text{with } a = -\frac{a'}{b'} \quad \text{and } b = \frac{1}{b'} \quad (4.6)$$

Taking this approach, it appeared that the calibration process diverged very quickly, for example, leaving many negative values for “A”. This was caused by poor correlations in the calibration regressions. To avoid this kind of problem, the test on R_{EFI}^2 had to be applied to CV_{EFI} (with a 10% threshold) as well. The outcome is presented in Table 4.5 and Figures 4.8 to 4.11.

Table 4.5 Outcome of Scenario #4. Superscript *R* means that the calculations have been repeated after the reference devices failing either test are discarded.

Trial	Device	Reference	R_{EFI}^2	CV_{EFI}
1,1	F09	Y	0,914	0,22
	F10	N	0,613	0,70
	F12	Y	0,882	0,29
	F13	Y	0,941	0,41
1,2	F01	Y	0,020	0,06
	F04	Y	0,777	0,29
	F06	N	0,798	0,29
	F07	N	0,171	0,07
1,2 ^R	F04	Y	0,826	0,29
	F06	N	0,701	0,29
	F07	N	0,078	0,07
1,3	F01	Y	0,850	0,12
	F02	Y	0,792	0,10
	F03	Y	0,905	0,12
	F08	N	0,285	0,24
2,1	F01	Y	0,722	0,16
	F04	Y	0,871	0,17
	F05	Y	0,941	0,16
	F06	Y	0,835	0,21
	F09	Y	0,339	0,14
	F10	Y	0,369	0,25
2,1 ^R	F14	Y	0,795	0,09
	F01	Y	0,754	0,16
	F04	Y	0,797	0,17
	F05	Y	0,949	0,16
2,2	F06	Y	0,829	0,21
	F02	Y	0,595	0,27
	F05	Y	0,869	0,08
	F08	N	0,690	0,33
	F12	Y	0,675	0,31
	F15	N	0,749	0,82
2,2 ^R	F02	Y	0,597	0,27
	F08	N	0,073	0,33
	F12	Y	0,948	0,31
	F15	N	0,407	0,82
2,3	F01	Y	0,454	0,10
	F03	Y	0,941	0,15
	F04	Y	0,944	0,41
	F11	N	0,708	0,61
	F13	Y	0,609	0,07
	F15	N	0,834	0,97
2,3 ^R	F03	Y	0,960	0,15
	F04	Y	0,963	0,41
	F11	N	0,861	0,61
	F15	N	0,922	0,97
3,1	F01	Y	0,891	0,34
	F06	Y	0,924	0,59
	F13	Y	0,934	0,27
3,2	F04	Y	0,791	0,15
	F05	Y	0,886	0,24
	F08	N	0,545	0,11
	F13	Y	0,224	0,13
	F14	Y	0,561	0,07
	F15	Y	0,786	0,19
3,2 ^R	F04	Y	0,675	0,15
	F05	Y	0,934	0,24

Trial	Device	Reference	R_{EFI}^2	CV_{EFI}
3,3	F08	N	0,342	0,11
	F15	Y	0,920	0,19
	F02	Y	0,736	0,45
	F03	Y	0,986	0,48
	F04	Y	0,981	0,43
	F05	Y	0,986	0,08
	F10	Y	0,963	0,37
	F11	Y	0,756	0,22
	F12	Y	0,920	0,25
3,3 ^R	F02	Y	0,776	0,45
	F03	Y	0,984	0,48
	F04	Y	0,977	0,43
	F10	Y	0,945	0,37
	F11	Y	0,715	0,22
	F12	Y	0,912	0,25

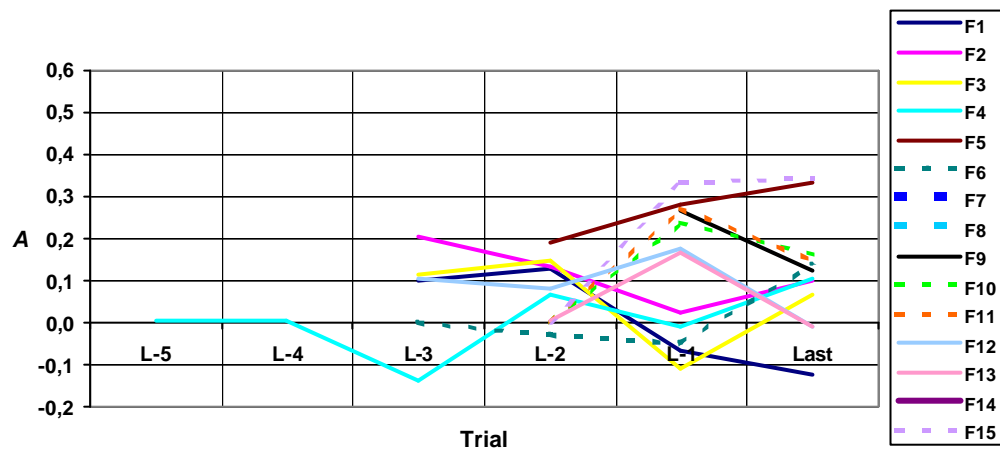


Figure 4.8 Evolution of "A" in Scenario #4

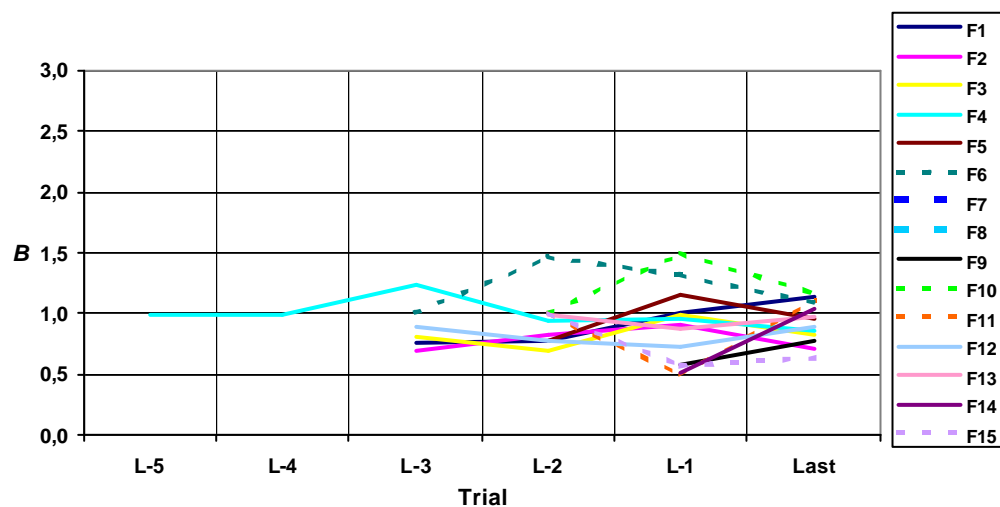


Figure 4.9 - Evolution of "B" in Scenario #4

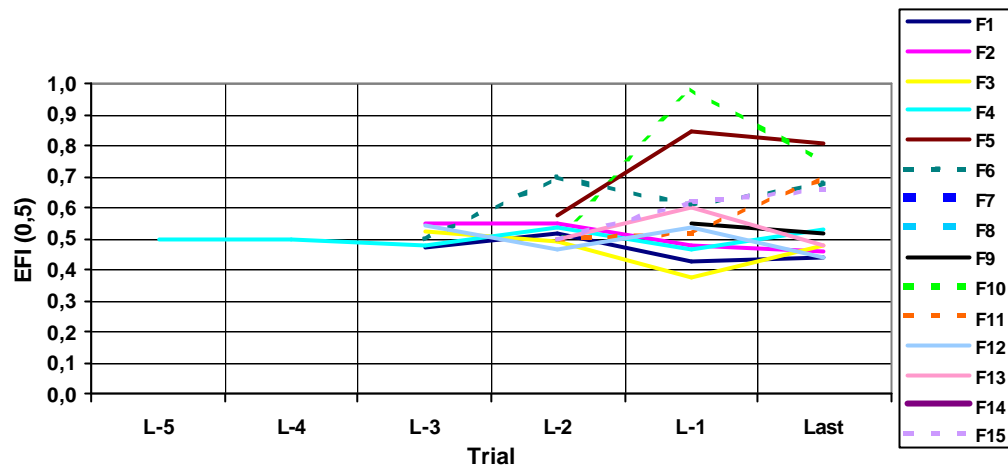


Figure 4.10 - Evolution of $EFI(0,5) = A + 0,5 B$ in Scenario #4

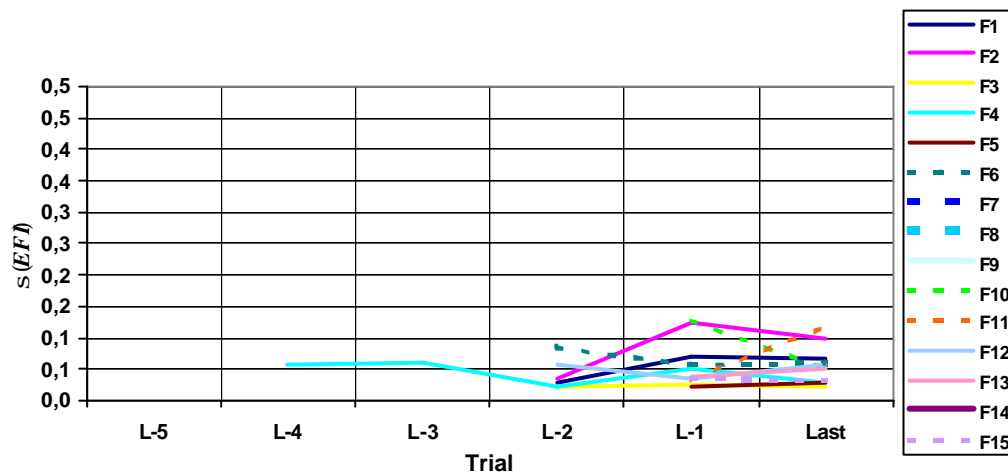


Figure 4.11 - Evolution of s_{EFI} in Scenario #4

In this scenario, “A” and “B” no longer exhibit any undesirable general trend. However, now, they evolve in a rather chaotic way. As the intercept “A” is generally far away from the cluster of data, a more realistic approach to evaluate the stability of the calibration parameters would be to consider the evolution that the value of EFI would take at a medium speed on a surface in the middle of the practical range of friction value, for example at $F_{30}=0,5$. Then, $EFI(0,5)=A+0,5B$. That is what Figure 4.10 shows. It does not seem that $EFI(0,5)$ has a tendency to stabilize. Regarding the precision of the calibration, s_{EFI} takes on values ranging from 0,023 to 0,119 with an average value of 0,062 in the 3rd round (last three trials).

4.7 Scenarios #5 to #7: forcing “A” to zero

As the first few attempts to prevent the undesirable trends of “A” and “B” have failed, the next step suggested in Section 2.4.12 is to force “A” to zero, which makes sense from a physical point of view since, ideally, EFI should vanish on a zero-friction surface (see 2.4.12). That option has been implemented in Scenario #5. Before following that process,

the initial B -values of the reference devices had to be re-calculated from the database⁶ of the *PIARC* International Experiment 1992 [1] with EFI re-defined as:

$$EFI = B \cdot F_{30} \quad (4.7)$$

Table 4.6 gives the initial values (B_0') to be used when $A_0 = 0$.

Table 4.6 Initial B -values (B_0') when “ A ” is forced to zero.

Friction device		Lab, country	Tyre	Measurement principle	Slip ratio	B_0'
Code	Name					
F01	DWW Trailer	DWW, NL	PIARC Blank	BFC	0,86	0,908
F02	ADHERA	LCPC, FR	PIARC Blank	BFC	1,00	1,089
F03	SCRIM	CEDEX, ES	AVON Blank	SFC	0,34	1,045
F04	SCRIM	MET, BE	AVON Blank	SFC	0,34	1,002
F05	GripTester	MET, BE	Findley-Irvine Blank	BFC	0,15	1,183
F06	ROAR	DRI, DK	ASTM E1551 Blank	BFC	0,20	1,000
F07	ROAR	DWW, NL	ASTM E1551 Blank	BFC	0,86	1,000
F08	Odoliograph	BRRC, BE	PIARC Blank	SFC	0,34	1,000
F09	PFT	TRL, GB	ASTM E524 Blank	BFC	1,00	1,049
F10	OSCAR	NRRL, NO	ASTM E524 Blank	BFC	0,18	1,000
F11	ROAR Mk2	NRRL, NO	ASTM E1551 Blank	BFC	0,18	1,000
F12	SRT-3	IBDIM, PL	Patterned	BFC	1,00	1,079
F13	SCRIM	TRL, GB	AVON Blank	SFC	0,34	1,002
F14	Odoliograph	MET, BE	PIARC Blank	SFC	0,34	1,065
F15	IMAG	STBA, FR	PIARC Blank	BFC	0,15	1,000

Figure 4.12 shows the evolution of “ B ” in Scenario #5.

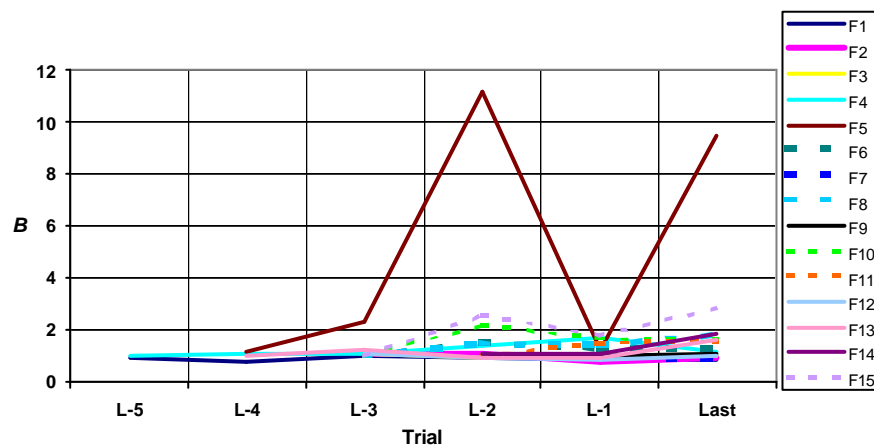


Figure 4.12 Evolution of “ B ” in Scenario #5 (A forced to zero)

The behaviour of device F05 is an obvious problem, introduced by the exponential model for friction against speed. The extremely high values of “ B ” that it reaches in some trials

⁶ Restricted to the devices in use in Europe.

affect the calibration of the other devices. Therefore, it was discarded and the calculations were repeated, to give Scenario #6. This time, F15 exhibited atypical behaviour (for the same reason) regarding both the evolution of “B” (Figure 1.13) of s_{EFI} , the residual standard deviation of EFI (Figure 4.14).

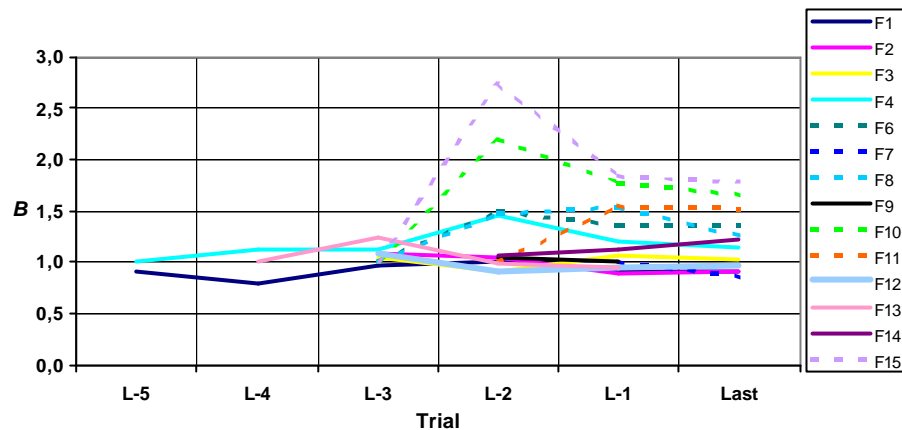


Figure 4.13 Evolution of “B” in Scenario #6 (Device F05 excluded)

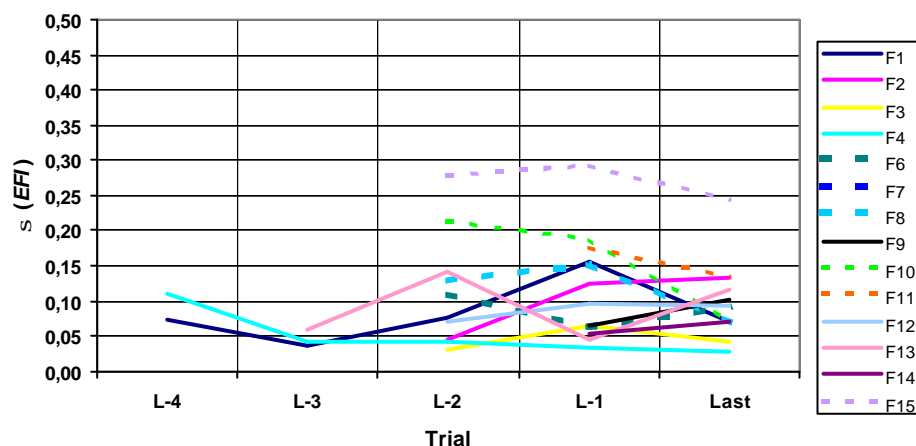


Figure 4.14 Evolution of s_{EFI} in Scenario #6 (Device F05 excluded)

For the same reason as for F05, F15 was discarded in the next round of calculations, which became Scenario #7, the results of which are presented in Figures 4.15 and 4.16. For completeness, all of the calibration graphs have been included in Annex G.

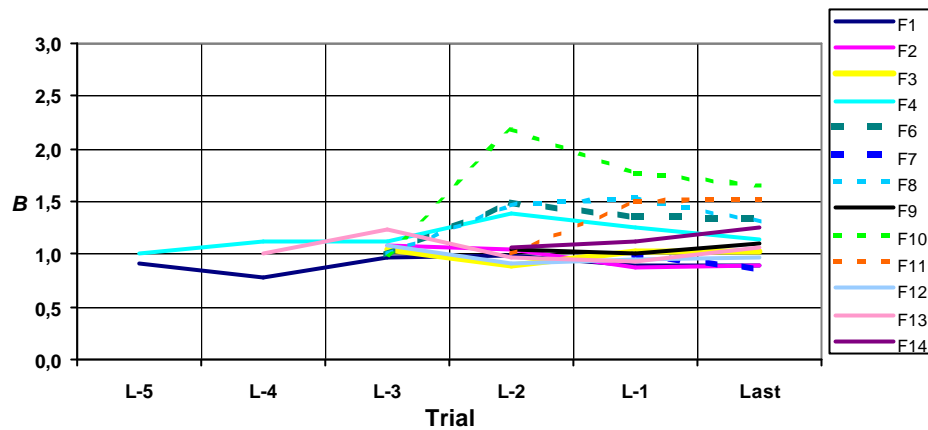


Figure 4.15 Evolution of “B” in Scenario #7 (Devices F05 and F15 excluded).

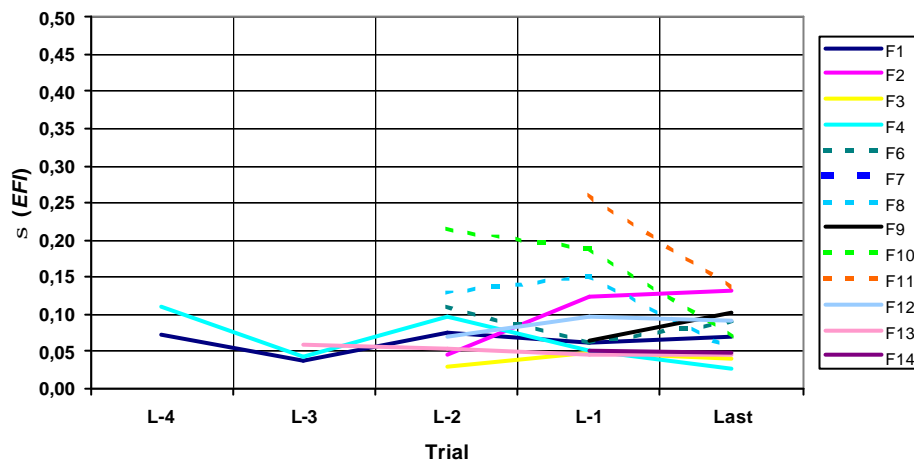


Figure 4.16 Evolution of s_{EFI} in Scenario #7 (Devices F05 and F15 excluded).

It can be concluded from Figure 4.15 that forcing “A” to zero solves the problem: “B” no longer decays. Instead, it shows a clear tendency to stabilise after one or two trials, which is the expected behaviour. This demonstrates that convening limited subsets of devices is sufficient to stabilise and maintain the *EFI* scale.

However, the benefit has a price: s_{EFI} in the last trial in which any given device took part, which is a measure of the precision of the calibration, ranges from 0,027 to 0,135 with an average of 0,081 (Figure 4.16). While the lowest figure is close to the repeatability of *F* (Section 2.4.6), which would be very satisfactory, the highest figure can hardly be considered acceptable. Table 4.7 ranks the devices according to their final value of s_{EFI} .

Table 4.7 Ranking of the devices according to the last value of s_{EFI} in Scenario #7 (F05 and F15 excluded)

Friction device		Lab, country	Measurement principle	Slip ratio	s_{EFI}
Code	Name				
F05	GripTester	MET, BE	BFC	0,15	*
F15	IMAG	STBA, FR	BFC	0,15	*
F04	SCRIM	MET, BE	SFC	0,34	0,027
F03	SCRIM	CEDEX, ES	SFC	0,34	0,040
F13	SCRIM	TRL, GB	SFC	0,34	0,045
F14	Odoliograph	MET, BE	SFC	0,34	0,047
F07	ROAR	DWW, NL	BFC	0,86	0,051
F08	Odoliograph	BRRC, BE	SFC	0,34	0,051
F01	DWW Trailer	DWW, NL	BFC	0,86	0,069
F10	OSCAR	NRRL, NO	BFC	0,18	0,070
F06	ROAR	DRI, DK	BFC	0,20	0,090
F12	SRT-3	IBDIM, PL	BFC	1,00	0,092
F09	PFT	TRL, GB	BFC	1,00	0,103
F02	ADHERA	LCPC, FR	BFC	1,00	0,133
F11	ROAR Mk2	NRRL, NO	BFC	0,18	0,135

Figure 4.17 shows that, regarding their s_{EFI} values, the devices fall into two populations representing the *SFC* and *BFC* measuring principles, regardless of the *slip ratio* (at least for *BFC* – all *SFC* devices in the trials had the same wheel angle). It could be argued that there is actually a third population, represented by F05 and F15. These two devices have a similar behaviour to one another that can be related to their rather low *slip ratio*, as shown in Chapter 3. As can be seen in Annex B, their *F*-values decrease with speed more rapidly than other devices and, because of a low *slip ratio*, their maximum slip speed is some way from the 30 km/h reference level. This generally results in extrapolated F_{30} values that are much lower than for other devices, which explains the low values of s_{EFI} with respect to $\langle\langle s_{EFI} \rangle\rangle$ and the high values of “*B*” and s_{EFI} .

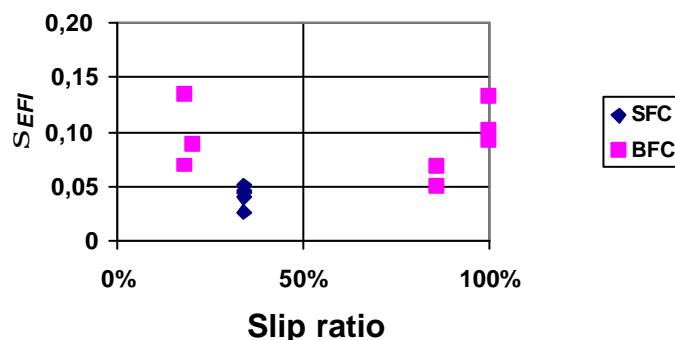


Figure 4.17 Values of s_{EFI} versus slip ratio and measuring principle (Scenario #7)

4.8 Scenario #8: treating *BFC*- and *SFC*-devices separately

In this scenario, the *BFC* devices and *SFC* devices, were processed as separate groups, as Scenario #8a or #8b respectively. The outcomes of the separate treatments are shown in Figures 4.18 and 4.19 for *BFC* devices and Figures 4.20 and 4.21 for *SFC*-devices. From the s_{EFI} values in the last trial of each device, it can be seen that considering *BFC* and *SFC* devices separately does not bring any improvement in either case. In terms of repeatability of *EFI*, the *BFC* group remains bad with $0,041 < s_{EFI} < 0,144$, whereas the *SFC* group remains rather good with $0,024 < s_{EFI} < 0,054$. The latter class includes the two Odoliographs and the three SCRIMs that participated in the trials. They all have the same *slip ratio* of 34% so they might be expected to perform better in terms of s_{EFI} .

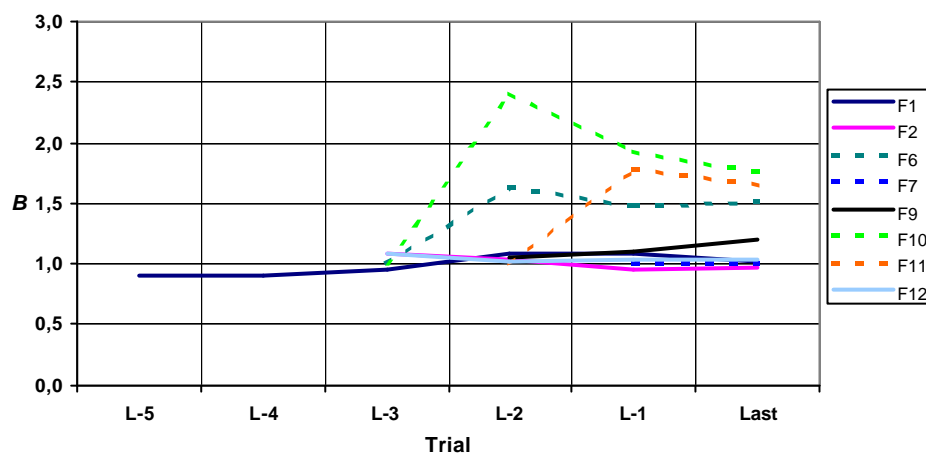


Figure 4.18 Evolution of "B" in Scenario #8a (*BFC*-devices only)

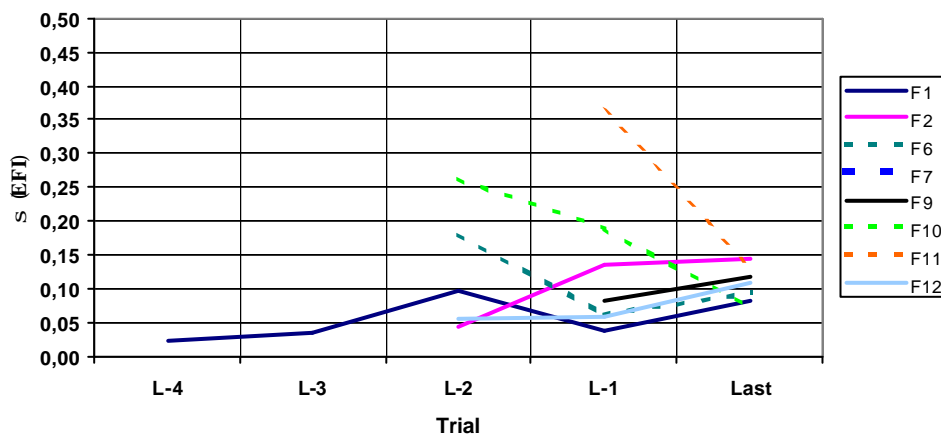


Figure 4.19 Evolution of s_{EFI} in Scenario #8a (*BFC*-devices only)

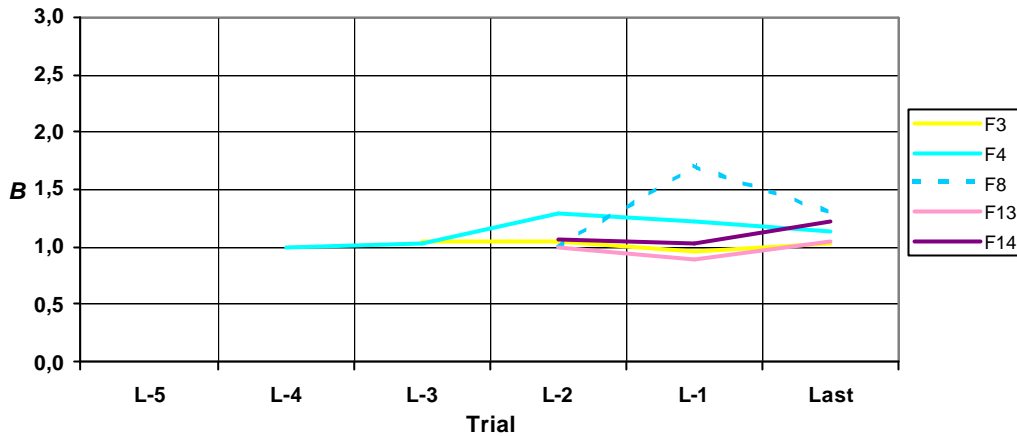


Figure 4.20 Evolution of "B" in Scenario #8b (SFC-devices only)

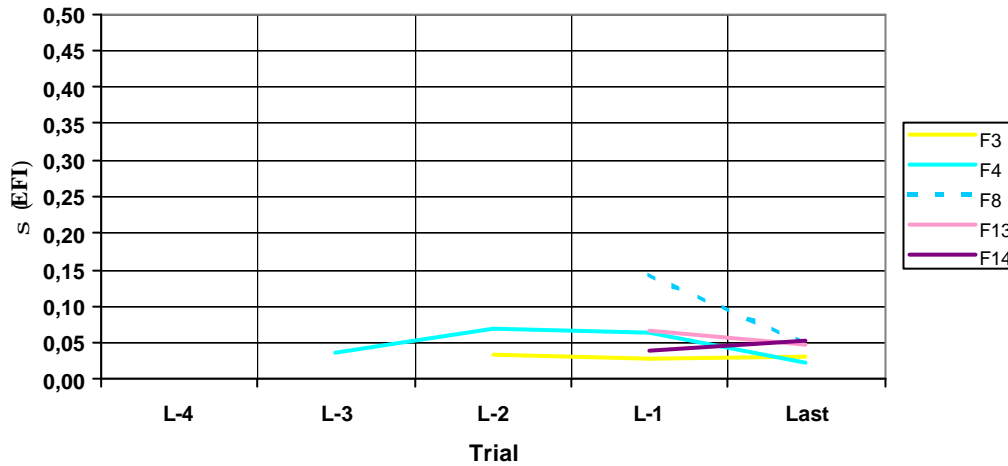


Figure 4.21 Evolution of s_{EFI} in Scenario #8b (SFC-devices only)

4.9 Scenarios #9 to #11: improved model for $F(S)$

In Chapter 3 it was shown that $F(S)$ could be better modelled by the following formula:

$$F = F_0 \cdot e^{-(S/S_0)^a} \quad (4.8)$$

With $a > 1$, measurement series exhibiting a negative curvature can be curve-fitted more closely than with the simple exponential model (the so-called *PIARC* model).

The model has now three undetermined parameters: F_0 , S_0 and a . Consequently, it can no longer be linearized. It can, however, still be treated in this way with respect to F and S^a by using the logarithm form:

$$\ln F = \ln F_0 - S_0^{-a} \cdot S^a \quad (4.9)$$

In order to determine the best curve fit to this formula, the linear regression of $\ln F$ versus S^a was calculated by the least squares method for each value of a from 0,05 to 9,95 in steps of 0,05. The value of a giving the lowest residual deviation was then selected. The different values obtained from the different measurement series made by a given device in a given trial were then averaged and that average was used in the subsequent processing. Figure 4.22 shows the average values of a obtained per device and per trial.

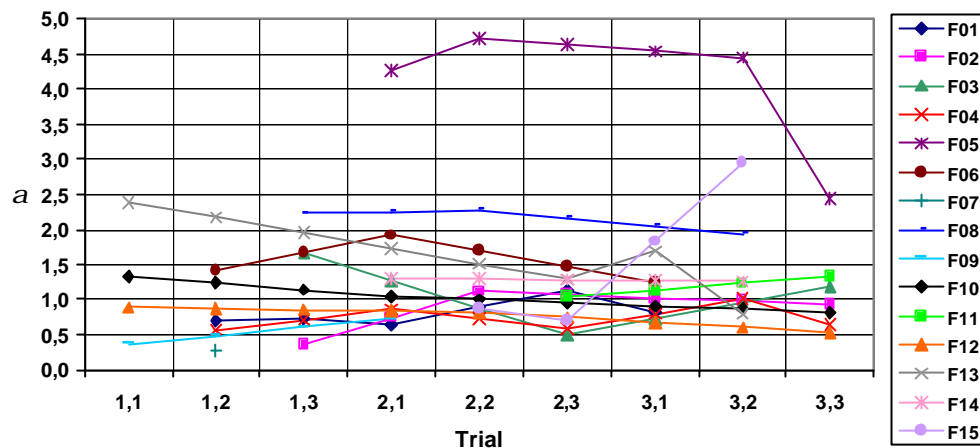


Figure 4.22 Values of a per device and per trial

It appears that, in general, a for a given device does not vary much from trial to trial, except for devices F05 and F15. Its average value per device, shown in Figure 4.23, seems to be related to the *slip ratio*: the lower the percent slip, the higher the value of a .

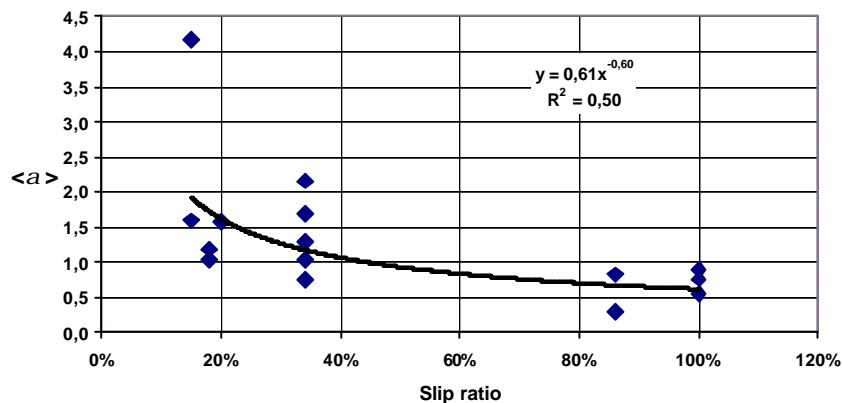


Figure 4.23 Values of a per device, averaged over the different trials

All of the regression curves using the new model (4.8) with the device-specific a values are shown in Annex H. In this new model, the the power law and the weighting as discussed in Section 4.2 continued to be used to relate S_0 to MPD .

Reprocessing the data using the new model is Scenario #9. It appeared that device F05 would have to be discarded again. Although the new model provides a better curve fitting for $F(S)$, as can be seen in Annex H, the extrapolation to the reference speed leads to still

lower values of F_{30} than were obtained with the original model. Figure 4.24 shows a typical example of the effect of that on the calibration regression.

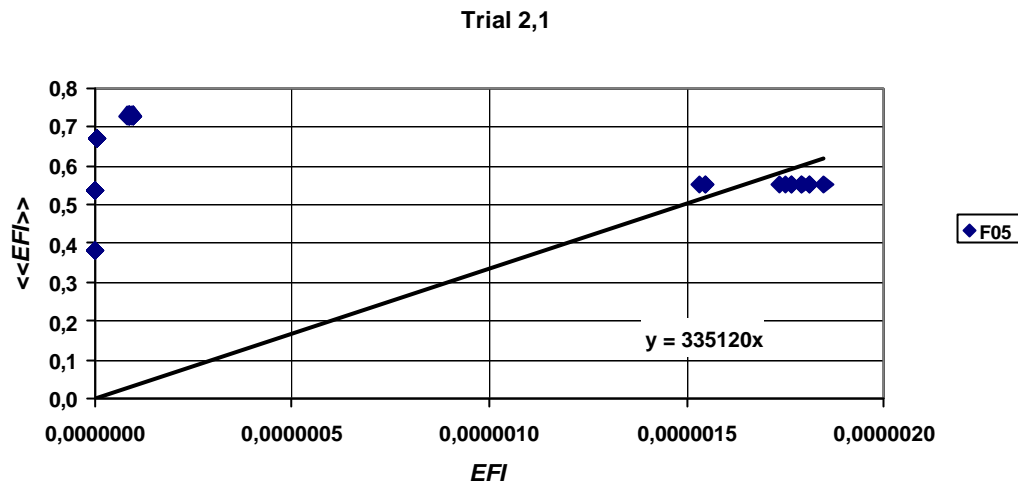


Figure 4.24 Example of impossible calibration of device F05.

The processing was then repeated without F05 (Scenario #10). As had occurred before, device F15 exhibited a behaviour resembling the case of F05 as Annex H (Trials 2,2 – 2,3 – 3,2) and Figure 4.25 show.

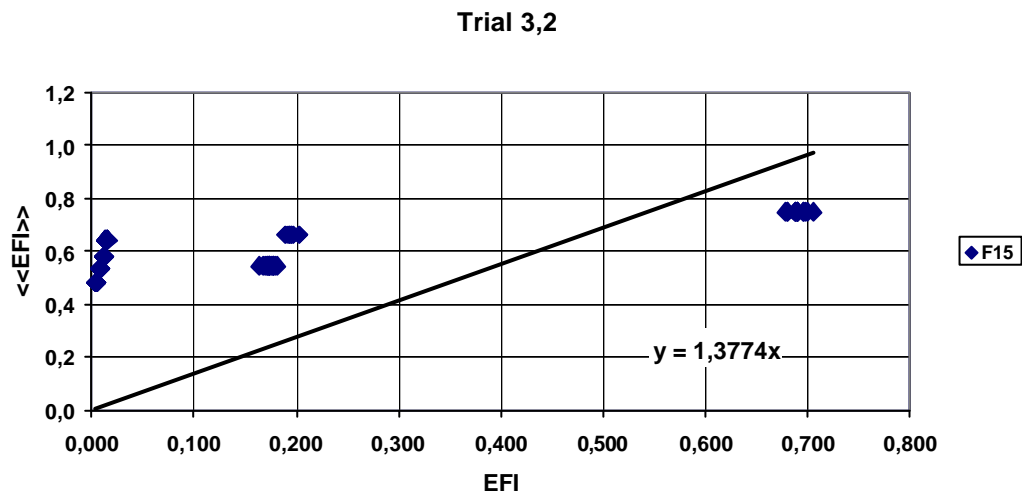


Figure 4.25 Example of unacceptable calibration result of device F15.

Eventually, a further set of calculations, Scenario #11, was made that excluded both F05 and F15. The results in the form of the evolution of “B” and s_{EFI} , are presented in Figures 4.26 and 4.27 respectively.

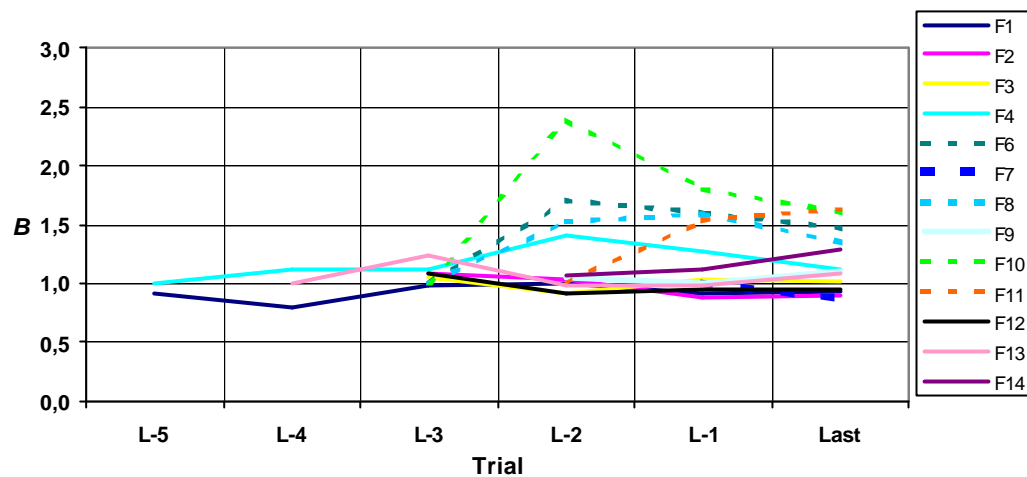


Figure 4.26 Evolution of “B” in Scenario #11 (F05 and F15 discarded).

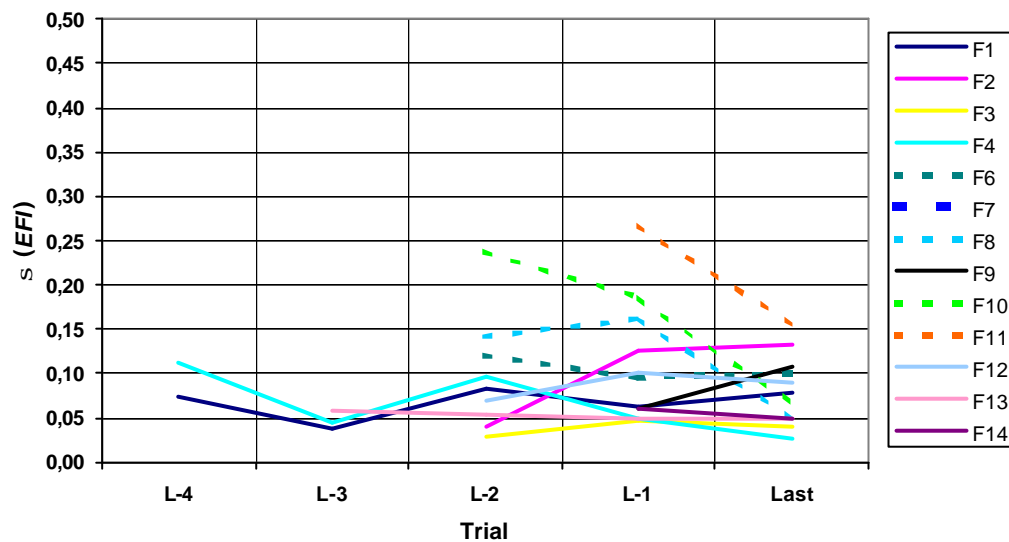


Figure 4.27 Evolution of s_{EFI} in Scenario #11 (F05 and F15 discarded).

In order to evaluate the possible benefit brought about by the improved model for $F(S)$, Figures 4.26 and 4.27 (Scenario #11) should be compared with Figures 4.15 and 4.16 (Scenario #7). It can be seen that the results are very similar.

The ultimate values of s_{EFI} for Scenario #11 (given in Table 4.8) range from 0,026 to 0,155 with an average of 0,085, which is slightly worse than with Scenario #7. Therefore, despite the fact that the improved model better fits certain measurement series, it does not seem to improve the precision of EFI .

Table 4.8 Final calibration precision in Scenario #11

Friction device		Lab, country	Measurement principle	Slip ratio	s_{EFI}
Code	Name				
F04	SCRIM	MET, BE	SFC	0,34	0,079
F03	SCRIM	CEDEX, ES	SFC	0,34	0,132
F13	SCRIM	TRL, GB	SFC	0,34	0,039
F14	Odoliograph	MET, BE	SFC	0,34	0,026
F07	ROAR	DWW, NL	BFC	0,86	0,100
F08	Odoliograph	BRRRC, BE	SFC	0,34	0,049
F01	DWW Trailer	DWW, NL	BFC	0,86	0,049
F10	OSCAR	NRRL, NO	BFC	0,18	0,108
F06	ROAR	DRI, DK	BFC	0,20	0,066
F12	SRT-3	IBDIM, PL	BFC	1,00	0,155
F09	PFT	TRL, GB	BFC	1,00	0,090
F02	ADHERA	LCPC, FR	BFC	1,00	0,050
F11	ROAR Mk2	NRRL, NO	BFC	0,18	0,050
BFC only					0,097
SFC only					0,043
All					0,085

4.10 Analysis of deviations

Essentially, there are four potential sources of errors that could explain the values of s_{EFI} :

1. Insufficient accuracy in the model for $F(S)$.
2. The repeatability deviations of F .
3. The deviation of the predicted S_0 with respect to the actual S_0 , due to the lack of accuracy of the model for S_0 (MPD).
4. The inaccuracy of the EFI concept itself due to some possible deficiency of the friction model.

In Section 2.4.6, the repeatability of F was evaluated. In Section 4.9 in this chapter it has been shown that improving the model for $F(S)$ does not bring any improvement. The following Sections of the report examine:

- The influence of the errors that occur when a predicted S_0 is used (Scenario #12).
- The repeatability of the EFI .
- The residual standard deviation, σ_{EFI} , of the calibration regression when the deviations due to errors of type 1, 2 and 3 above have been averaged out (Scenario #14).

4.11 Scenario #12: using actual values of S_0 instead of predictions

The purpose of Scenario #12 is to evaluate the influence of the errors that arise from using a prediction of S_0 to determine F_{30} by using actual values of S_0 instead. The processing was otherwise identical to Scenario #7, i.e. using the original model for $F(S)$ with ($\gamma = 1$). Although it is possible to make the calculations here, using the *HERMES* data, this approach cannot be considered as a practical solution to the problem. This is because, in a real situation, measurements are not repeated at different speeds and S_0 therefore cannot be determined. In normal circumstances it will only be possible to use a predicted value of S_0 based on a texture measurement.

The results of this analysis are presented in Table 4.9 and Figure 4.28. The range of final values of s_{EFI} is 0,032 to 0,133 with an average of 0,072, which is not significantly better than was obtained using the approach in Scenario #7. In some cases, s_{EFI} increases in Scenario #12. This can happen because successive calibrations are influenced by the results of those preceding. So, s_{EFI} in the last trial does not depend only on the improvement of the extrapolation to obtain F_{30} .

Table 4.9 Comparison of the final calibration precision in Scenarios #7 and #12

Friction device		Lab, country	Measurement principle	Slip ratio	s_{EFI}	
Code	Name				Sc.#7	Sc.#12
F01	DWW Trailer	DWW, NL	BFC	0,86	0,069	0,055
F02	ADHERA	LCPC, FR	BFC	1,00	0,133	0,080
F03	SCRIM	CEDEX, ES	SFC	0,34	0,040	0,034
F04	SCRIM	MET, BE	SFC	0,34	0,027	0,032
F06	ROAR	DRI, DK	BFC	0,20	0,090	0,087
F07	ROAR	DWW, NL	BFC	0,86	0,051	0,059
F08	Odoliograph	BRRC, BE	SFC	0,34	0,051	0,055
F09	PFT	TRL, GB	BFC	1,00	0,103	0,089
F10	OSCAR	NRRL, NO	BFC	0,18	0,070	0,073
F11	ROAR Mk2	NRRL, NO	BFC	0,18	0,135	0,133
F12	SRT-3	IBDIM, PL	BFC	1,00	0,092	0,079
F13	SCRIM	TRL, GB	SFC	0,34	0,045	0,045
F14	Odoliograph	MET, BE	SFC	0,34	0,047	0,041
BFC only					0,093	0,082
SFC only					0,042	0,041
All					0,081	0,072

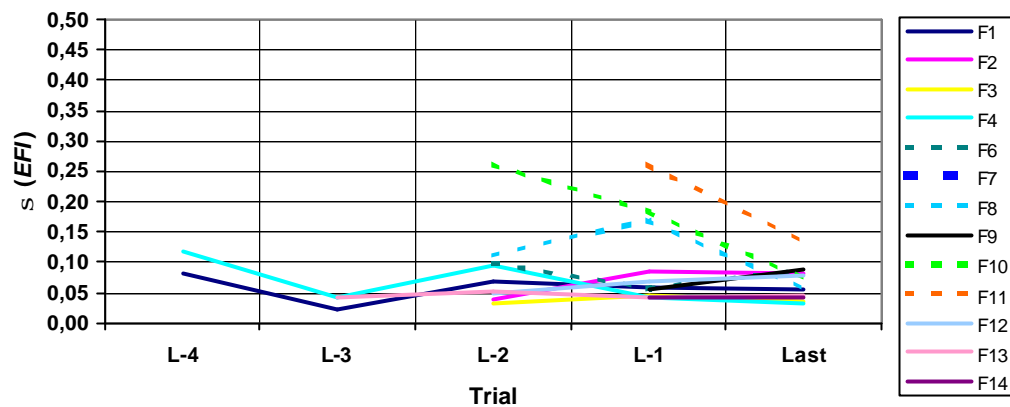


Figure 4.28 Evolution of s_{EFI} in Scenario #12

4.12 Repeatability of EFI

The repeatability of EFI , is represented by the standard deviation of the EFI values reported by a given device on a given surface from repeated measurements at different speeds. The overall repeatability standard deviation of EFI essentially contains two components:

- The repeatability errors in the friction measurements themselves.
- The errors that arise as a result of the inaccuracy of the models that relate friction to speed, $F(S)$, and the speed constant to texture, $S_0(MPD)$ which, in turn, are reflected in the extrapolated values of F_{30} used to convert F into EFI .

Table 4.10 provides a comparison of the repeatability of EFI with the repeatability of F , using the process described in Scenario #7. The table gives the average repeatability standard deviation (s_r) of EFI for each device at each trial it attended, together with the overall average and the average for the last trial round. These values are compared with the average repeatability of the original friction measurements, $s_r(F)$, both overall and for the last trial round. The averages incorporate the values of the repeatability of EFI , calculated from each measurement series for each device and surface, weighted by the number of measurements retained after the test on R_F^2 (Table 4.11). Devices F05 and F15 are excluded.

Clearly, an increase in s_r would be expected when changing from F to EFI and this is generally reflected in the summary columns of Table 4.10 (those showing the “average” and “final” values). However, comparing the “final” columns, which represent the values obtained when all the devices had been calibrated at least once, the increase found when moving from $s_r(F)$ to $s_r(EFI)$ is moderate, especially when “all” devices are considered.

This observation suggests that little further improvement can be expected from the quest for better models.

Table 4.10 Repeatability of EFI in Scenario #7 compared to the repeatability of F (Section 2.3.6, Table 2.12). "Final" means the three trials in the third round

Device	$s_r(EFI)$ at individual trials									Summary values			
										$s_r(EFI)$		$s_r(F)$	
	1,1	1,2	1,3	2,1	2,2	2,3	3,1	3,2	3,3	Average	Final	Average	Final
F01		0,024	0,030	0,019		0,036	0,025			0,027	0,025	0,016	0,018
F02			0,047		0,142				0,073	0,096	0,073	0,018	0,017
F03			0,034			0,022			0,028	0,029	0,028	0,028	0,023
F04		0,059		0,023		0,028		0,033	0,022	0,036	0,022	0,035	0,020
F06		0,014		0,031			0,022			0,024	0,022	0,027	0,029
F07		0,031								0,031	0,031	0,017	0,017
F08			0,027		0,050			0,036		0,037	0,036	0,026	0,022
F09	0,055			0,055						0,055	0,055	0,029	0,029
F10	0,013			0,045					0,039	0,032	0,039	0,027	0,023
F11						0,015			0,024	0,021	0,024	0,021	0,018
F12	0,041				0,025				0,029	0,033	0,029	0,016	0,016
F13	0,022					0,043	0,030	0,025		0,030	0,025	0,028	0,037
F14				0,028				0,030		0,029	0,030	0,022	0,017
BFC	0,035	0,023	0,037	0,038	0,084	0,026	0,024	-	0,041	0,044	0,040	0,025	0,021
SFC	0,022	0,059	0,030	0,025	0,050	0,031	0,030	0,031	0,025	0,033	0,028	0,025	0,025
All	0,036	0,038	0,035	0,035	0,092	0,030	0,026	0,031	0,040	0,042	0,036	0,025	0,023

Table 4.11 Number of measurements retained after the test on R_F^2 .

n	1,1	1,2	1,3	2,1	2,2	2,3	3,1	3,2	3,3	Total
F01		90	90	81		75	120			456
F02			90		90				90	270
F03			90			75			90	255
F04		90		87		75		57	90	399
F06		66		76			105			247
F07		70								70
F08			90		60			73		223
F09	103			69						172
F10	100			62					57	219
F11						62			89	151
F12	120				90				90	300
F13	120					75	120	69		384
F14				85				86		171
Total	443	316	360	460	240	362	345	285	506	3317

4.13 Scenario #13. Averaging out the repeatability deviations of EFI

In Scenario #13, the repeatability deviations of EFI have been averaged out by correlating the grand average $\langle\langle EFI \rangle\rangle$ to the average values $\langle EFI \rangle$ over each measurement series instead of the individual values of EFI . By doing this, not only are the repeatability deviations of F eliminated but the errors due to the imperfection of the models for $F(S)$ and $S_0(MPD)$ are removed as well. Apart from this, the processing is exactly as in Scenario #7. Figures 4.29 and 4.30 show the evolution of “ B ” and s_{EFI} , respectively. The values of “ B ” are quite close to those in Scenario #7, as expected.

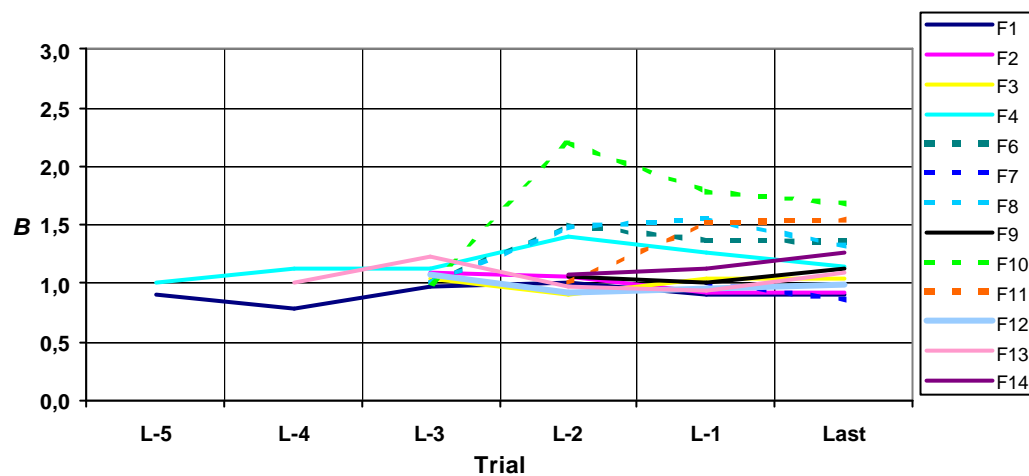


Figure 4.29 Evolution of “ B ” in Scenario #13

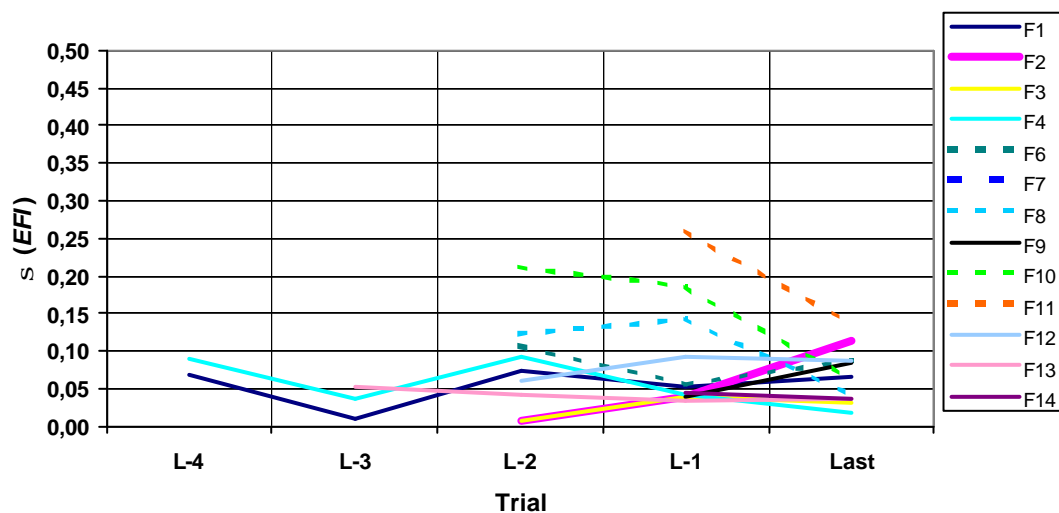


Figure 4.30 Evolution of s_{EFI} in Scenario #13

Table 4.12 provides a comparison between σ_{EFI} in Scenarios #7 and #13. The range of final values of s_{EFI} is now 0,019 to 0,135 with an average of 0,073. It shows that repeatability deviations do not contribute very much to s_{EFI} .

Table 4.12 Comparison between final calibration precision of EFI (Scenario #13) and final repeatability of EFI (Scenario #7). The devices are ranked according to s_{EFI} .

Friction device		Lab, country	Measurement principle	Slip ratio	s_{EFI}	
Code	Name				Sc. #13	Sc. #7
F04	SCRIM	MET, BE	SFC	0,34	0,019	0,027
F03	SCRIM	CEDEX, ES	SFC	0,34	0,031	0,040
F13	SCRIM	TRL, GB	SFC	0,34	0,036	0,045
F14	Odoliograph	MET, BE	SFC	0,34	0,036	0,047
F08	Odoliograph	BRRC, BE	SFC	0,34	0,041	0,051
F07	ROAR	DWW, NL	BFC	0,86	0,045	0,051
F10	OSCAR	NRRL, NO	BFC	0,18	0,062	0,070
F01	DWW Trailer	DWW, NL	BFC	0,86	0,065	0,069
F09	PFT	TRL, GB	BFC	1,00	0,085	0,103
F06	ROAR	DRI, DK	BFC	0,20	0,088	0,090
F12	SRT-3	IBDIM, PL	BFC	1,00	0,089	0,092
F02	ADHERA	LCPC, FR	BFC	1,00	0,113	0,133
F11	ROAR Mk2	NRRL, NO	BFC	0,18	0,135	0,135
BFC only					0,085	0,097
SFC only					0,033	0,043
All					0,073	0,080

Sets of three graphs showing the calibration lines for the trials in each round are shown in Figures 4.31 to 4.33 for Rounds 1 to 3 respectively (See also Annex I).

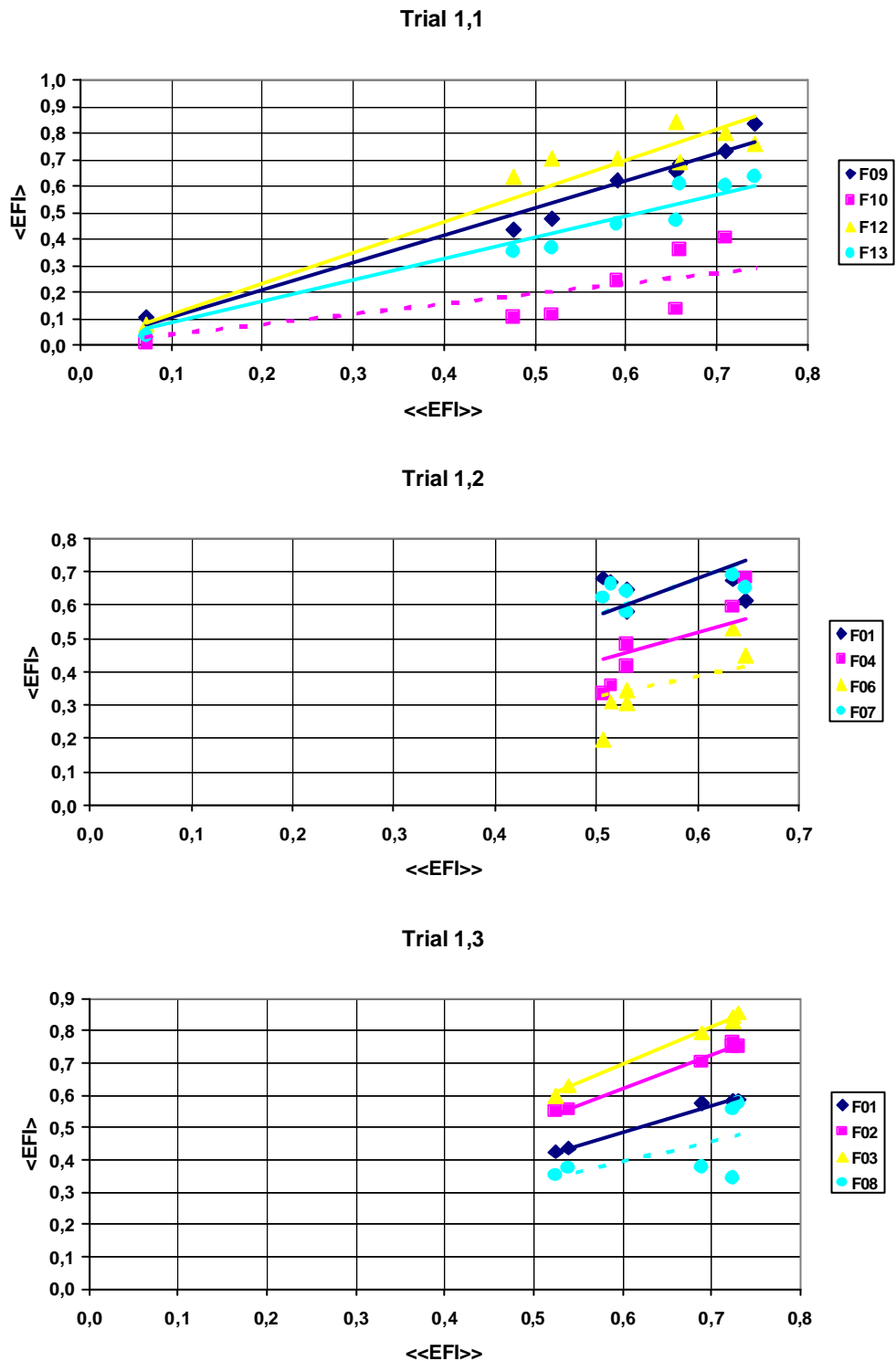


Figure 4.31 Comparison of EFI-values delivered by the devices participating in each trial in Round 1 (Scenario #13). Solid lines represent reference devices taking part in a Type-1 calibration in that trial. Dotted lines represent non-reference devices taking part in a Type-2 calibration.

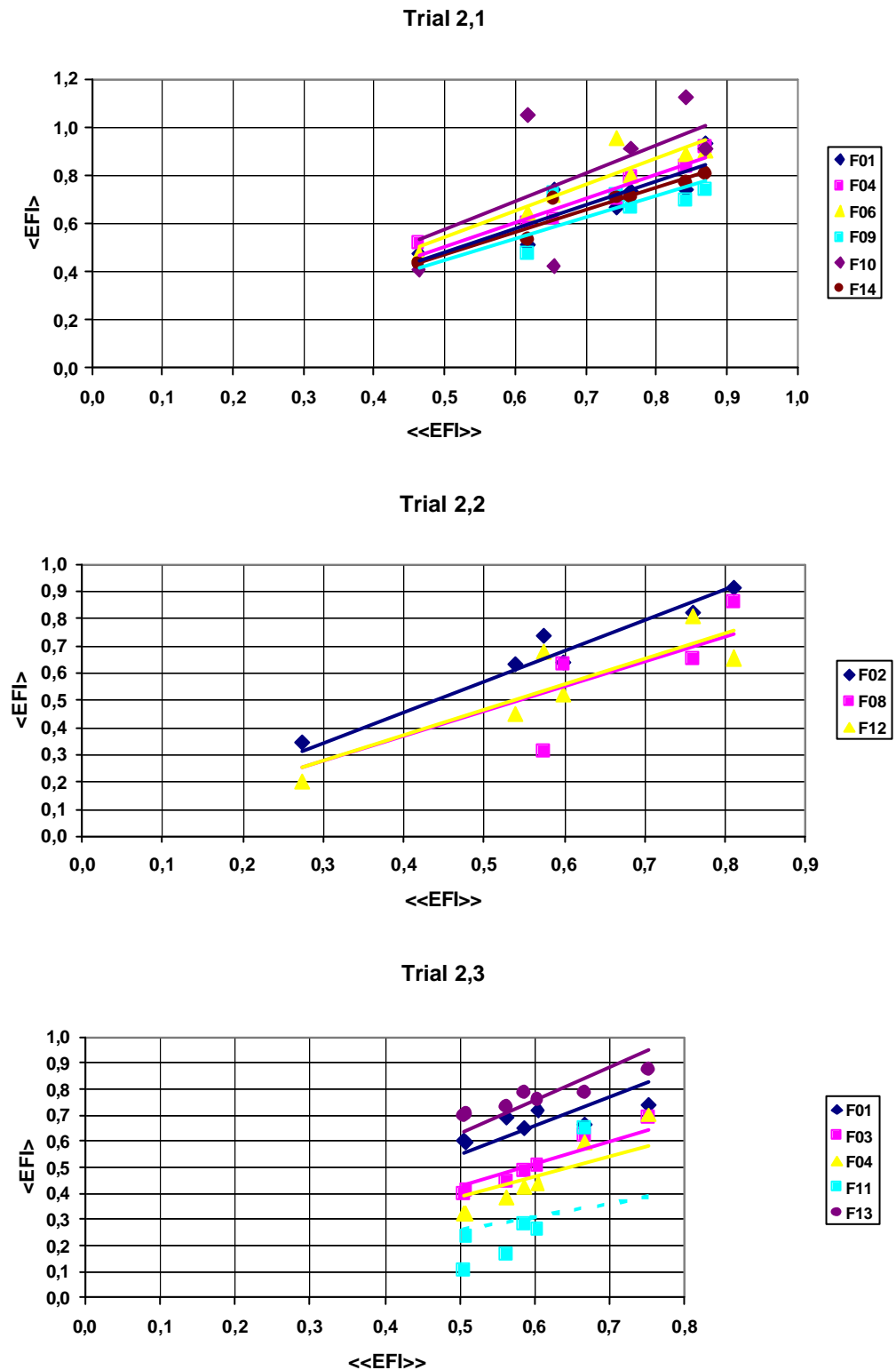


Figure 4.32 Comparison of EFI-values delivered by the devices participating in the trials in Round 2 (Scenario #13). Solid lines represent reference devices taking part in a Type-1 calibration in that trial. Dotted lines represent non-reference devices taking part in a Type-2 calibration

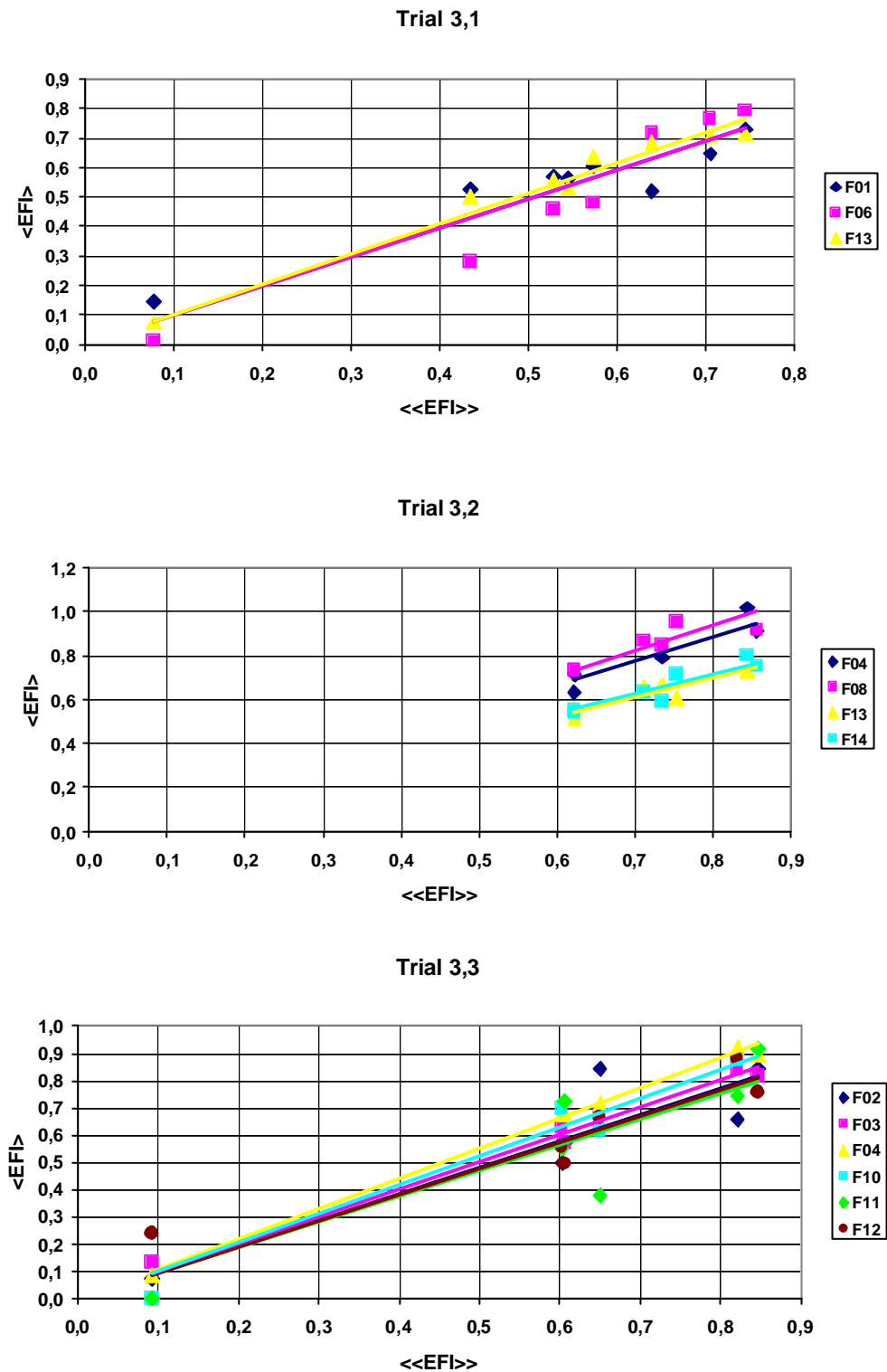


Figure 4.33 Comparison of *EFI*-values delivered by the devices participating in the trials in Round 3 (Scenario #13). Solid lines represent reference devices taking part in a Type-1 calibration in that trial. Dotted lines represent non-reference devices taking part in a Type-2 calibration

4.14 Recapitulation

Table 4.13 summarises the various processes used in the analyses described in the earlier parts of this Chapter. There is a column for each of the fourteen data processing scenarios described. An “X” in a box indicates which variant was used for each component of the analysis in that scenario.

Table 4.13 Recapitulation of the different data processing scenarios applied in Section 2.3. and Chapter 4.

	Scenario =>	#0	#1	#2	#3a	#3b	#4	#5	#6	#7	#8a	#8b	#9	#10	#11	#12	#13
F-model	$F = F_0 \cdot e^{-S/S_0}$	X	X	X	X	X	X	X	X	X	X	X				X	X
	$F = F_0 \cdot e^{-(S/S_0)^a}$												X	X	X		
S ₀ -model	$S_0 = 57 + 56 \cdot MPD$	X	X														
	$S_0 = a \cdot MPD^b$ ⁽¹⁾			X	X	X	X	X	X	X	X	X	X	X	X		X
	Actual S ₀ -value from F(S)															X	
EFI-model	$EFI = A + B \cdot F_{30}$	X	X	X	X	X	X										
	$EFI = B \cdot F_{30}$							X	X	X	X	X	X	X	X	X	X
Calibration method	$\langle\langle EFI \rangle\rangle = a + b \cdot EFI$	X	X	X	X	X											
	$EFI = a' + b' \cdot \langle\langle EFI \rangle\rangle$						X										
	$\langle\langle EFI \rangle\rangle = b \cdot EFI$							X	X	X	X	X	X	X	X	X	
	$\langle\langle EFI \rangle\rangle = b \cdot \langle\langle EFI \rangle\rangle$																X
Statistical tests	$F > 0.01$	X	X	X	X	X	X	X	X	X	X	X	X	X	X	X	X
	$S_0 > 0$	X	X	X	X	X	X	X	X	X	X	X	X	X	X	X	X
	$s_r(F) < 0.04$	X	X														
	$s_{EFI} > 0.07$	X															
	$R_F^2 > 0.5$			X			X	X	X	X	X	X	X	X	X	X	X
	$R_{EFI}^2 > 0.5$			X	X	X	X										
	$CV_{EFI} >$				10%	5%	10%										
	“k-test” (0,5%)			X													
	“h-test” (0,5%)			X													
Discarded devices									F05	F05 F15	F05 F15 SFC	BFC (²)	F05	F05 F15	F05 F15	F05 F15	F05 F15
⁽¹⁾ With weighting . ⁽²⁾ F05 and F15 were also discarded here since they are of BFC-type																	

4.15 Discussion

In Figures 4.31 to 4.33, the *EFI*-values delivered by the different devices in the first round of trials were compared. Some of the devices (represented by solid lines in the graphs) were regarded as reference devices from the start of the exercise because they had participated in the 1992 *PIARC* International Experiment [1]. Their initial *B*-values (B_0) were derived from the database of that experiment.

Using those values should have enabled them to deliver equal *EFI* values. Generally, however, this was not the case. In Trial 1,1, devices F09, F12 and F13 provided widely differing *EFI* values even though they were initially reference devices. In Trial 1,2, devices F01, F04 and F07 were in the reference group. In this trial, devices F01 and F07 agreed with each other, the only case where this occurred, while F04 disagreed with them both. In Trial 1,3, F02 and F03 were close but not equal⁷. This demonstrates the necessity of calibrating *EFI*.

Figures 4.37 to 4.39 compare the *EFI*-values delivered by the different devices in the last round of trials. At this stage of the exercise, having participated in at least one earlier calibration, all devices were now reference devices and so they should have delivered similar *EFI*-values. This appears to have occurred quite well in Trial 3,1, albeit with some scatter, and again, but not quite so well, in Trial 3.3. However, the improvement was not so clear in Trial 3,2, in which two pairs of devices agreed well with each other, but not with the other pair.

Now, it is possible that some devices might change some of their characteristics in the interval between two rounds 6 months apart, and this could explain the discrepancy between the two sets of devices in Trial 3,2. This point has already been made in relation to the direct comparison between devices F04 and F13 (Figure 2.24). Taking that possibility into account (which, incidentally illustrates why calibrations are required), it appears that the concept of convening small sets of devices in separate trials and on various test sites instead of bringing all the devices together actually works. This is further illustrated by the fact that the *B*-value of each device more or less stabilises at the end of the series of trials (Figure 4.15).

Table 4.14 gives the results of the calculations of the repeatability and reproducibility standard deviations of the calibrated *EFI* after each trial in Scenario #7, in accordance with *ISO 5725-2* [5]. The overall values were obtained by weighting the variances with respect to the number of measurements.

The rounded overall values were 0,04 for the repeatability and 0,10 for the reproducibility. These values should be compared to the overall repeatability of *F*, which ranges from 0,016 to 0,035 (Table 2.12) and to the reproducibility of *F* by similar devices, which ranges from 0,041 to 0,171 (Table 2.13).

⁷ In that trial, F01 was no longer using B_0 since it had been re-calibrated in trial 1,1.

Table 4.14 Repeatability and reproducibility standard deviations of the calibrated *EFI* after each trial in Scenario #7, according to ISO 5725-2 [5]

Trial	$s_r(EFI)$	$s_R(EFI)$	n
1,1	0,037	0,112	443
1,2	0,040	0,094	316
1,3	0,038	0,072	360
2,1	0,034	0,101	460
2,2	0,079	0,137	240
2,3	0,030	0,122	362
3,1	0,025	0,082	345
3,2	0,031	0,045	285
3,3	0,039	0,099	506
Overall	0,040	0,099	3317

The increase of repeatability standard deviation in moving from *F* to *EFI* is due to the extra deviation introduced into F_{30} by using the value S_0 "predicted" from *MPD* instead of the actual value derived from the exponential regression for $F(S)$. That extra deviation appears as a speed influence as explained in Section 2.4.13. As was apparent in Table 4.9, which showed the effect of using the predicted S_0 on the calibration precision of *EFI*, the extra repeatability deviations due to the imperfection of the model for $S_0(MPD)$ were rather moderate. Little could be gained by further improving the model.

In summary, a general conclusion to this Chapter could be that the *EFI* concept neither improves nor worsens the reproducibility of friction measurements by different devices but, at least, it does seem to provide them with a stable common scale.

5 Alternative approaches to reference levels

5.1 Introduction

It was recognised at the outset of the *HERMES* project that there could be problems in using the *EFI* concept and associated the calibration procedure to provide a reliable common scale for the comparison of measurements of skid resistance made by different devices in Europe.

Anticipating this, the project included two supplementary tasks that had the objective of investigating alternative solutions to the problem of providing references against which devices could be calibrated and these are discussed in this Chapter.

The first of these, described in Section 5.2, was to develop proposals for a set of specifications for a single reference device that, conceptually at least, could be used either as a means of calibrating existing devices or, in the longer term become the standard measurement method.

It was also recognised that any real device, even if it is based on a standard specification, will need to be calibrated or checked somehow and to do this would require stable and reproducible reference surfaces that could provide and maintain known levels of friction. The second approach, covered in Section 5.3, discusses the topic of reference surfaces and presents proposals for a set of requirements for such surfaces.

5.2 A single reference device

5.2.1 Purpose

As outlined in the introduction to this Chapter, one objective of the *HERMES* project was to develop a specification for a single friction and texture measurement device. This device would, at some time in the future, take over the role of the calibration process in the draft standard *prEN* [3] by providing a direct reference, rather than the current proposal in which the “grand average” of all devices provides a floating reference and groups of different combinations of devices meet at different places at regular intervals for calibration purposes.

In the long term, a fleet of devices of this type could possibly replace the many different devices now in used in Europe.

5.2.2 Approach

In approaching its objective, the *HERMES* working group proposed that the “reference device” should be a Friction Testing Device to which any device currently in use could be compared. It was recognised that, for the foreseeable future, the friction measurement would have to rely on the basic principle of a test tyre running on a wetted road surface and the likely requirements were developed on that basis.

It was also considered important that the design should not necessarily be a perpetuation of present practice. Although it would be wise to draw on current experience, the

reference device should, in effect, represent a “new generation” of devices and that therefore the proposed specifications would not correspond to any existing device.

A lesson learnt from current experience in some countries that have operated large fleets of similar devices over many years was that careful and consistent control of equipment was essential to maintain consistent results between ostensibly similar machines. (Evidence of this kind of problem was to emerge from the HERMES exercises, as noted in Section 2.4.7 of this report.) Therefore, it was also considered particularly important that the specifications for the new device should be designed to provide the best level of reproducibility that would be practicable.

The *HERMES* team, therefore took into account these various aspects when considering the requirements for a reference device. This included a questionnaire survey of *FEHRL* member laboratories to canvass their views. Having established what the basic principles should be, a draft specification was incorporated into a draft standard for making friction measurements using the reference device, prepared in a format suitable for proposal to *CEN*, which is included as Appendix K. The draft proposal for a test method would, of course, be subject to revision and review through the normal channels before formal adoption.

The following sections discuss the background and underlying ideas behind the proposed specification.

5.2.3 Historic and technical background

Each European country uses at least one device to measure friction and texture. Historically, some countries have developed their own devices; others have used devices developed elsewhere. The earliest developments were made before the Second World War, continuing in the 1950s. In the UK, for example, devices such as the Pendulum tester and early side-force skid cars and brake-force devices were developed in this period, but most devices in current use were developed in the late 1960s and 1970s.

An important driving force behind the development of friction measuring devices was the need to explain why it appeared that, on certain sections of the road network, there would be an accumulation of accidents under certain conditions. At the same time, developments were made in order to satisfy the needs of the different countries for research and, in due course, to provide for acceptance tests on new works, and network surveys of various kinds. In parallel, there was an increasing desire to be able to measure friction on airfield runways.

Many new types of equipment were devised and developed in different European countries, for example (in no particular order): Adhera, μ Meter, Odoliograph, SCRIM, Skidometer, Stradograph, Stuttgarterreibungsmesser (SRM), and others in their turn. Some of these are still in use while others have been replaced by more recent developments. At the start of the *HERMES* project it was estimated that there were around 18 different devices in use in Europe alone.

Over the last ten years or so it seems to have become increasingly important for the European national Road Authorities to be able to know the level of the surface characteristics of their own networks. This knowledge is an important aid to the optimising of budgets used to maintain a good service level for road users. Skidding resistance and

texture also have an important role in relation to safety, especially when road surfaces are wet.

Apart from the UK, which had developed its side-force motorcycle combination in the 1920s, early knowledge of the skid resistance characteristics of a road surface in most European countries was very often obtained by static devices or methods. What became known as micro texture was characterised with a pendulum measurement and macro texture was characterised by a volumetric measurement (the "Sand Patch" technique). The introduction of dynamic methods for skid resistance measurement enabled the influence of another important parameter, the test speed, to be explored. This had first been observed in the 1930s by the UK team working with their motorcycle equipment. This led on to the understanding of the relatively greater influence of micro texture at low test speeds and the important influence of macro texture as test speed increased.

In the last past 20 years laser technology has been used to evaluate the macro texture. Although the dynamic measurements of this parameter can now be made at normal traffic speeds (on a dry surface), this is still not possible for micro texture. Lasers and digital imaging technology can be used to assess micro texture but currently this is only possible with static measurements on a laboratory scale and the translation of the technology to a vehicle moving at traffic speeds for routine use will be some years in the future. At present, therefore, there is still a need for a direct friction measurement to evaluate the influence of micro texture.

Many experts consider that, today, the best way to evaluate the likely friction characteristics of a road surfacing is to associate a skid resistance measurement made at a very low speed (allowing micro texture evaluation) with a laser-based profile measurement (allowing macro texture evaluation). However, direct measurements at low speeds may be difficult to obtain on a trafficked road.

It would appear, therefore, that the best practical approach to the problem would be to use a system that can associate a laser macro texture measurement with a friction measurement made at a low slip speed for the test wheel to assess micro texture. The advantage of this approach is that, although the test vehicle may be running at a normal traffic speed (60 km/h or 80 km/h), the test wheel slip speed can be very much lower (for example 30 km/h). These lower slip speeds can be obtained with a test wheel set at an angle (in which case slip speed is equal to the test speed multiplied by the sine of the cornering angle) or with a *slip ratio* imposed by a mechanical or hydraulic system while the test is being made.

In practice, all existing devices for dynamic skid resistance measurement operate on one of these principles, which have been referred to elsewhere in this report as the *SFC* (sideway-force coefficient, ie angled wheel) or *BFC* (brake-force coefficient, ie in-line braking of some kind) principles. The *BFC* principle encompasses the full range of *slip ratio*, up to the locked-wheel condition (100% *slip ratio*), in which the slip speed is the same as the test speed.

5.2.4 European needs

All of the available techniques are used across Europe, with different countries having adopted different methods to meet their own particular requirements. In different countries, the measurements may be made for various purposes:

- On airfield surfaces in real conditions, to give the information about runway condition to the pilots before landing.
- On new works to control the quality level of the work.
- In network-scale surveys of skid resistance characteristics of in-service roads to assist in identifying areas requiring treatment and to prioritise and optimise maintenance work.
- For accident investigation.
- For research (for example, developing new friction models, assessing the behaviour of new types of surfacings, testing the influence of different parameters on skid resistance).

Although initially the principal purpose of the “reference device” would be to calibrate existing devices, there was also the idea that the device might become a Europe-wide standard device in the longer term. With this in mind, it was decided that, before drawing up a specification, it would help if there was a proper understanding of the needs within Europe and to see whether it was possible to conduct all these tests with a single device.

To this end, a questionnaire (Annex K) was sent to all *FEHRL* members. The questionnaire identified the main potential areas of use for the device (excluding accident investigation, which in this context was regarded as a special case of the research category) and asked respondents to indicate which principles and key parameter ranges they thought would best meet their needs. In the latter case, the respondents were asked to “agree” or “disagree” with the proposal that the device should use the feature concerned. A question was included as to whether simultaneous measurements of macro- or megatexture would be required.

Twelve replies were received and syntheses of the results of this enquiry are shown in Tables 5.1 & 5.2. Table 5.1 summarises the majority view regarding the key operating principles broken down by the various types of use and Table 5.2 gives the percentage of responses regarding detailed features. Figure 5.1 illustrates graphically the responses to the 21 questions covered by Table 5.2 regarding network surveys.

Not surprisingly, the responses reflected to some extent the experience of the particular organisation replying, the devices already used in their country and purposes for which they were currently used. It was also apparent that the main common needs related to conducting acceptance tests of new works and for routine network surveys.

Table 5.1 Main results of the responses to the reference device questionnaire.

Operational Feature	Preferred option for each proposed use of device			
	Airfields	New works	Research	Network survey
Type of measurement	Continuous	Continuous	?	Continuous
Principle	<i>BFC</i> fixed ratio	<i>BFC</i> fixed ratio	?	<i>BFC</i> fixed ratio <i>SFC</i>
Test speed	Up to 140 km/h	50 – 80 km/h	All speeds	50 – 80 km/h
Test tyre	Smooth	Smooth	Smooth	Smooth
Water depth	0,5 mm	0,5 mm	0,5 mm to 3 mm	0,5 mm
Operating range	Up to 5 km	10 – 100 km	10 – 100 km	Up to 100 km

Load on test wheel	200 daN	200 daN	Variable	200 daN
Wheel path	Variable	The more loaded wheel path	Variable	The more loaded wheel path
Macro texture	Yes	Yes	Yes	Yes
Mega texture	Yes	Yes	Yes	Yes

Table 5.2 Main results of the enquiry

Question asked	Agree:	Disagree:
1) Continuous type of measurement	75%	25%
2) SFC principle	33%	0%
3) BFC slip ratio	58%	0%
4) BFC fixed ratio > 80%	25%	0%
5) BFC variable ratio	17%	0%
6) BFC locked wheel	17%	0%
7) Blank tyre	67%	8%
8) PIARC tyre	58%	0%
9) Test speed low 30 – 50 km/h	0%	0%
10) Test speed medium 50 – 80 km/h	83%	0%
11) Test speed high > 80 km/h	33%	0%
12) water depth = 0,5 mm	100%	0%
13) Test wheel load = 200 daN	58%	42%
14) Wheel path - the most trafficked	92%	8%
15) Operating range < 10 km/h	0%	0%
16) Operating range 10 – 100 km/h	42%	0%
17) Operating range > 100 km/h	58%	0%
18) No texture measurements	17%	0%
19) Macro texture	33%	0%
20) Mega texture	0%	0%
21) Both Macro and Mega texture	50%	0%

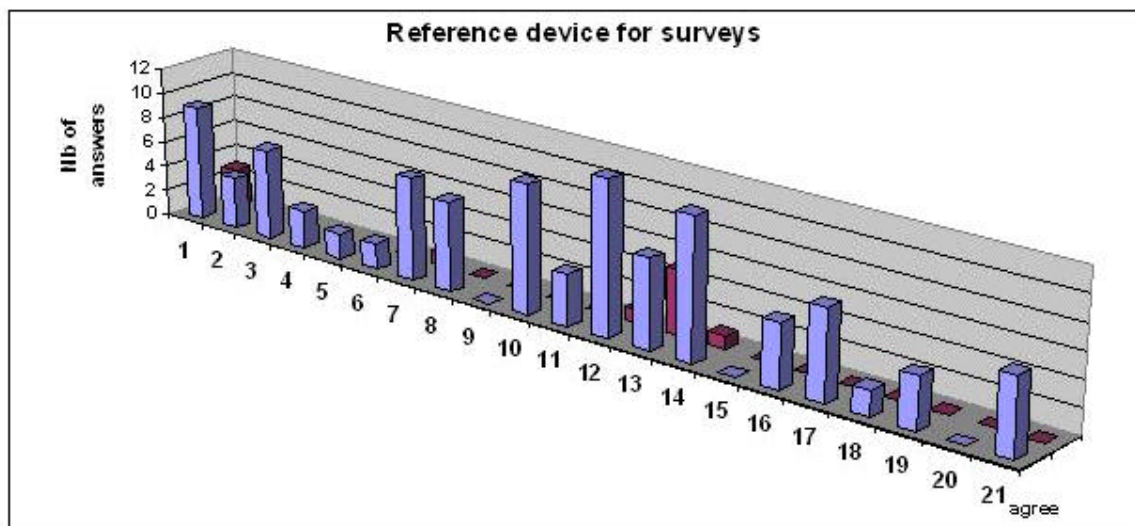


Figure 5.1 Results of the enquiry for surveys reference device.

5.2.5 Proposed specification requirements

Initially, there might be only one device built but eventually more than one may be needed, either to increase flexibility for calibration of existing devices in different countries or to replace those devices in the longer term. Experience over many years has shown that as soon as more than one device is made, even following an identical specification and detailed design, differences can occur between them. Therefore, the specifications for the reference device have been chosen bearing in mind the need to keep the precision of the measurements (i.e., the repeatability and reproducibility) as small as possible. As well as the issue of precision, the specification requirements reflect the initial decision by the HERMES group not to replicate existing devices.

A draft formal specification, in a format suitable for proposal to CEN has been prepared and is included as Annex L. In the following paragraphs, the main aspects of the proposed specification and the reasoning behind them are discussed briefly.

(1) *Continuous measurements*

It should be borne in mind that the primary purpose of the reference device is to provide a means of calibrating other devices, with the secondary potential to become a routine tool. In that regard, it would need to be capable of continuous surveys. In either case, the device should be able to carry out repeated tests on long sections of road without serious short-term deterioration of the test tyre.

(2) *Measurement principle: Brake Force Coefficient (BFC) using controlled slip.*

Because this was to be a reference device, in order to minimise concerns over possible adverse effects such as transverse deformation of the tyre during a test and the uneven tyre wear that can occur using an angled wheel, it was decided that in-line braking should be used. To meet the continuous measurement requirement, a locked-wheel system would not be suitable and therefore the basic operating principle of the device should use in-line controlled slip to give BFC.

(3) *Normal operating speeds of 40, 60 and 80 km/h*

Three normal operating speeds are proposed: 40, 60 and 80 km/h. This range of speeds will assist safe operation on most types of road, for example, 40 km/h for urban roads, 60 km/h on main roads and 80 km/h on motorways. This also provides a range of speeds for comparative tests with other devices for calibration purposes. Clearly, for research use, other speeds may also need to be used.

(4) *Use of a variable slip ratio to provide a constant, low, slip speed*

For calibrating other devices with *EFI* the device should, ideally, record its measurements directly at the reference slip speed of 30 km/h. However, since the device will need to operate at different speeds in practice, this imposes a special requirement on its operation.

In order to achieve a constant slip speed, the actual speed of the test wheel will need to be measured and compared with the vehicle speed so that the slip ratio can be varied depending upon the vehicle speed:

- A test speed of 40 km/h requires a *slip ratio* of 75%.
- A test speed of 60 km/h requires a *slip ratio* of 50%.
- A test speed of 80 km/h requires a *slip ratio* of 37.5%.

This proposed approach to using a variable slip ratio to maintain a constant slip speed, so far as the Authors are aware, is new and has not been applied on any friction measurement devices in current use. Some tests have been made on three of the surfaces used in the *HERMES* trials in France (FR1, FR2 and FR3) using a device that was able to measure the all points on the friction/slip curve ($BFC = f(\text{slip ratio})$) at different test speeds. These suggest that by using a different *slip ratio* in order to obtain the same slip speed for different test speeds leads to a reduction in the variations in the measured braking force coefficient as speed increases (Figure 5.2).

The *BFC* friction measurements obtained on the same surface using each of the three proposed test speeds will not necessarily be equivalent, even though the slip speed should be the same. However, the apparatus, after calibration and calculation of its “A” and “B” values, will be able to calculate an *EFI* value for each of these test speeds and these *EFIs* should be equivalent. The slip speed of 30 km/h has been chosen so that it matches the reference speed for the *EFI* and therefore can be expected to minimise the repeatability of the *EFI* value.

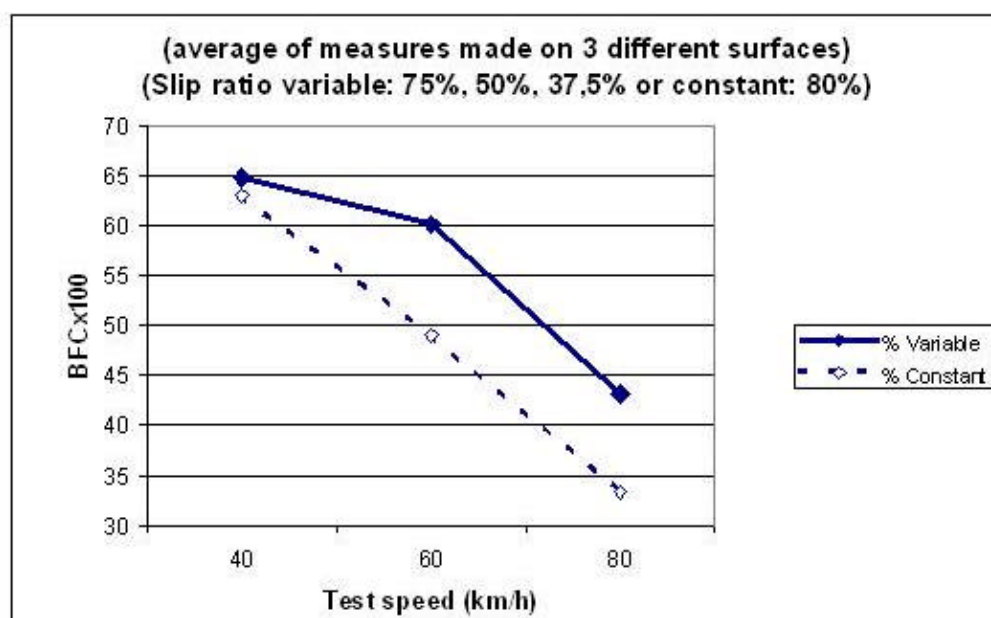


Figure 5.2 Influence of slip ratio on the *BFC* obtained at different test speeds

(5) Static Vertical Load of 3kN

The majority of answers to this question in the enquiry favoured a 2kg (200daN) vertical load on the test wheel but it was clear that this had been influenced by the fact that this is the standard load for a SCRIM. For the reference device, a value of 3kN (300daN) was chosen, not just to be different from existing devices, but because it was more representative of the average load of a normal quarter passenger car.

(6) Measured dynamic vertical load

Even with critical damping on the test wheel suspension, roughness or unevenness of the road can induce variations in the vertical load applied to the test wheel. Additionally, the response of the vehicle suspension relative to the test wheel (when entering, leaving or negotiating a curve, for example) may also have an effect on the dynamic load. For this

reason, the reference device should continuously measure the vertical load and use this value when converting the frictional force to BFC.

(7) *“Theoretical” water film thickness of 0.5mm, independent of speed.*

As with all skid resistance measurement devices, the reference device will make measurements on a wet road and it should carry its own water supply to wet the road just in front of the test wheel.

The theoretical water film thickness can be defined as the water depth obtained on a perfectly flat, smooth and waterproof surface. The actual water film thickness will depend on the surface to which it is applied and will be affected by the texture and porosity of the surface as well as the way in which it is applied. Other practical issues such as air currents (both from side winds and the vehicle slipstream) may also influence the actual application of water.

The constant theoretical thickness will be achieved by regulating the flow rate to match the area over which the water is applied and the test speed. Careful design of the application nozzle will also be required to maintain an even distribution of water across the width of the wetted area.

The chosen value of 0,5 mm is already widely used by current European devices. It is also a value that should give a reasonable operating range for the reference device.

(8) *Test tyre*

It was obvious that test tyre used by the reference device would also have to be standardised and that therefore a special reference tyre would be needed. It was decided that the device should use a tyre that was similar to a normal passenger car tyre under worst conditions, i.e., with a smooth tread (smooth) so that the device would test the road surface characteristic and not the wear level of the tyre.

Proposals for such a tyre were already being developed through *PIARC* Committee C1 in parallel with this work, so it was decided that the *HERMES* reference device should use the tyre defined in that proposal [19] which, in addition to the smooth tread, covers other characteristics such as compound, size, inflation pressure, hardness/resilience and storage conditions.

(9) *Other parameters to be measured or controlled*

As well as the matters discussed above, a number of other parameters will need to be either measured or controlled in some way.

Clearly, the horizontal force must be measured during the test, as must the distance travelled. The vehicle speed should be measured and recorded (the speed is also needed in order to determine and control the *slip ratio*).

In order to ensure that the measurements at different speeds reflect any the variations along the road, the sampling interval (i.e. the period over which instantaneous values of the forces are aggregated in order to provide a sample) should be based on distance travelled, not on elapsed time. It was decided that a sample value should be obtained at least every 100 mm (ie a sampling frequency of up to 220 Hz at 80km/h).

Inevitably there will be significant “noise” in the data as a result of vibrations in the dynamic system and local irregularities in the surface being tested. To damp out these

effects, the horizontal and vertical force samples will be averaged over 10 m before making the calculation of the *BFC*.

5.3 Reference surfaces

The objective of this task within the *HERMES* project was to evaluate the feasibility of designing stable reference surfaces for calibrating friction-testing devices. It was recognised that it was unlikely that a full specification could be produced at this stage. Rather, the task would review key aspects of the topic and make proposals that could be developed in the future.

The work carried out by the project partners in this process included:

- A literature review on the general topic.
- Contacts with operators of test tracks in the motor industry and with other contacts in the field in different countries.
- General discussion and pooling of expertise within the core group.

5.3.1 The purpose of reference surfaces

The reason that a friction index such as *EFI* is being considered is that there is no absolute measure of skid resistance that all devices will record. Differences in measurement method and operational parameters all influence the values recorded. The characteristics of most conventional road surfaces also vary widely and change with time, ambient conditions and the influence of traffic.

Section 5.2 discussed options for a reference device against which others could be compared or which, in the long term, could become universally used. However, such a device must itself be calibrated and in an ideal world it would also be checked against known levels of friction.

Therefore, even though a harmonising index may be necessary to enable measurements from different devices to be compared, it would be better to be able to calibrate devices against standardised surfaces rather than against combinations of each other.

The purpose of a reference surface, therefore, is to provide a stable, known, level of skid resistance that can be used for calibration purposes.

5.3.2 Requirements for reference surfaces

Ideally, a reference surface should have the following general characteristics:

- It should have a known, possibly predictable, level of skid resistance.
- The skid resistance should be stable over time (i.e., it does not change with use).
- The surface should have reproducible characteristics (so that more than one can be made or a replacement can be produced).

If reference surfaces are to be used for calibration purposes, then it must be possible to test any device over its practical range of operation. Therefore, several reference levels are required. Also, for as long as different devices are to be used together with a

harmonised scale, the practical range of operation will have to include a range of speeds as well as of friction levels.

The two main surface characteristics that contribute to skid resistance are micro texture and texture depth (macro texture), governing the underlying friction level and the change in skid resistance with speed. Therefore, any set of reference surfaces should include combinations of these two parameters.

Clearly, it would not be realistic to attempt to produce examples of all possible combinations. Neither is it necessary, for calibration purposes, for surfaces to be specifically representative of any particular type of road surfacing.

It is considered that a practical number of reference surfaces, therefore, would be four. The different combinations of texture that could be encountered should be covered, in broad terms, as suggested in Table 5.3.

Table 5.3 Proposed combinations of texture parameters

	Micro texture	Macro texture
Surface HH	High	High
Surface HL	High	Low
Surface LH	Low	High
Surface LL	Low	Low

At this stage, it is not clear how these parameters should be specified, but before any device calibration testing were undertaken on such surfaces, the skid resistance and texture would need to be validated in some way.

Ultimately, the reference device could be used but, until its development, the texture depth, at least, could be measured using a standard procedure: either the volumetric texture depth test (*MTD*) using glass beads or the mean profile depth (*MPD*). Friction levels would probably need to be checked in the first instance using existing devices representing the three main principles (in-line low *slip ratio*, side force intermediate *slip ratio* and in-line locked-wheel or high *slip ratio*).

However, it is likely that the reference surfaces would need to be made to quite close tolerances in order to ensure that the surfaces and the skid resistance values obtained are reproducible. Current test methods may not be sufficient for this purpose, and this is a point to bear in mind when considering any future specification.

5.3.3 Past experience and existing practice

5.3.3.1 Some historic background

Dynamic measurements of road skid resistance have been made in some countries for decades. In the UK, for example, the first side force device was developed in the late 1920s, and locked-wheel devices were used from the 1950s. Accurate measurement of skid resistance on roads became of increasing importance in the 1970s and since that time there have been many attempts to establish appropriate reference standards. While it has always been possible to carry out static calibration checks on force transducers,

there has always been a desire to establish surfaces on which the whole friction measurement system could be checked in a dynamic test.

In a laboratory exercise in 1974, Britton et al [13] investigated the criteria needed for the design of primary standard reference pavement surfaces. Model surfaces were created using particles of known and easily-controlled geometry on a flat substrate, such as spheres set in epoxy resin. Adhering artificial or natural fines controlled the micro texture. A wide range of macro texture was tested and several materials were used. The different particles had the same shape factor but represented different chemical structures. The friction measurements were made with a British Portable Skid Resistance Tester (the "pendulum tester") and the friction values reported as the *BPN* (British Pendulum Number). Over 600 samples were made for the experiment.

No evident difference was observed between the samples made of different materials and of the same particles size, within the limit of the sensitivity of the experiments, but the effects of macro texture, size and shape were found to be more significant. Their work indicated that pavement tyre/friction was influenced by both the macro texture (size of aggregate, spacing and shape) and the micro texture (size of the fines, spacing and shape), which, of course, had already been observed in practical work on roads. The use of synthetic aggregates was investigated and the more promising type appeared to be synthetic burnt clay aggregates.

Viewed from the present time, however, a limitation of this exercise was the use of the pendulum test, which is not able to discriminate reliably between the relative effects of micro texture and macro texture. (The test was originally designed to indicate the level of friction when a patterned tyre (of the 1960s) skids at 50km/h on a medium-textured road surface).

In 1983, Dunlop Limited (UK) investigated the creation of reference surfaces and proposed a standard reference surface to the relevant International Organisation for Standardisation (*ISO*) committee [14]. This proposal involved replica surfacings to which quartz sand was applied to simulate micro texture. The polished stone value (PSV) was measured for the different replicas, which were found to behave in a similar way to many granite natural aggregates. The replicas reproduced micro texture to a high degree of accuracy but, in use, the micro texture was removed rapidly by the tyre in a similar way to that expected from traffic action had a natural aggregate been used.

Therefore, this could not be considered as a standard reference surface specification but was a starting point that was taken into account in a further review in 1986, when *ISO* published a technical report detailing the process for creating a standardised test surface for high friction tests [15]. The work carried out to investigate this type of surface indicated that the best results were achieved with a surface dressing of fine (passing 1.2mm retained on 0.6mm sieves) silica sand (natural Leighton Buzzard sand) spread, without rolling, on to a bitumen-expanded epoxy binder. With this surface, the high friction depended almost entirely on the micro texture produced by this aggregate. Silica sand was selected because it represented the most wear-resistant material known.

In the mid-1970s, three field test centres were set up in the USA under the auspices of the Federal Highway Administration (FHWA) in order to improve and standardise the measurement of skid resistance [16]. At these centres, which were in separated geographical locations, various "primary reference surfaces" (PRS) were constructed. The surfaces were replicated in each location using the same contractor and similar selected naturally occurring materials, including silica sand and river gravel, all in an epoxy seal

coat. Initially, each centre had five primary reference surfaces 4.6m wide by 158m long. Friction measuring devices (complying with the ASTM standard) from the various state authorities were correlated individually against the PRS. A standard vehicle based at each centre was used to provide a reference skid measurement system and provide a correction to take account of variations in the PRS over time. Although three centres had been set up initially, it soon became evident that only two were needed to service the population of skid testers and one station was closed after only one year of operation.

Although five primary reference surfaces were constructed at each site, there were difficulties in achieving the required target levels of skid resistance. Initially, all the surfaces had higher levels than anticipated. As a result the roughest surface, which was abrading the test tyres of the candidate equipment, was abandoned and further primary surfaces were constructed later to provide low skid resistance. In addition, some of the other primary surfaces at one of the centres were affected by surface distress probably brought about by defects in the original binder and by construction joints propagating from the underlying base material.

Even though the primary reference surfaces were only trafficked during the testing process, it was found that all exhibited significant variations in measured friction during the year. It was also found that there could be significant variation over time: on one surface, the Skid Number (the value recorded by ASTM devices) reduced from 63 to 46 over the nine year period of the operation of one of the centres [17].

Thus, although so-called durable reference surfaces were made, the experience shows the difficulty in defining and achieving skid resistance using natural materials and in making materials that maintain a consistent value over time. In this situation a reference device (but of the same type as the devices being calibrated) had to be used as well in order to provide a correction to take account of the variations in the surfaces, but there was no real standard against which that device could be compared.

5.3.3.2 Comparisons of devices on airfields

For some years, regular comparisons of friction devices (mostly for airfields) have been made in the USA at the NASA airfield test site at Wallops Island [18]. Many different surfaces have been laid on runways and taxiways to provide a range of friction and texture levels and studied on regular basis since 1993. Although some 35 different surfaces or variations have been included or added over the years, the eight surfaces that have been included throughout and therefore on which most attention has been focussed are described as:

- Concrete surface.
- Concrete surface with 1x1/4x1/4 inch grooves and canvas belt finishing.
- Surface with 1x1/4x1/4 inch grooves and burlap drag finishing.
- Aggregate asphalt.
- Aggregate asphalt with 2x1/4x1/4 inch groove.
- Aggregate asphalt with 1x1/4x1/4 inch groove.
- Aluminium plate.
- Driveway seal coated asphalt.

Measurements have included sand patch, *MPD*, *BPN*, and outflow meter for texture. Various friction devices have made measurements, including some from Europe. A review of data provided to the *HERMES* team by the organisers of the trial showed that considerable variability has been observed both between devices (as might be expected)

and over time. Each friction device made measurements at a range of test speeds, with the expected decrease in measured friction with increased speed.

However, it is the stability of the friction and texture measurements over time, which is the major factor of interest here. Some variation in texture depth was observed (the cement concrete surfaces appear to have been the most consistent). Measurements of friction at one test speed were compared over time for individual devices on those sections for which most data were available for the period. Considerable variation could be observed from year to year, the extent of which varied depending on the device making the measurements. Although this exercise has provided many useful comparisons, the analysis is still dependent upon using the average of all devices as a basis for them. Because of the instability observed over time, it is considered that none of these surfaces has the potential to become a long-term reference surface, although some of the ideas could probably be developed.

Attempts to harmonise airfield friction devices have been made in recent years in Norway on a calibration test track at Oslo Airport. These trials utilised a purpose built Calibration Test Track. The test surfaces were of different asphalt mixes but here, as at Wallops, the average of devices was used as a reference level for harmonisation in a similar way to that proposed by the International Friction Index. Comparisons from trials from 1998 to 2000 using tests with examples of GripTesters and the Swedish BV11 devices showed variation in friction level from year to year.

5.3.3.3 Test tracks operated by road research organisations

FEHRL members with research test tracks, such as LCPC and TRL have built test surfaces over the years, some of which were used in the HERMES calibration meetings. They, too, have found that it is possible to obtain different friction levels using different combinations of materials. In fact, surface GB15 was prepared, partly for use in the HERMES work, with the specific intention of providing an intermediate level of skid resistance. It was based upon small particles (nominally 3mm) of gravel (with smooth surfaces and hence no micro texture) fixed to the underlying asphalt surface with epoxy resin (Figure 5.3).

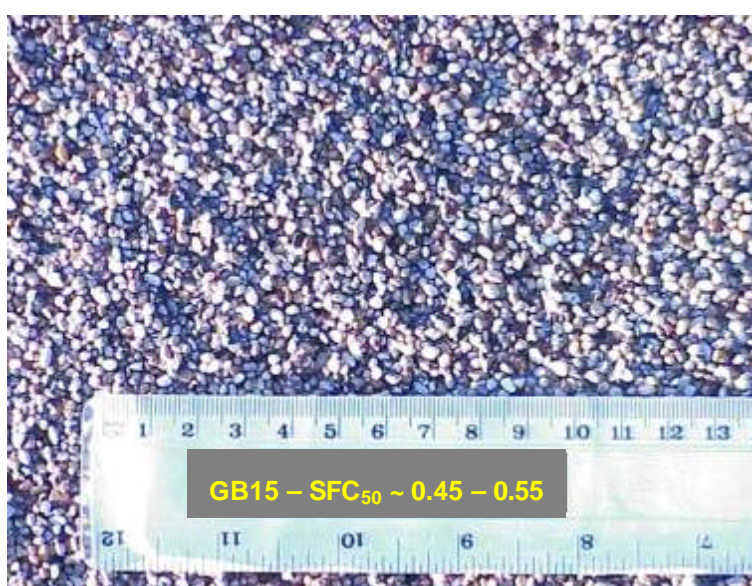


Figure 5.3 The "pea gravel" surface GB15

While this technique successfully produced an intermediate friction level, it was not possible to predict what that would be or to guarantee that it would remain stable over time.

These various test track surfaces are all used for regular comparison of devices or for correlation of devices of the same type, such as the annual SCRIM correlation trials held at *TRL* each April. However, the correlation process relies on the comparative measurements of the devices rather than a stable reference level from the surfaces themselves.

5.3.3.4 The Motor Industry

The motor industry in different parts of the world uses proving grounds to evaluate the performance of tyres and braking systems. However, although they may have surfaces designed to give different friction levels and some materials are commonly used (such as polished basalt tiles or ceramic to provide low friction), they do not have standardised friction characteristics. Rather, they provide a means for comparative testing and friction is deduced from the braking performance of the vehicle or tyre.

In Spain, for example, *IDIADA* - Instituto De Investigación Aplicada Del Automóvil (Applied Automotive Research Institute) built a test pavement on their research track. The pavement friction was tested at the end of the construction work, using the British Pendulum tester. However, no dynamic skid resistance measurements with standardised devices have been carried out. Instead, friction values are estimated from the braking distance of the different commercial vehicles visiting the site. This process of calculation was considered sufficient to characterise the surfaces since the vehicles had already been officially approved by some standard.

In this context, the friction can be even more variable than with standard friction test devices given the range of systems, tyre compounds and tread patterns likely to be used. Some organisations carry out regular friction tests on their test surfaces using standard methods (TRC, in the US, for example monitors its surfaces every two weeks using the *ASTM* Skid trailer (similar to device F09 in the *HERMES* project) but because the sites are out-doors, the surfaces are still subject to the variations that are associated with changing seasonal conditions.

It is clear that the problem of specifying and producing surfaces with predictable characteristics and stable friction levels that would be suitable for reference calibration purposes has yet to be solved. In the remainder of this Section the various issues that need to be addressed are considered and proposals for further work are made.

5.3.4 Possible solutions

In considering possible solutions to the issue of reference surfaces in the context of calibrating devices for comparison with a European skid resistance index, several aspects must be considered including:

- Where the surfaces are to be based.
- Where and how they are to be used.
- How they are to be made.

These considerations, in turn, lead to further questions regarding the detail of the way in which calibration reference surfaces might be used in Europe. This Section discusses the general issues and Section 5.2.5 summarises the ideas in the form of some initial suggestions for an outline specification.

5.3.4.1 Where should the reference surfaces be based?

Having established that the reference surfaces would need to be specially laid or manufactured for this purpose, it follows that a dedicated site would be required. That would need certain specific features, discussed later, but an important issue is where it should be.

In an ideal world there would be one site, with one set of reference surfaces, reasonably centrally located, which all devices that were to be included in the skid resistance index would have to visit for regular calibration checks. This would avoid problems of reproducibility between replicate surfaces. However, Europe covers a very large area, so it would be unrealistic to consider just one location. Devices from as far apart as Norway, and Spain took part in the *HERMES* exercises but while this was reasonably practical (as discussed in Section 2.1.3), some devices did place constraints upon where they would be prepared to go, given the travelling distances involved.

In principle, any country that can identify a suitable site and organisation to take responsibility could build and maintain a set of reference surfaces. However this would be a significant investment and might not be practical for some European countries. It would be better, perhaps, to establish a limited number of separate test locations so that there is one within a reasonable distance of most countries. It is recommended that at least three sites should be established in Europe: one in the north and west, one in a central area and one in the south or eastern region.

Conceptually, each site could have its own set of reference surfaces. Alternatively, a common set of surfaces could be built with a modular structure, stored in one location and then transported to a particular test site (designed to accommodate them) when required for a calibration exercise.

5.3.4.2 What should a test site be like?

The *HERMES* project partners have carefully considered what would be required from a test site in order to provide an effective location for carrying out calibrations using reference surfaces.

Clearly, any test surfacing must be built on a structure or foundation that is capable of carrying repeated passes of the weight of the test vehicles. In many cases the test wheel is in line with the vehicle road wheels, either on the same chassis or a trailer. Because they carry large water tanks, some are necessarily large goods vehicles with axle loads of up to eight tonnes. (The Dutch ROAR in the *HERMES* exercises and a SCRIM that has recently entered service in Belgium, for example, are both built on three-axle truck chassis). Other devices have the test wheel on a trailer offset from the wheel path and so the vehicle must pass with its wheels slightly to one side. Whatever form of construction is chosen, it should be able to accommodate vehicle of these sizes.

As well as being able to carry the weight of the vehicles repeatedly, the test road structure will also need to have adequate drainage to remove the water deposited by the test devices. Ideally, a system that could positively remove excess water between passes would be an advantage.

Each test section also needs to be long enough to accommodate the necessary test passes, including an allowance for accelerating to the required test speed and decelerating afterwards. Although the length of surface on which friction will be measured may only be 100 m or so long, some devices, usually those using a variable slip control system, need a certain length in which to stabilise the required *slip ratio* at the particular speed and friction level. This could require a test surfacing some 300 m long, together with an approach and exit lane to allow for acceleration and braking when higher test speeds are needed.

A crucial aspect of reference surfaces is that their characteristics should remain stable over time. This means that ideally, they should be kept clean and should not be exposed for long periods to extremes of weather, particularly frost, rain and strong sunlight. Therefore, a test facility should include some means of protecting the test surfaces from the elements when they are not in use. Consideration should also be given to how any build-up of tyre deposits on the surfacings as a result of repeated testing can be removed without adversely affecting the friction characteristics.

While it will be important that the characteristics should be stable and durable, the working life of a reference surfacing need not be very long, provided that it can be reproduced and replaced easily and reliably.

There are essentially two choices for the method of construction: the creation of four permanent surfaces, or the creation of modular surface sections. Permanent surfaces would probably be quicker to test, especially if laid in-line with one another, and would be relatively easy to control. However, a large test site would be required and it would be potentially rather difficult to keep clean and protect from the weather.

The general requirements suggest, therefore, that a modular form of construction that allows surfaces to be removed and stored when not required could be the preferred approach. An arrangement that enables the sections to be laid adjacent to one another with approach and exit areas common to all sections would reduce the length of road required compared with a linear structure where sections were laid one after the other. This would allow the test surfaces to be relatively narrow (say 1m wide), with neutral areas the width of a normal traffic lane to each side that would potentially allow either left- or right-handed machines to test them without unnecessary wear and tear on the test sections.

Ideally, the reference component of the test surfaces (i.e. the part where the calibration friction levels will actually be measured rather than the approach length) should be under cover, perhaps in a large hangar that is also equipped with water supplies and other ancillary facilities. The building could include space for cleaning and storing modular surface sections when they are not being used. Blank modules or slats could be provided for the test area when it is not in use. This concept is illustrated schematically in Figure 5.4. In principle, an alternative might be to use a single line layout, with modules removed and replaced with different surfacings during a test session. However, this is only likely to be worthwhile if the modules can be changed quickly and this may not be a practicable option. A separate storage building, possibly with a protective tunnel to covering the test area might also be considered.

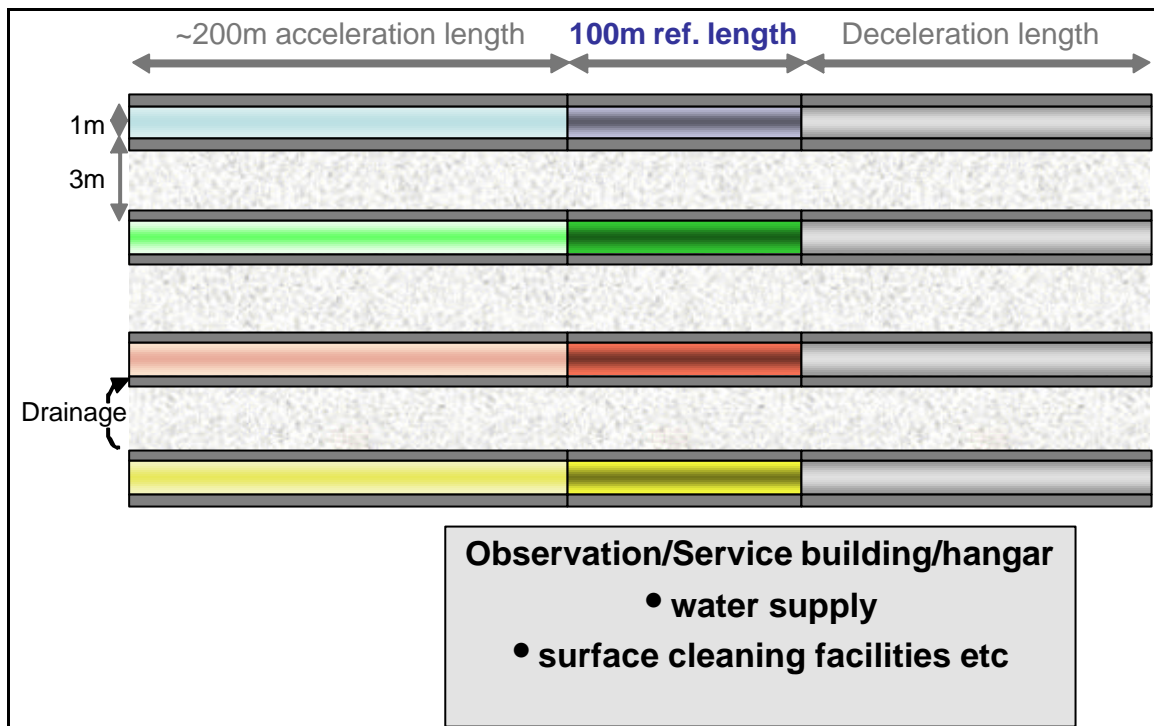


Figure 5.4 Concept of using parallel modular reference sections

Another advantage of the modular approach is that the sections could be transported relatively easily from one facility to another if this were required. It would also be much easier to provide identical, interchangeable and replaceable surfaces. Spare modules would need to be built for the different surfaces to allow for possible damage during handling and use. If a typical module was in the form of a 1m x 5m slab, around 70 slabs (60 + 10 repairs) would be needed for each surface, assuming a section is 300m long.

The essential feature of a reference surface is that its characteristics should be clearly defined, easily reproduced and consistent through its working life. An individual module need not last for a very long time if it can quickly be replaced by another with the same characteristics.

5.3.4.3 What materials might be used?

The calibration surface itself could be made from three basic types of material:

- Natural aggregate with either a bitumen binder or in a Portland cement concrete.
- An artificial aggregate (such as a ceramic) fixed to a substrate with a resin-based binder.
- A completely fabricated surface using man-made materials.

(1) Natural aggregates

Although crushed rock aggregates are easy and relatively cheap to obtain, their natural characteristics are likely to be very variable in the context of creating a reference surface. Natural aggregates are already known to change their characteristics with time due to weathering and wear, particularly polishing by traffic.

The use of bitumen as a binder is also a marked disadvantage because there is a strong possibility of initial contamination of the aggregate surface. This might be avoided with a surface dressing technique, but this is unlikely to be a successful way of producing a

material that will retain its texture depth with the repeated passage of test vehicles. Similarly, it would be difficult to prepare a surface using cement as a binder because of the risk of contamination.

Conventional asphalt mixes would be inappropriate for reference surfaces, not only because of the contamination risk but also because where the asphalt matrix forms part of the surface, this can be expected to change over time as the bitumen weathers. Cement concrete mixtures are also likely to gradually wear.

In theory it might be possible to make a surface using conventional materials and then to condition it in some way before use as a reference. However, the difficulty with this approach is to know when the correct condition has been reached and what the friction level would be.

Some gravel aggregates, particularly flint, may have naturally smooth, hard surfaces and so it might be possible to use such materials to provide a combination of low micro texture and intermediate or higher macro texture.

However, experience on test tracks using natural aggregate surfaces where skid resistance devices are regularly compared has shown that their characteristics can change as a result of repeated testing.

For all these reasons, it is not recommended that natural aggregates or normal asphalt or concrete mixes should be used

(2) An artificial aggregate and a resin binder

There has been a great deal of research over the years into the production of artificial (or synthetic) aggregates. Artificial aggregates can be produced with characteristics that can be controlled and remain relatively stable. Most are derived from naturally-occurring minerals, which are then treated in some way, for example by calcination (heating to high temperatures).

Synthetic aggregate particles can be expected to be identical and regular in shape and these therefore, fixed to a substrate with a suitable binder (such as epoxy resin) could be a possibility for the creation of reference surfaces. The different levels of the two components of texture could be achieved by varying the final particle sizes and the asperities in the surface.

Examples of artificial aggregates that might be explored are listed in Table 5.4.

Table 5.4 Artificial aggregates that might be used in a reference surfacing

low friction	high friction
Ceramics	Calcined bauxite
Calcined Flint	Burned clay

(3) Man-made materials

Using man-made materials means that pre-determined shapes and profiles can be manufactured and replicated. The techniques might utilise moulded shapes using, for example, fibreglass and resin, as was tried for special external drum surfaces by Dunlop and *TRL* during the 1990s. The shapes could be basic geometric shapes such as

hemispheres, cuboids tetrahedra or cylinders (Figure 5.5) or castings taken from actual road surfaces.

An alternative to moulding surface profiles would be to machine or press them from a metallic plate, although this technique might not allow some of the more complex patterns to be easily reproduced over large areas.

The advantage of this type of technique is that it would allow very repeatable surfaces to be made and would permit different forms and scales of macro texture to be produced.

Using casts from real roads, although theoretically possible, might not be appropriate for developing reference surfaces. Apart from deciding what general type of road surface should be used, this approach would make it difficult to ensure homogeneity, both along each modular section and along the length of the assembled test surface.

A major limitation of this type of approach, however, is that the materials would be unlikely to have a “natural” micro texture and so this would have to be added somehow, which has proved a problem in the past. On the other hand, this approach could be useful to make a low micro-, high macro texture surface (type LH in Table 5.3).

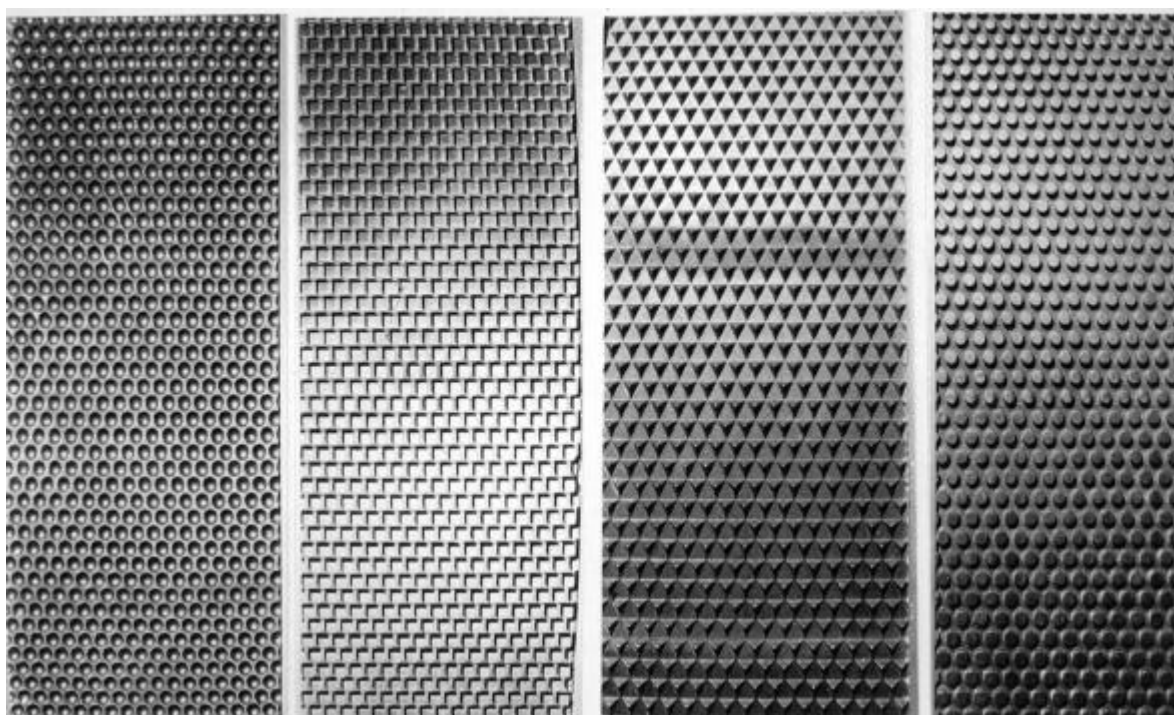


Figure 5.5 Specially formed surfaces using geometric shapes (l-r): hemispheres, cubes, tetrahedra, cylinders.

5.3.5 Outline specification for calibration reference surfaces

The discussion of the various aspects of reference surfaces in Section 5.2.4 leads to the view that, at the present time, it is not possible to develop a definitive specification for reference surfaces suitable for use for the routine calibration of friction measuring devices against a harmonised index. Further research is needed to take this idea forward (Section

5.2.6), but an outline specification can be suggested here to provide a framework for future investigations.

Table 5.5 gives this suggested outline specification, based on the assumption that a modular form of construction would be used, allowing surfaces to be set up at a number of sites or to be moved between suitable locations as required. Some of the details such materials to be used, the layout of the site or facilities needed that have been discussed above have not been included in this table since they would need to be finalised in the light of experience from any future research.

Table 5.5 Outline requirements for Calibration Reference surfaces

General Property		General Requirements	Other Comments
Alignment		Straight and level, no cross-fall	These requirements would apply to the track on which vehicles run as well as the test surface. With no cross-fall, suitable drainage or other mechanisms will be needed to rapidly clear excess water from the test surfaces.
Length		100 metres minimum	This is the minimum test length. A longer length (up to 300m) may be required to accommodate some devices that use a fixed <i>slip ratio</i> controlled by a servo system that responds to changing surface friction.
Width		1 metre wide test surface	There will also be a need for space either side of the test surface when installed to allow for the passage of the test vehicle, depending upon the relative alignment of the test wheel and the main vehicle's tyres.
Construction		Similar interlocking modules Module size to be chosen to suit ease of construction and handling.	The load bearing capacity for the installed module and associated roadway will need to be able to support normal lorry axle-weights in order to accommodate the larger test vehicles.
Surface characteristics	General	Texture (micro and macro) of the surfacing should be homogeneous along its length and across its width. The texture should not be so aggressive that it causes excessive test tyre wear.	Each module should be similar, with no significant boundary edges in the surface where the modules join. Joints will need to be secure and not collect dirt or allow passage of water (unless suitable sub-surface drainage is provided).
	Surface HH	$BFC_{20} = 0.75-0.85$ $MPD = 1.5-2.0$ mm	These are tentative suggestions of target ranges for the key texture parameters. Eventually, a more precise specification will be needed. BFC (locked-wheel) values at 20km/h have been used here as a suggested indicator of the micro texture level needed: in practice, other low slip-speed measurements could be used.
	Surface HL	$BFC_{20} = 0.75-0.85$ $MPD = 0.2-0.4$ mm	
	Surface LH	$BFC_{20} = 0.25-0.35$ $MPD = 1.5-2.0$ mm	
	Surface LL	$BFC_{20} = 0.25-0.35$ $MPD = 0.2-0.4$ mm	
Surfacing materials		To be determined.	Should not be bitumen-based or use untreated crushed-rock aggregate.
Stability		Should maintain defined skid resistance and texture depth over a practical temperature range for at least 3 years. Friction should not change over a short period of repeated testing.	To assist this, it may be necessary to keep and use the surfaces in a controlled environment.
Durability		Should maintain defined skid resistance and texture depth for up to 1000 repeated test passes with up to 500kg test wheel load.	The suggested number of passes is sufficient to check up to 5 devices (making 5 test passes at 3 speeds plus some additional passes) 3 times a year for 3 years.

5.3.6 Further research

It is clear that further research is necessary to develop practical reference surfaces. It is not practical to develop a full research proposal here, but some suggestions of what might be included can be made.

5.3.6.1 Suggestions for materials to include in the investigation

As discussed in Section 5.2.4.3, the choice of suitable materials to achieve predictable and stable performance will be difficult, so work to identify materials that could be reliably specified for use for the reference surfaces will be a fundamental aspect of the research. The challenge is to find suitable combinations of a regular and repeatable form and level of macro texture with appropriate treatments or additives to provide predictable, controlled and durable micro texture.

As a starting point, some or all of the following could be investigated:

- Castings of geometric shapes using resin/fibreglass to represent controlled macro texture forms (such as in Figure 5.5).
- Cut or pressed shapes or patterns in metal.
- Proprietary anti-slip or high friction materials/coatings.
- Paints with suitable additives to provide micro texture (variations on some road marking materials might prove suitable).
- Conventional materials, either to prove that, as expected, they would not be suitable or to assess whether in certain conditions they might be used.

These suggestions assume an approach in which the required surfacing is applied as some form of overlay to a suitable substrate. An alternative might be to use a material that can be “refreshed” in some way to a standardised level.

Another aspect that could be considered would be the inclusion of porous or permeable materials, since these are used on the network and a calibration check on the devices with this type of surfacing might be appropriate.

5.3.6.2 Module structure

Although the main emphasis on the research would be to establish suitable test surfaces, consideration should also be given to the structure of the modules on which they would be used and how they should be supported at road level on the test site.

The research on this would initially be a desk study to assess how the modules might be engineered, followed by practical tests on the most promising designs.

Possible forms of construction for the bearing surface might include:

- A timber bed.
- Concrete slabs.
- Steel/alloy plates.

All would need a suitable support framework, together with a carefully designed mechanism to ensure that they would interlock reliably. Some might be ruled out as impractical in order to achieve a workable size and weight for individual modules.

Tests using the surface materials applied to fixed substrate might also be considered to allow for the possibility of a permanent installation.

5.3.6.3 Outline research programme

In outline, the research might comprise a three-stage process involving the following ideas:

- (1) *Investigation on a laboratory or pilot scale of suitable materials*
 - Tests to explore suitable material combinations to achieve the required levels of friction and texture depth.
 - Accelerated wear testing of the best of the possible materials.
 - Comparisons of indoor and outdoor tests.
- (2) *Design and testing of a suitable form of construction*
 - Desk study to explore suitable forms of construction for the modules that would carry the test surfaces.
 - Practical durability tests on pilot-scale modules.
- (3) *Full-scale trial exercise*
 - Assess both weathering and wear-and-tear under repeated testing over a 3-year period.

Testing of the reference surface materials would need to include measurements using friction devices covering the three main principles, plus measurements of physical characteristics using all suitable techniques available to assess gradual changes.

For accelerated wear tests on the surfaces, consideration should be given to using laboratory scale indoor test machines or larger-scale outdoor machines such as the *LCPC* carousel at Nantes.

For tests on the durability of the module construction, facilities such as the Pavement Test Facility at *TRL*, which allows repeated passing of a lorry-sized wheel under controlled load, might be used.

Clearly, this is a large programme of work that, as with the *HERMES* project, would require co-operation between several organisations to achieve. It might be worthwhile therefore, to limit the work initially to a feasibility study that concentrated on (1), the desk component of (2) and limited tests for (3).

6 Conclusions

The *HERMES* project was developed through *FEHRL*, and was carried out under the guidance of a steering group comprising experts from six *FEHRL* member laboratories. The project had the primary objective of testing the procedures for establishing and maintaining a harmonised skid resistance index proposed by *CEN* in *prEN13036-2* [3]. In addition to testing the practical aspects, the project also was to consider possible improvements to the models used to calculate the index and to explore alternative approaches for possible future consideration. The findings of the the project in relation to these main tasks are summarised below.

(1) *Experimental procedures*

The procedures described in Annex B of the *prEN* [3] have been tested in as realistic conditions as possible. Nine calibration trials involved fifteen friction devices from eight countries, covering virtually all the measurement principles normally used to measure skid resistance at traffic speeds. Seven different devices (but all complying with the relevant *ISO-CEN* standards [4]) were used to measure texture depth.

The trials took place in five different countries, either on public roads or on test tracks. The test surfaces covered a wide range of materials and textures, including porous surfaces. The trials were grouped in “rounds”, with three trials in each round being carried out in the space of about one month. Further rounds were carried out at six-month intervals, thus giving some opportunity for the characteristics of the devices to undergo changes and for seasonal or weather influences to have an effect, as would be expected to happen in practice.

The project has shown that the proposed methodology for bringing different groups of devices together for calibration trials is practical to achieve and can be carried out successfully. However, the process can be expensive, with costs broadly in the range 3 000 - 5000 euros and 150 - 200 hours of staff time required to organise a trial and from 1500 to 5000 euros and 50 - 100 hours of time for a device to attend a trial, depending upon how far it has to travel to the test location. Lessons learnt progressively from the running of the trials have been used to develop a Guideline that can be used as the basis for organising such exercises in future.

(2) *Analysis methods and improved models*

The application of the analysis method specified in the *prEN* [3] revealed a number of drawbacks:

1. The statistical tests proposed in the *prEN* for discarding outlying results are too severe and not in line with those commonly used in international standards such as *ISO 5725* [5].
2. The exponential model for the variation of the friction coefficient (F) with slip speed (S) did not fit the experimental data in a significant number of cases.
3. The prediction of the speed parameter (S_0) from texture depth (MPD) is much too imprecise, and this leads to a significant residual operating speed influence on *EFI*.

4. As the calibration is repeated trial after trial, the calibration parameters (*A* and *B*) of any given device evolved in such a way that the sensitivity of *EFI* to the actual friction characteristics of the surfaces decreased dramatically, leading for example to unacceptably high values on very low friction surfaces.

In order to remedy those defects, a number of possible improvements have been considered:

- (i) Applying the statistical tests specified in *ISO 5725-2* [5] ("k-test" and "h-test") to remove outlying combinations of devices and sites.
- (ii) Applying, as alternative statistical tests, the rule: $R^2 > 0,5$ to the regressions.
- (iii) Applying an additional condition on the coefficient of variation of *EFI* ($CV_{EFI} > 5\%$ or 10%) in order to discard measurement series bearing on too narrow a range of friction levels.
- (iv) Using alternative forms of regressions to *F* against *S*, namely polynomial and Stribeck's curve in order to provide a better fit to the data.
- (v) Considering the relationship S_0 versus *MPD* as device-specific in order to reduce the scatter of data with respect to the "universal" law specified in the *prEN* [3].
- (vi) Using a power law for S_0 versus *MPD* instead of a linear law to fit the data better.
- (vii) Applying a weighting on the regression of S_0 against *MPD* to reduce the influence of outlying values.
- (viii) Trying to relate S_0 to texture parameters other than *MPD* to further improve the prediction of S_0 .
- (ix) Forcing calibration parameter "*A*" to zero with a view to preventing the loss of sensitivity of *EFI* referred to in point 4 above.
- (x) Calculating first the regression of *EFI* against its grand average $\langle\langle EFI \rangle\rangle$ and then back calculating $\langle\langle EFI \rangle\rangle$ against *EFI* by reversing the equation.

Fourteen different attempts have been made to improve the consistency and precision of the calibration procedure by resorting to different combinations of the alternative treatments (i) – (x) above. It was found that better, although still not ideal, results were obtained by adopting the following options:

Retaining the original exponential model proposed in the *prEN* [3] for the relationship between friction and slip speed, i.e.

$$F = F_0 e^{-S / S_0} \quad (6.1)$$

Use a new model for the relationship between texture depth (expressed as *MPD*) and the speed parameter S_0 , with device-specific coefficients "*a*" and "*b*", i.e.

$$S_0 = a * MPD^b \quad (6.2)$$

Apply the following weighting in the regression calculation to determine “a” and “b”:

$$w = (S_0 / s_{S_0})^2 \quad (6.3)$$

where s_{S_0} is the residual standard deviation of S_0 with respect the exponential regression of F against S .

In the definition of EFI , “A” is forced to zero to give:

$$EFI = B * F_{30} . \quad (6.4)$$

Both in the regression $F(S)$ and in the regression yielding the value of “B”, the correlation coefficient R^2 must be higher than 0,5 otherwise, the corresponding measurement series is discarded.

In the model chosen, both in the *prEN* and in the further analyses, a reference slip speed of 30km/h was selected because this was close to that used by many devices in practice. However, it was found that the GripTester and IMAG devices did not fit the chosen model well. A possible explanation for this is that these devices have only a narrow range of slip speeds over the practical range of operating speeds: this leads to unavoidable extrapolation when relating these devices to the reference speed. It is important to stress that this is a function of the models, not a criticism of the devices themselves. Including the results of the GripTester and IMAG unacceptably disturbed the whole calibration process of the other devices; therefore, they were discarded from the data set.

Further, it was found that two families could be distinguished within the remaining thirteen devices, namely those using the *BFC* and the *SFC* measuring principles. The latter group comprised the *SCRIMs* and the *Odoliographs*, both types of device having the same *slip ratio* of 34%. Although it could be assumed that the participating devices were in good condition, direct comparison of devices revealed that significant changes may have occurred to some of them from one trial to the next. However, it is not known to what extent this could have influenced the outcome of the whole experiment.

(3) General conclusions from the experimental and analytical studies

In the light of the conditions applied in the analysis summarised above, the main results of the experimental part of the project can be summarised as follows:

1. Regarding consistency, it was concluded that the calibration method works satisfactorily: the procedure leads to a stable *EFI*-scale even though limited subsets of devices operating on different sets of test surfaces are compared in each calibration exercise.
2. Regarding precision, it was concluded that the reproducibility of the *EFI* value delivered by different devices was acceptable for *SFC* devices with the same *slip ratio* but not for *BFC* devices, which use a wider variety of measurement principles.

3. Analysis of the sources of deviations has shown that further improvements to the models used for $F(S)$ and $S_o(MPD)$ are unlikely to improve the reproducibility of EFI .

An important conclusion from the project is that it appears that, based on the data from this study and using the models developed so far, it is not yet practical to harmonise satisfactorily all the device principles currently used in Europe by using the EFI approach.

(4) *Alternative approaches*

An alternative approach to the common scale and calibration process associated with the EFI concept has been considered, in the form of a single reference device. Such a device could, in the longer term, replace existing devices and itself become a Europe-wide standard. A set of proposed specifications for a single friction and texture measurement method based on this device has been prepared in a form that can be proposed to *CEN*. The specifications take into account the views of *FEHRL* laboratories based on their responses to an enquiry.

Although learning from experience from developing and using present equipment, the proposed device is intended to be completely new and, so far as the authors are aware, it uses a different approach to the measurement of skid resistance to that followed by existing devices. It was decided that the reference device should have the following key features:

- Simultaneous measurement of friction and macro texture on the same test line to enable immediate evaluation of EFI at any test speed.
- Friction measurement on the BFC controlled-slip principle, but with a *variable slip ratio, controlled to provide a constant slip speed of 30 km/h*.
- Three standard operating speeds (40, 60 and 80km/h).
- Simultaneous
- A standardised reference tyre based on a technical specification currently being proposed by *PIARC* [19].

A mega texture indicator will be also given by this device on this same measurement line. Any real device, even if it is based on a standard specification, will need to be calibrated or checked somehow and to do this would require stable and reproducible reference surfaces that could provide and maintain known levels of friction. A set of requirements for such surfaces has been developed.

(5) *Additional findings*

Finally, it is noted that two interesting by-products emerged from the work carried out during the course of the project:

- The quest for a better model for predicting S_o yielded a new relationship that included not only the macro texture of the surface but also the *slip ratio* of the device.
- As a result of the participation of seven texture profilers, the reproducibility of the Mean Profile Depth (MPD) as defined by *ISO 13473-1:1997* [4] has been determined. It is characterized by an average relative standard deviation of 5%.

7 Recommendations

In the sections below, the current situation in the light of the work in the HERMES project is reviewed and specific recommendations are made as to how to move forward.

7.1 Review of the current situation

The underlying problem in harmonising skid resistance measurements is the absence of a fixed reference friction level. The principle of *EFI* attempts to overcome this problem by using the average of all machines to define a “correct” level. An alternative would be to use a reference device for direct comparison. However, this still needs to be calibrated to validate that it is stable. Another alternative is to use reference surfaces to provide stable (over time), known levels of friction with which all devices can be compared and hence linked to some form of common scale. However, the reference surfaces must also be calibrated to verify that they continue to provide the expected level of friction. This would need a “reference device”. Neither the reference device or reference surfaces remove the need for an “*EFI*” kind of scale where different devices using different principles are used.

This gives rise to four possible “scenarios”, reflecting progress from the current position to a fully-standardised situation:

1. No one type of device gives the same results as another (the current situation).
2. Devices are calibrated against one another on any kind of surface, using the *EFI* approach to harmonise the results.
3. During a transition period, different measuring principles will be in use as countries decide to change (or not) their current practices and devices. These devices must be calibrated against a “reference device” using a set of representative “reference surfaces” and correcting for the influence of various factors such as texture etc. using the *EFI* approach.
4. In a “standardised” world, all devices would use the same principle – the “reference device” would become, in effect, a “standard device”. The reference surfaces would then be needed to verify that each individual “standard device” was actually measuring the standard values.

In brief, the *HERMES* project found that:

- The procedure specified in the draft *CEN* standard [3] works (in the sense that it allows a common, stable scale of friction to be kept between the various devices that participated in the calibration exercises) in fully realistic conditions.
- The reproducibility of *EFI* has proved to be rather poor in comparison with the reproducibility between devices of a similar type, which makes the procedure as yet unsuitable for a mandatory application.
- The project has paved the way to alternative solutions by drawing up specifications for a proposed reference device and by setting up general specifications and possible designs for reference surfaces.

7.2 Specific recommendations

In view of the need to improve the present situation, the possible scenarios above and the results of *HERMES*, it is recommended that:

- (a) For the short term (less than 4 years):
 - *CEN/TC227/WG5* should be advised to set up a provisional testing and calibration method based on the experiences gained in the experiments carried out in *HERMES*. The purpose of this recommendation is to make the results provided by various devices comparable through a common scale, even though it is not perfect.
 - The calibration routine initiated by *HERMES* should be kept running using the harmonized procedure on a voluntary basis. It is recommended that for the full operation of the *CEN* procedures, the co-ordination of trial meetings and the allocation of devices to them should be the responsibility of a single overseeing body
 - Further analysis of the data collected by *HERMES* and additional equipment comparisons should be carried out, with a view to improving the precision of *EFI*.
 - The prototype of a reference device should be developed.
 - A feasibility study into the design of reference surfaces is begun.
- (b) For the medium term (4-8 years):
 - A second generation of the standard for dynamic measurement of skid resistance should be prepared, based on a reference device associated to reference surfaces for calibrating the existing systems, possibly using an improved version of *EFI*.
- (c) For the long term (more than 8 years):
 - The reference device should be progressively substituted for existing measuring devices.

Finally, it is recommended that the *FEHRL Working Group* on “Harmonization of friction, texture and evenness measurement methods” that designed and launched the *FILTER* and *HERMES* projects should be re-convened, in order for that extended group to evaluate the situation and develop action plans.

Anticipating these future developments, the *HERMES* Group has prepared three documents in addition to the general report:

- A proposal for the revision of the *prEN 13036-2-Annex B* (drafted as Annex J in this report).
- Guidelines for organizing the calibration of skid resistance testing devices (drafted as a stand-alone document accompanying this report).
- A proposal of a standard reference device for dynamic skid resistance testing of pavements (drafted as Annex L of this report).

References

- [1] WAMBOLD J.C., ANTLE C.E., HENRY J.J., RADO Z., DESCORNET G., SANDBERG U., GOTHIE M., HUSCHEK S., "International *PIARC* Experiment to Compare and Harmonize Skid Resistance and Texture Measurements", *PIARC* Publication n°01.04.T, Paris, 1995.
- [2] DESCORNET G., "Proposal for a European standard in relation with the skid resistance of road surfacings", Final report, Research contract SSTC NO/C3/004, Belgian Road Research Centre, Brussels, 1998.
- [3] *CEN/TC 227/WG5 5*, *prEN 13036-2:2003* "Surface characteristics of road and airfield pavements - Procedure for determination of skid resistance of a pavement surface", *CEN*.
- [4] *ISO 13473-1:1997*, "Characterization of pavement texture by use of surface profiles: Part 1: Determination of Mean Profile Depth", *ISO*.
- [5] *ISO 5725-2:1994*, "Accuracy (trueness and precision) of measurement methods and results – Part 2: Basic method for the determination of repeatability and reproducibility of a standard measurement method", *ISO*.
- [6] VAN DEN BOL M.E., BENNIS T.A., "Measuring Systems for the Evaluation of Skid Resistance and Texture – Relation between the friction Measurements from Different Devices and the International Friction Index", Proceeding of the 4th International Symposium on Pavement Surface Characteristics of Roads and Airfields, pp. 137-182, Nantes, 2000.
- [7] JACOBS M.M.J., GERRITSEN W., WENNINK M.P., VAN GORKUM F., "Optimization of Skid Resistance Characteristics with Respect to Surface Materials and Road Function", Proceedings of the 3rd International Symposium on Pavement Surface Characteristics, pp. 283-298, 1996.
- [8] EMMENS W.C., "The Influence of Surface Roughness on Friction", Proceedings of the 15th Vienna Congress of IDDRG, pp. 63-70, 1988.
- [9] VAN DEN BOL M.E., Personal communication, March 2003.
- [10] MANCOSU F., PARRY A., LA TORRE F., "Friction Variation Due to Speed and Water Depth", Proceedings of the 4th International Symposium on Pavement Surface Characteristics of Roads and Airfields, pp. 249-258, Nantes, 2000.
- [11] KENNEDY J.B., NEVILLE A.M., "Basic Statistical Methods for Engineers and Scientists", Thomas Y. Crowell Company, Inc. 2nd edition, pp. 335-244, 1976.
- [12] GOTHIE, M.G. "Proposal for Specification for a Standard Test Tyre for Friction Coefficient Measurement of a Pavement Surface: Smooth Test Tyre (1)", *PIARC C1* (Committee on Surface Characteristics), Paris, 2003.
- [13] S.C. BRITTON, W.B LEDBETTER, AND B.M.GALLAWAY. "Estimation of Skid Numbers from Surface Texture Parameters in the Rational Design of Standard Reference Pavements for Test Equipment Calibration". Journal of testing and Evaluation, JTEVA, Vol 2 , N°2 p73-83, 1974.
- [14] *ISO/TC22/SC 9*. "Vehicle dynamics and road-holding ability", *ISO*.
- [15] *ISO/TR 8350-1986 (E)*. "Road vehicles - High Friction test track surface- Specification", *ISO*.

[16] HUCKINS, H.C. "FHWA Skid Measurement Test Centres". Public Roads. Federal Highway Administration. Washington D.C. September, 1977.

[17] ELDRIDGE A. WHITEHURST. E. A AND NEUHARDT. J. B. "Time-History Performance of Reference Surfaces. Page 61-71. The Tire Pavement Interface". Pottinger/Yager edition. ASTM. Baltimore, 1986.

[18] J WAMBOLD, J HENRY, "NASA Wallops Tire/Runway Friction Workshops". NASA report. NASA Langley Research Centre Hampton, VA 23681-2199, 2002.

[19] *PIARC* STRATEGIC THEME 1, COMMITTEE C1, SURFACES CHARACTERISTICS, Technical document: "Specification for a standard test tyre for friction coefficient measurement of a pavement surface: Smooth test tyre", *PIARC*.